NAVAL POSTGRADUATE SCHOOL

MONTEREY, CALIFORNIA

THESIS

ELECTRICAL AND THERMAL ANALYSIS OF GALLIUM NITRIDE HEMTS

by

Yuchia Wang

June 2009

Thesis Advisor:	Todd R. Weatherford
Second Reader:	Gamani Karunasiri

Approved for public release; distribution is unlimited

THIS PAGE INTENTIONALLY LEFT BLANK

REPORT DOCUMENTATION PAGE			Form Approved OMB No. 0704-0188
Public reporting burden for this collection of information is estimated to average 1 hour per response, including the time for reviewing instruction, searching existing data sources, gathering and maintaining the data needed, and completing and reviewing the collection of information. Send comments regarding this burden estimate or any other aspect of this collection of information, including suggestions for reducing this burden, to Washington headquarters Services, Directorate for Information Operations and Reports, 1215 Jefferson Davis Highway, Suite 1204, Arlington, VA 22202-4302, and to the Office of Management and Budget, Paperwork Reduction Project (0704-0188) Washington DC 20503.			
1. AGENCY USE ONLY ***(Leave blank)***	**2. REPORT DATE** June 2009	**3. REPORT TYPE AND DATES COVERED** Master's Thesis	
4. TITLE AND SUBTITLE Electrical and Thermal Analysis of Gallium Nitride HEMTs		**5. FUNDING NUMBERS**	
6. AUTHOR(S) Yuchia Wang			
7. PERFORMING ORGANIZATION NAME(S) AND ADDRESS(ES) Naval Postgraduate School Monterey, CA 93943-5000		**8. PERFORMING ORGANIZATION REPORT NUMBER**	
9. SPONSORING /MONITORING AGENCY NAME(S) AND ADDRESS(ES) N/A		**10. SPONSORING/MONITORING AGENCY REPORT NUMBER**	
11. SUPPLEMENTARY NOTES The views expressed in this thesis are those of the author and do not reflect the official policy or position of the Department of Defense or the U.S. Government.			
12a. DISTRIBUTION / AVAILABILITY STATEMENT Approved for public release; distribution is unlimited.		**12b. DISTRIBUTION CODE**	

13. ABSTRACT (maximum 200 words)

The purpose of this thesis was to build a transient model and to study the electrical and thermal characteristics of the AlGaN/GaN HEMT. We first used Method 3104 of MIL-STD 750D to determine the location of HEMT structure that gate voltage measurement relates to. Secondly, we investigated the performance of single pulse and multiple pulses. Thirdly, we studied and compared the performance between the DC model and the Transient model (multiple pulses) with the same power. Finally, we compared the self-heating effect between various substrates and discussed the observation of unique transistor heating. Based on the analysis of these simulation results, we would be able to predict the performance of the AlGaN/GaN HEMT.

14. SUBJECT TERMS Gallium Nitride, HEMT, High Electron Mobility Transistor, Silivaco, ATLAS, modeling, Transient, Self-heating, Pulse			**15. NUMBER OF PAGES** 109
			16. PRICE CODE
17. SECURITY CLASSIFICATION OF REPORT Unclassified	**18. SECURITY CLASSIFICATION OF THIS PAGE** Unclassified	**19. SECURITY CLASSIFICATION OF ABSTRACT** Unclassified	**20. LIMITATION OF ABSTRACT** UU

NSN 7540-01-280-5500 Standard Form 298 (Rev. 2-89)
Prescribed by ANSI Std. 239-18

THIS PAGE INTENTIONALLY LEFT BLANK

Approve for public release; distribution is unlimited

ELECTRICAL AND THERMAL ANALYSIS OF GALLIUM NITRIDE HEMTS

Yuchia Wang
Captain, Taiwan Army
BSEE, National Defense University, 2000

Submitted in partial fulfillment of the
requirements for the degree of

MASTER OF SCIENCE IN APPLIED PHYSICS

from the

NAVAL POSTGRADUATE SCHOOL
June 2009

Author: Yuchia Wang

Approved by: Todd R. Weatherford
Thesis Advisor

Gamani Karunasiri
Second Reader

James H. Luscombe
Chairman, Department of Physics

THIS PAGE INTENTIONALLY LEFT BLANK

ABSTRACT

The purpose of this thesis was to build a transient model and to study the electrical and thermal characteristics of the AlGaN/GaN HEMT. We first used Method 3104 of MIL-STD 750D to determine the location of HEMT structure that gate voltage measurement relates to. Secondly, we investigated the performance of single pulse and multiple pulses. Thirdly, we studied and compared the performance between the DC model and the Transient model (multiple pulses) with the same power. Finally, we compared the self-heating effect between various substrates and discussed the observation of unique transistor heating. Based on the analysis of these simulation results, we would be able to predict the performance of the AlGaN/GaN HEMT.

THIS PAGE INTENTIONALLY LEFT BLANK

TABLE OF CONTENTS

LIST OF FIGURES

LIST OF TABLES

THIS PAGE INTENTIONALLY LEFT BLANK

LIST OF EQUATIONS

.

THIS PAGE INTENTIONALLY LEFT BLANK

EXECUTIVE SUMMARY

In this thesis we used the modeling program Silvaco Atlas© to build a transient model and to study the electrical and thermal characteristics of the AlGaN/GaN HEMT. We first used Method 3104 of MIL-STD 750D to determine the location of HEMT structure that gate voltage measurement relates to. The simulation result suggests that the specific location is inside the gate electrode above the channel, and is dynamic rather than fixed.

Secondly, we investigated the performance of single pulse and multiple pulses. As a result, the single pulse had the higher maximum temperature of 394.62 K, 105.33% of 374.62 K in multiple pulses. But single pulse had a better performance on average power of 6 W, 183.5% of 3.27 W in multiple pulses.

Thirdly, we studied and compared the performance between DC model and Transient model (multiple pulses) with the same power. We used time constant technique to predict the peak temperature and average drain current of multiple pulses in equilibrium and obtained the values were respectively as 402.61 K and 0.4737A. The average power was 2.37 W. With the same power in DC modeling, the temperature in equilibrium was 527.01 K. The simulation suggests that running multiple pulses in GaN HEMT instead of DC modeling will reduce the self-heating effect.

Finally, we compared the self-heating effect between various composition ratios of diamond in substrate and discussed the observation of unique transistor heating. In multiple pulses simulation, increasing the substrate composition ratio of diamond from 76% to 95% would lead to the temperature decrement from 1.97 ^{o}C to 5.07 ^{o}C as well as the average power increment from 2.83% to 4.56%. Pertaining to the observation of transistor heating, the simulation results appeared that the Joule heat power accumulated with increasing time at both sides. Therefore, there were two hot spots in the beginning of the pulse. Then we presumed that the heat gradually dissipated through gate electrode in the end of the pulse after gate electrode was filled with the accumulated Joule heat. Eventually, the two hot spots began to diffuse into one hot spot.

The simulation work done in this thesis can help to understand more thoroughly the electrical and thermal characteristics of AlGaN/GaN HEMTs in transient processing.

ACKNOWLEDGMENTS

Several people played an important role in the accomplishment of this thesis paper. First, I would like to thank my advisor, Professor Todd R. Weatherford, for his ample support and invaluable guidance throughout the thesis, especially for his supervision in the simulation process. Professor Weatherford had helped me developed a deeper understanding of the theories by always being readily available to answer the questions I had. I gratefully appreciate his time and effort.

I would also like to thank Professor Gamani Karunasiri for being the second reader of my thesis.

Finally, and most importantly, I have to thank God for giving me a chance to study at NPS and the strength to finish my study. He also blessed me with a lovely girlfriend and many friends who support me while I am away from my family.

THIS PAGE INTENTIONALLY LEFT BLANK

I. INTRODUCTION

A. BACKGROUND

There has been a long-standing desire to replace Traveling Wave Tube Amplifiers (TWTAs), which are pervasive in nearly all Electronic Warfare (EW), Information Warfare (IW), Radar, and Communication System, with lower cost solid-state components. In the past couple of years, DoD has kept funding GaN technology research. According to DoD Fiscal Year 2009 budget Estimates [1], DoD spent $6.676 million in 2007 and 2008, and are planning to spend $5.392 millions in 2009 for the Disruptive Manufacturing Technologies (DMT) program as in Table 1. The DMT program will merge Polystrata and GaN technologies to eliminate the need for monolithic microwave integrated circuits (MMICs).

Program	FY 2007	FY 2008	FY 2009
Disruptive Manufacturing Technologies (DMT)	$3.008	$3.368	$5.392

Table 1. DMT Program of DoD FY 2009 Budget Estimate (in millions) [From 1].

Comparing with Solid State Power Amplifier (SSPA) technology, Traveling Wave Tube Amplifiers (TWTA) technology has disadvantages of shorter life cycle, poor linearity and requiring a higher voltage to amplify. However, a Si or GaAs-based SSPA has a challenge of offering a high output power though it has not been considered as a potential replacement of TWTA until the availability of GaN Transistor technology.

In the past few years, Gallium Nitride (GaN) has attracted a lot of attention and is considered to be a candidate for next generation high-power electronics due to wide bandgap, high electron saturation velocity, high critical breakdown field, and the potential to form lattice-matched heterojunctions with other group III-Nitride materials [2]. The electrical and thermal characteristics of GaN compared to other materials are listed

as Table 2. For military communication and navigation systems, GaN HEMT technology offers tremendous new capabilities and is expected to transform the future of power amplifiers from UHF to Q-Band frequencies [3].

Although GaN has so many advantages that make it a promising technology, significant technological development is still required to improve the reliability and thermal management of devices constructed with this material. Self-heating is one of the critical factors that adversely affect device performance and reliability. Channel temperature can reach several hundred degrees above ambient base temperature due to self-heating. The temperature increases not only reduce the performance of the devices but also accelerate their degradation. Severe self-heating effect may deteriorate the gate electrode and can burn metal wires connecting the chip to the package, and hence cause device failures and reliability problems [4]–[5].

	InAs (AlSb/ InAs)	Si (SiGe/Si)	GaAs (AlGaAs/ InGaAs)	InP (InAlAs/ InGaAs)	4H SiC (------)	**GaN (AlGaN/ GaN)**	Diamond
Bandgap(eV)	0.36	1.1	1.42	1.35	3.26	**3.49**	5.45
Electron mobility (cm^2/Vs)	33000 (25000)	1500 (2800)	8500 (8000)	5400 (10000)	700	**900 (>2000)**	4000
Saturated (peak) electron velocity ($x10^7 cm/s$)	(4.0)	1.0 (1.0)	1.0 (2.1)	1.0 (2.3)	2.0 (2.0)	**1.5 (2.7)**	2.8
2DEG sheet electron density (cm^{-2})	$<6x10^{12}$	$2x10^{12}$	$<3x10^{12}$	$<4x10^{12}$	NA	**$1\text{-}2x10^{13}$**	NA
Critical breakdown field (MV/cm)	0.04	0.3	0.4	0.5	2.0	**3.3**	10
Thermal conductivity (W/cm-K)	0.27	1.5	0.5	0.7	4.5	**>2.0**	2.2
Relative dielectric constant(ε_r)	15.1	11.8	12.8	12.5	10	**9.0**	5.5

Table 2. Semiconductor Material Comparison [From 6].

Fortunately, many researchers have studied reliability and performance and the results may be satisfactory.

In a wearout reliability assessment [7] of AlGaN/GaN HEMTs fabricated on SiC at 48V , the activation energy based on the results of the 3-temperature test, was 2.47 eV with a 60 % confidence interval of [2.00, 2.94] eV and a 90% confidence interval of [1.55, 3.39] eV. Figure 1 showes the estimate of MTTF (Mean Time to Failure) based on the results of the 3-temperature AlGaN/GaN HEMT life test. The triangles show MTTF at junction temperatures of 257, 273 and 289 ^{o}C based on log normal fit to the TTF (Time to Failure) data at each temperature, using the method of maximum likelihood. The dotted lines show the 60% and 90% confidence bounds on the estimate of MTTF at any desired channel temperature. The estimated MTTF at 200 ^{o}C was [1.0 x 10^{6}, 3.0 x 10^{7}] hours within a 60% confidence interval and [2.0 x 10^{5}, 1.5x10^{8}] within a 90% confidence interval. The estimated MTTF at 150 ^{o}C was [3.2 x 10^{8}, 1.6 x 10^{11}] hours within a 60% confidence interval and [1.7 x 10^{7}, 3.0 x 10^{12}] within a 90% confidence interval.

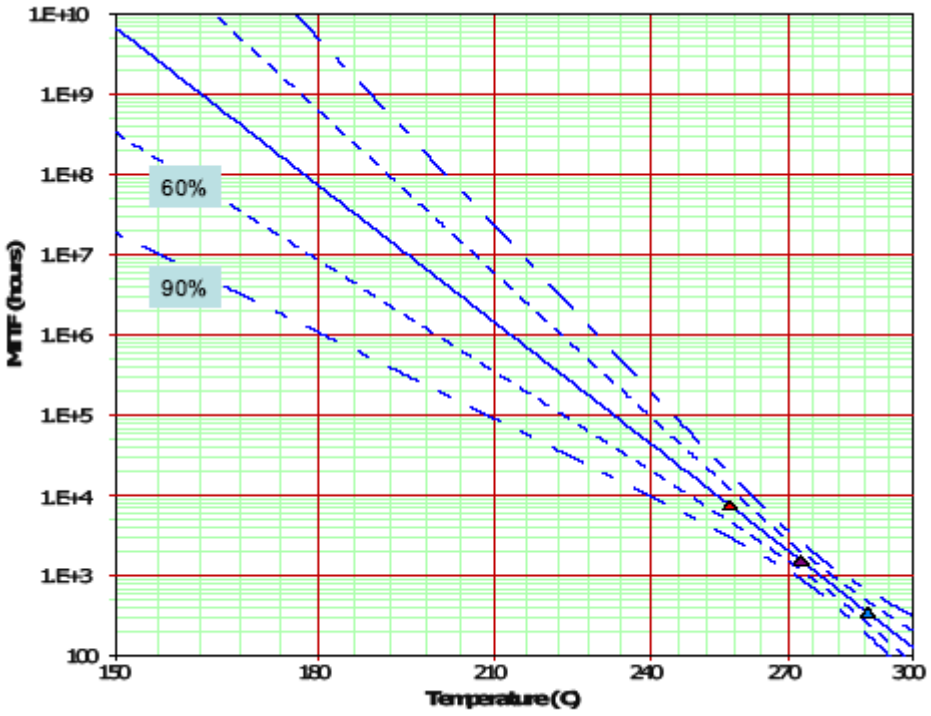

Figure 1. MTTF Estimation [From 7].

As mentioned in McGlone's thesis [8], since GaN is generally unavailable in a single crystalline substrate, it is often deposited on a substrate of different material such as silicon, sapphire, silicon carbide, and most recently, silicon-on-diamond (SOD). The thermal conductivity of the substrate becomes important when discussing the thermal management of the device. Commercially available devices are currently constructed with various substrates such as silicon-carbide (SiC) or sapphire. The current market availability and scientific knowledge of silicon makes it a convenient choice for substrate material, but its thermal transferability is poor compared with other available materials. Silicon-carbide has become a popular choice for substrate because of its thermal transfer properties, but its cost remains high compared with other substrate options, in addition to its 3-inch limiting size. Diamond has a large thermal conductivity compared with that of most materials including SiC. Due to the large thermal conductivity, diamond appears to be a good alternative to SiC for its heat transfer ability. The SILVACO© model developed in this thesis examines the current sp3, Air Force Research Laboratory (AFRL) constructed device and the thermal impact of using a SOD substrate.

B. RESEARCH PROGRAMS ON GAN HEMT

We introduced two programs pertaining to GaN HEMTs in this chapter. The first one is WBGS-RF program funded by DARPA. The second one is SOD technology funded by the Missile Defense Agency (MDA).

1. WBGS-RF Program of DARPA

In the past years, the Defense Advanced Research Projects Agency (DARPA) has been funding a series of researches pertaining to the development of the GaN HEMTs. One important program of them is WBGS-RF (Wide Bandgap Semiconductor for RF applications). It is a three-phase program [9]**.**

Phase I of DARPA's WBGS-RF initiative, conducted between 2002 and 2004, contributed significantly to the availability of low-defect, high-resistivity SiC substrates. In early 2005, the three-year WBGS-RF Phase II program began. By its conclusion in 2008, it is expected that many types of GaN-on-SiC devices with the potential for

enabling additional military and commercial applications and vastly improving the characteristics of many existing types of systems will be realized. Subsequent to the demonstration of the program's Phase II objectives, a two-year Phase III program is planned, which will culminate with demonstrations of several types of high performance MMICs and several types of modules. It is expected that robust fabrication processes will be in place, coupled with advanced design capabilities. Collectively, these will make it possible to produce numerous additional types of MMICs that have stable, reliable operation and can be produced at an affordable cost.

In October 2007, DARPA published a paper [10] that reported the latest advances in GaN-on-SiC HEMT Reliability and Microwave Performance within the WBGS-RF Program. The WBGS-RF program has three distinct performance tracks. The goals of these tracks are shown in Table 3.

Type Integration Level Track	Unit	WBGS-RF Phase II Program					
		24 month Status Device			36 month Go/No Go Criteria Device		
		X	Q	WB	X	Q	WB
Drain Bias	V	40	28	40	40	28	40
Cell Size	µm	1250	500	400	1250	500	1250
Operating Frequency	GHz	10	40	10	8-12	>40	8-12
Output Power*	W/mm	7.9	1.5	3.1	7.94	1.58	7.94
Power Density*	W/mm	6.4	3.0	7.9	6.4	3.2	6.4
Power Added Efficiency	%	55	34	55	60	35	60
Gain at Power	dB	11	7.7	12.4	12	8	12
RF Yield‡	%	> 50	94	67	50	50	50
Output Power Uniformity†	dB	1.5	0.2	0.36	1	1	1
PAE Uniformity†	% pts	4	1.8	2.9	3	3	3
Small Signal Gain Uniformity†	dB	1	0.3	0.52	1	1	1
Long Term Performance**	hrs	1.E+05	> 100	1.E+05	1.E+05	1.E+05	1.E+05

Table 3. WBGS-RF Program Status and Goals [From 10].

* Measured at compression corresponding to maximum PAE

† Uniformity defined as the standard deviation in measured values from 100 devices/MMICs on all validation wafers

‡ The fraction of devices from all validation wafers meeting or exceeding all relevant GNG requirements

** Failure is defined as one dB decrease in output power compared with its level at the time that testing commences

Metrics that are being used to identify progress towards program goals can be grouped into three categories that include RF performance, stability and degradation, and producibility.

For RF performance, the Raytheon/Cree team has simultaneously achieved power added efficiency (PAE) of 55% with 7.9 W output power and gain of 11 dB for the Track oen X-band power amplifiers. For Track two, the Northrop Grumman team has achieved 40 GHz device operation with 1.5 W output power (3 W/mm), 34% PAE and 7.7 dB gain. For Track three, the TriQuint team has achieved power density of 7.9 W/mm with greater than 55% PAE and greater than 12 dB gain using small gate periphery devices.

For stability and degradation, although the full planned battery of RF and DC reliability testing was not completed yet, initial RF life tests at multiple elevated temperatures, performed on an earlier generation of devices operated at 28 V drain-source bias, are encouraging. Based upon this elevated temperature testing, projected mean-time-to-failure (MTTF) for many of these devices is in excess of 10^5 hours, at a junction temperature of 150° C. Initial RF life tests on a more recently fabricated device, biased at 48V, have demonstrated operation for more than 750 hours with a negligible drop in output power.

For producibility, high quality 100 mm SiC substrates have become available, and their use within the program is becoming routine, replacing 3-inch substrates. Initial devices fabricated on 100 mm diameter SiC wafers have shown comparable epitaxial uniformity and similar RF performance to that of devices fabricated on 3-inch diameter substrates. The use of 100 mm substrates is expected to result in significantly reduced production costs in the future.

2. SOD Substrate Research

The Silicon-on-Diamond (SOD) structure is basically equivalent to an SOI device structure, but the insulator in SOD is diamond, rather than silicon dioxide. The key advantage with diamond is its very high thermal conductivity—ten times that of silicon and more than double that of SiC, the most commonly used substrate for GaN electronics. This advantage is beneficial in the following two aspects (1) It leads to a significant

reduction in the thermal degradation of the device electrical characteristics, and (2) it allows a more uniform distribution of temperature in the device active region, that, in turn, enhances heat removal [11]. Therefore, SOD is viewed as a substrate solution for wide-bandgap electronics.

In June 2006, Diamond wafer specialist SP3 Diamond Technologies received $0.75 million from the Missile Defense Agency (MDA) to pursue work on a diamond-based substrate material suitable for wide-bandgap electronics [8]. In the Phase I part of the project, SP3 developed SOD wafers with a GaN top surface. NPS performed detailed computer simulations, suggesting that a HEMT built on diamond would reduce junction temperature in the transistor by 80 ^{o}C and increase power output by 37 %. In collaboration with GaN wafer and component developers at Nitronex and TriQuint, SP3 will use the Phase II contract from the MDA to deliver GaN on silicon-on-diamond (SOD) technology.

In April 2009, SP3 Inc. released the news [12] that announced commercial availability of SOD wafers for high-power and high-frequency devices. The SOD wafers are delivered as structured substrates with a top layer of device-quality float-zone silicon. They provide diamond heat spreading directly under the junction and can achieve more than 100% increase in power levels compared to silicon substrates alone, and a 50-80% increase when compared to SiC, at a fixed junction temperature. At fixed power, they can reduce junction temperature by more than 50^{o}C compared to GaN on silicon or SiC. GaN growth on SOD yields epi films equivalent to GaN on silicon, and SP3 can scale wafer size up to 300mm.

C. SUMMARY OF PREVIOUS NPS RESEARCH

Since the first NPS research studied in GaN HEMTs was presented in 2001 , there have been six students who have contributed their efforts to exploring the characteristics of GaN HEMTs. The contributions of the first five students have been mentioned and discussed in [8]. Here, we will only discuss McGlone’s research.

The work in McGlone's thesis was modified from Gibson's model [13] primarily, instead of a SOD substrate. We will discuss the model in detail later. In his simulation, the low field mobility model (Albrecht's model) was used to simulate DC IV data to a GaN HEMT fabbed on SOD material. He finally suggested using a high field mobility model to improve the simulation capability to predict DC self-heating.

D. OBJECTIVE

In the previous NPS researches, a lot of work has been done on the DC analysis of AlGaN/GaN HEMT, using the simulation software Silvaco©. The purpose of this thesis is to utilize Silvaco© software to build a transient model and to study the transient electrical and thermal characteristics of AlGaN/GaN HEMTs. We will also use Method 3104 of MIL-STD 750D [14], that will be discussed later as we investigate techniques to predict transistor thermal characteristics.

II. HIGH ELECTRON MOBILITY TRANSISTOR (HEMT)

A. FUNDAMENTALS OF ALGAN/GAN HEMT

In this chapter, we introduce the formations of heterostructure and Two Dimensional Electron Gas (2DEG), as well as the operation of AlGaN/GaN HEMT.

1. Heterostructure and 2DEG

HEMT is also called Heterostructure FET (HFET), or Modulation Doped FET (MODFET). A HEMT is a field effect transistor incorporating a junction between two materials with different band gaps (i.e., heterojunction) as the channel instead of a doped region, as is generally the case for MOSFETs. The unique feature of HEMT is the heterostructure in which the wide-energy band gap material is doped, and carriers diffuse to the undoped narrow band gap material where the channel is formed. Also, due to this modulation doping, carriers in the undoped heterointerface are spatially separated from the doped region and have extremely high mobilities because there is no impurity scattering. The idea of modulation doping was proposed at Bell Laboratories in the late 1970s, and then in 1980, the first HEMT was demonstrated by Mimura et al. [15].

In Mishra's paper [16], it was clearly demonstrated that when Aluminum Gallium Nitride (AlGaN) is grown on top of a layer of a similar crystal, such as Gallium Nitride (GaN), a heterojunction occurs at the boundary between the two different crystals as shown in Figure 2. This heterojunction is a major contributor to Gallium Nitride's outstanding high-frequency characteristics.

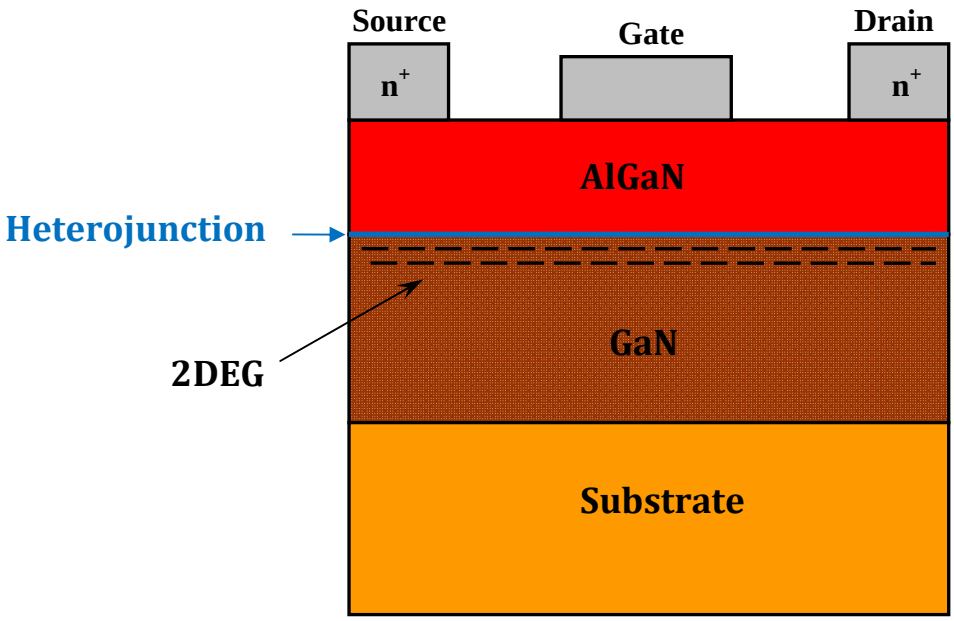

Figure 2. Heterojunction of AlGaN/GaN HEMT.

Inside the Gallium Nitride crystal, as in any similar crystal, the individual atoms are electronically charged, or ionized, and the large Gallium and small Nitrogen atoms are arranged somewhat irregularly with respect to each other, because of the difference in size. This combination of ionization and irregularity leads to a spontaneous electrical polarization within the crystal, or a separation of charge into countless, regularly spaced negative and positive atoms. Figure 3 from [15] illustrates the ionization and the irregularity inside the GaN crystal.

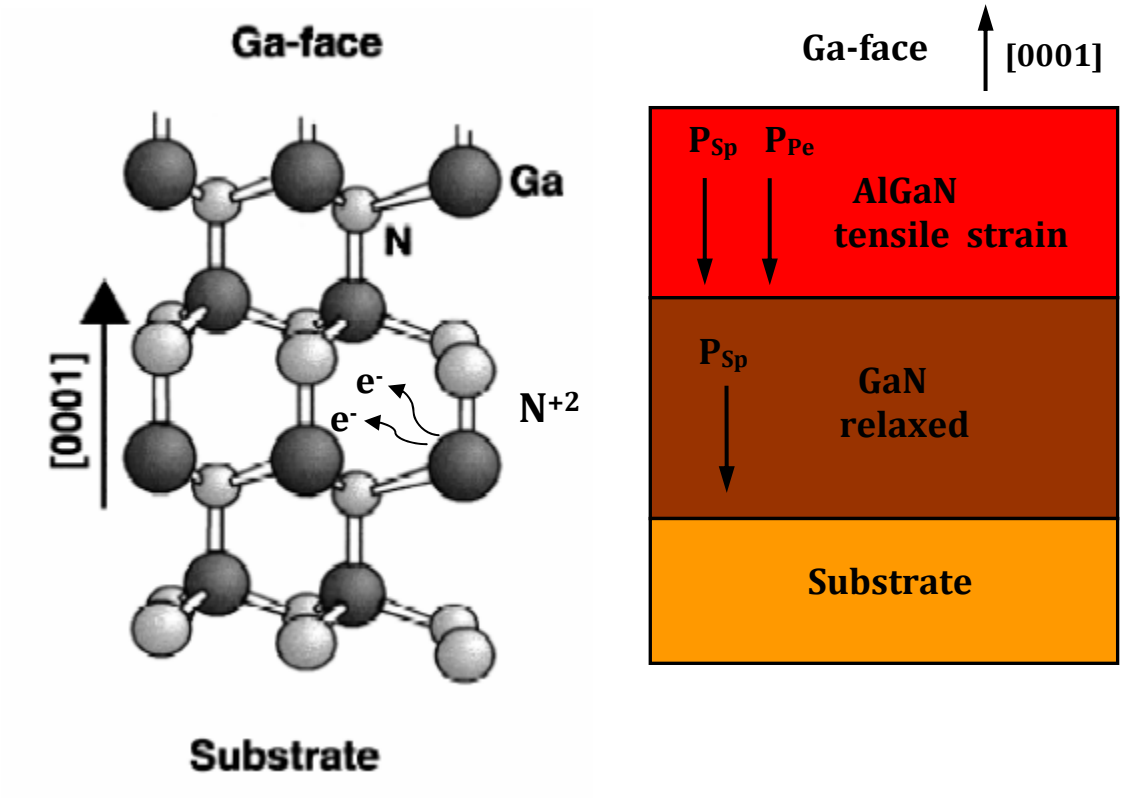

Figure 3. Atomic Structure of GaN Layer [From 15].

In an ordinary GaN crystal, the polarization does not accumulate, because the oppositely charged regions cancel out overall. But that canceling doesn't occur where the GaN crystal ends suddenly, for example, at a heterojunction with another crystal, such as Aluminum Gallium Nitride. In that case, the abrupt change at the interface gives rise to an electrically charged region in the immediate vicinity of the boundary. That charged, polarized region is augmented, furthermore, by a piezoelectric polarization, which arises from the strain caused by the coming together of the two different crystal lattices.

These combined polarizations, in turn, induce an excess of free-moving electrons in the Gallium Nitride. The electrons concentrate near the polarization region, hard against the Aluminum Gallium Nitride but without straying into it because the material's higher bandgap acts as a barrier. Thus, a dense two-dimensional "gas" (2DEG) of charge-carrying electrons spontaneously forms in the Gallium Nitride, very close to the boundary with the Aluminum Gallium Nitride as shown in Figure 4.

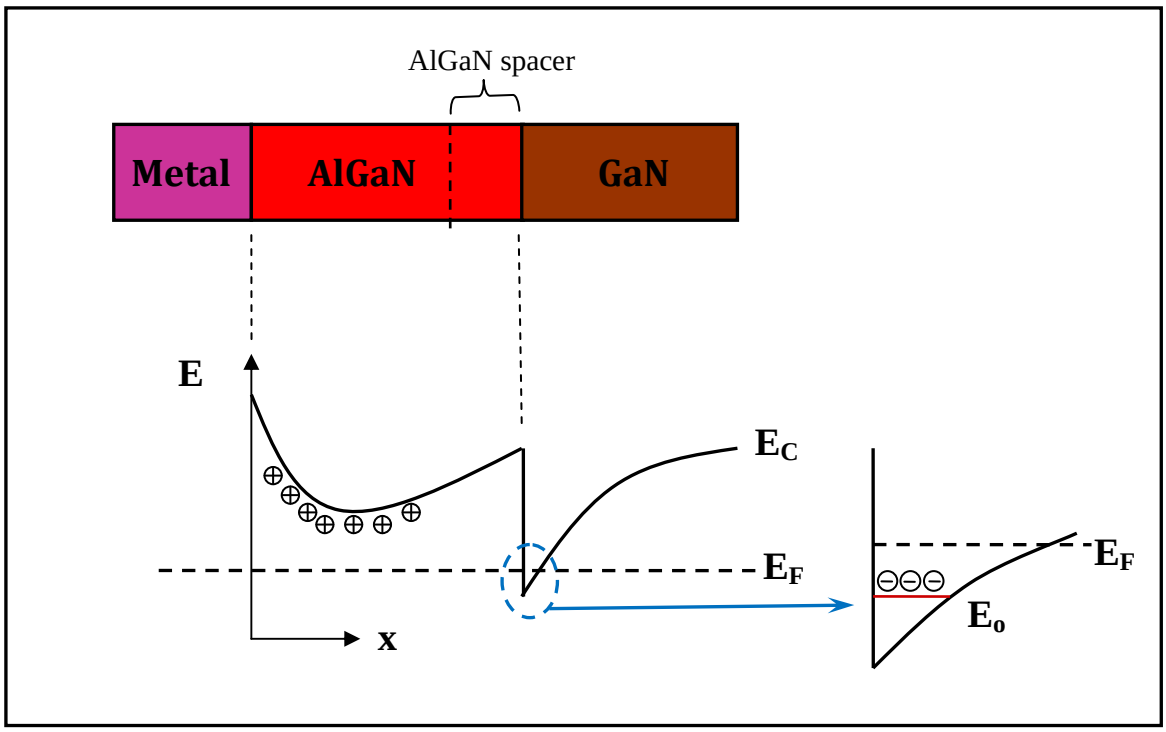

Figure 4. Energy band diagram and 2DEG.

In fact, due to the piezoelectric and spontaneous polarization, AlGaN/GaN HEMTs are able to achieve 2DEG with sheet carrier concentrations of up to $2\text{x}10^{13}\text{cm}^{-2}$ close to the interface, which excess those observed in other III-V material systems [15].

As mentioned in previous thesis [8], the sheet carrier density showing the control of the gate voltage can be modeled by equation (1) and the threshold voltage can be modeled by equation (2).

$$n_s(m) = \frac{2q\varepsilon(m)D}{\varepsilon(m) + 2q^2 D(d_d + d_i)}(V_{gs} - V_{th}(m) - V(x)) \quad (1)$$

$$V_{th}(m) = \phi(m) - \Delta E_c(m) - \frac{qn_d d_d^2}{2\varepsilon(m)} - \frac{\sigma(m)}{\varepsilon(m)}(d_d - d_i) \quad (2)$$

where

$\varepsilon(m)$ is the dielectric constant of the AlGaN barrier layer

q is the electron charge

d_d , d_i are AlGaN layer thickness and spacer layer thickness, respectively

$D = \frac{4\pi m^*}{h^2}$ is conduction band density of state of 2-DEG system

V_{gs} is gate-to-source voltage

$V(x)$ is channel potential at a distance x

$V_{th}(m)$ is the threshold voltage of gate bias

$\phi(m)$ is the Schottky barrier height

$$\sigma(m) = \left| P_{spontaneous}(Al_mGa_{1-m}N) - P_{spontaneous}(GaN) + P_{piezoelectric}(Al_mGa_{1-m}N) \right| \frac{C}{m^2}$$

$$P_{piezoelectric}(Al_mGa_{1-m}N) = \left[\frac{2(a(0)-a(m))}{a(m)} \right] \times \left[e_{31}(m) - \frac{e_{33}(m)C_{13}(m)}{C_{33}(m)} \right] \frac{C}{m^2}$$

$$P_{spontaneous}(Al_mGa_{1-m}N) = -0.052m - 0.029 \frac{C}{m^2}$$

The constants not listed above are contained in Table 4.

Wurtzite	AlN	GaN	InN	BN
a_0(Å)	3.112	3.189	3.54	2.534[e]
c_0(Å)	4.982	5.185	5.705	4.191[e]
c_0/a_0	1.601	1.627	1.612	1.654[e]
	1.619 [a]	1.634 [a]	1.627 [a]	···
u	0.380 [a]	0.376 [a]	0.377 [a]	0.374 [e]
P_{SP}(C/m^2)	−0.081 [a]	−0.029 [a]	−0.032 [a]	···
e_{33}	1.46 [a]	0.73 [a]	0.97 [a]	···
(C/m^2)	1.55 [b]	1 [c]	···	···
		0.65 [d]	···	···
	1.29 [e]	0.63 [e]	···	−0.85 [e]
e_{31}	−0.60 [a]	−0.49 [a]	−0.57 [a]	···
(C/m^2)	−0.58 [b]	−0.36 [c]	···	···
		−0.33 [d]	···	···
	−0.38 [e]	−0.32 [e]	···	0.27 [e]
e_{15}	−0.48 [b]	−0.3 [c]	···	···
(C/m^2)		−0.33 [d]	···	···
ϵ_{11}	9.0 [b]	9.5 [f]	···	···
ϵ_{33}	10.7 [b]	10.4 [f]	14.6 [g]	···

Table 4. Various Semiconductor Constants [From 8].

2. Operation of AlGaN/GaN HEMT

All the different types of HEMTs operate in a similar way. By applying a positive voltage to the gate, one may induce electrons into the narrow channel in Gallium Nitride at the heterointerface. The composition and doping profile of the AlGaN layer determine the device threshold voltage.

The electron gas induced at the heterointerface is similar to the electron gas in the inversion layer in silicon MOSFETs. But different to silicon MOSFETs, the 2DEG already exists naturally in the GaN layer of AlGN/GaN HEMT. Figure 5 and Figure 6 illustrate how the AlGaN/GaN works compared to Silicon FET.

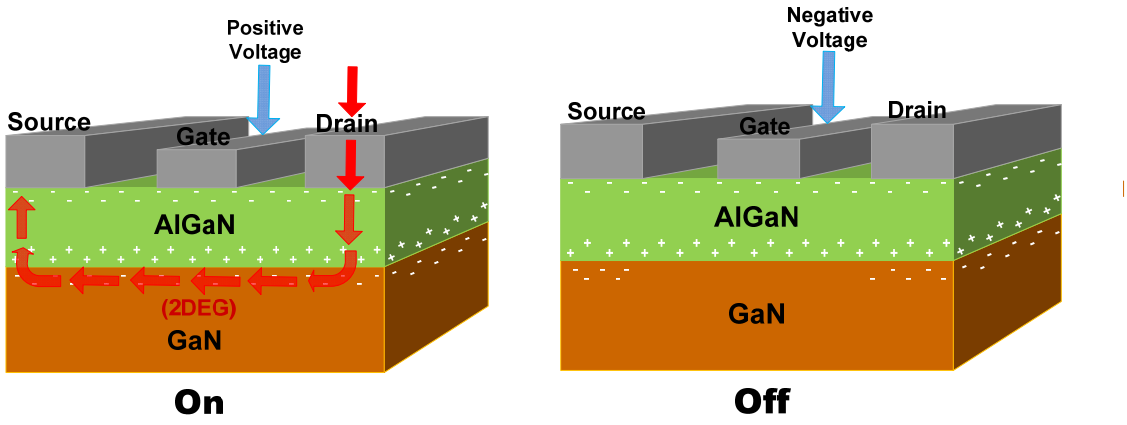

Figure 5. Operation of GaN FET [From 16].

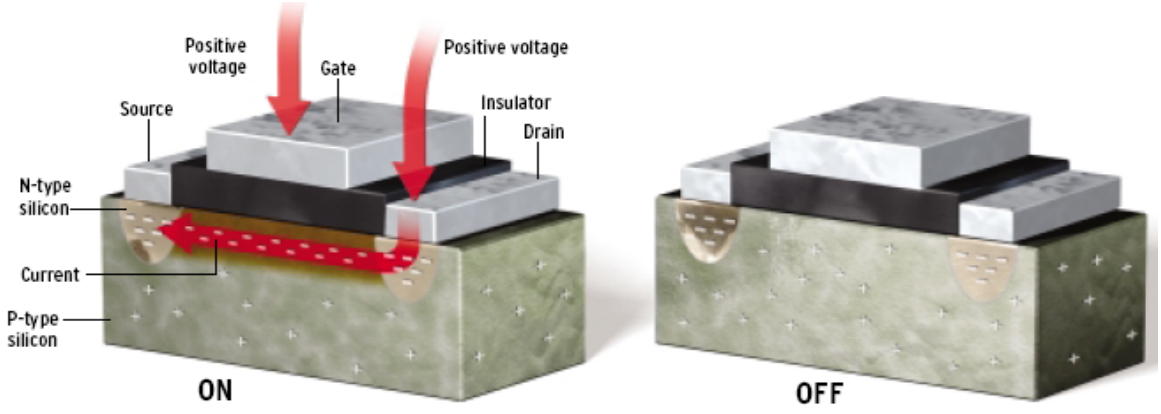

Figure 6. Operation of Silicon FET [From 16].

3. Thermal Issues of AlGaN/GaN HEMT

Many researchers of GaN-based HEMTs have focused on the thermal effects. Self-heating is one of the critical effects that seriously affects the device performance and reliability. For reducing the effect of self-heating and enhancing heat dissipation, the thermal properties of substrate becomes very important.

a. Self-Heating

Due to self-heating, channel temperatures can reach several hundred degrees above the ambient base temperature. The temperature increases can significantly degrade the performance of the transistor, for instance the decrease in the channel electron mobility, the maximum drain current and the maximum power density and also the increase in the gate leakage, etc.

Figure 7 and Figure 8, from Manju's paper [4], specifically illustrate the relationships between temperature, low field mobility and sheet carrier concentration.

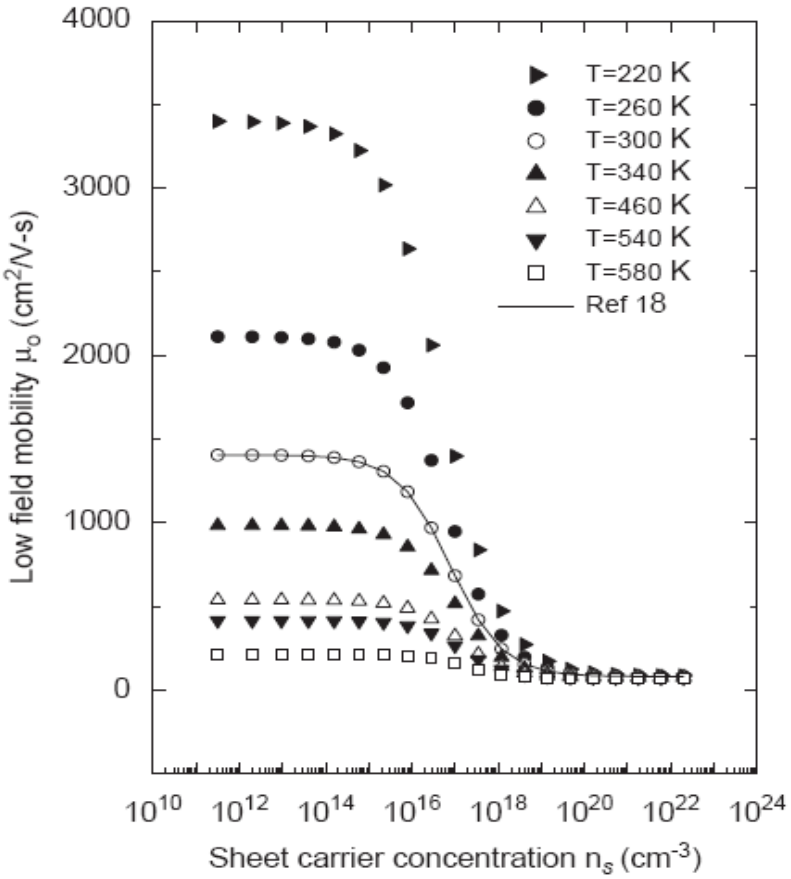

Figure 7. Low-field mobility μ_o(cm^2/Vs) variation with sheet carrier concentration n_s(cm^{-3}) [From 4].

Figure 7 shows the dependence of mobility on sheet carrier concentration. Mobility values at all temperatures reduce to similar value for very high sheet concentration (**>**10^{20} cm^{-3}). For small sheet carrier concentration, lower temperature gives higher carrier mobility. Table 5 lists the mobility values and the corresponding temperature at $n_s=10^{11}$ cm^{-3}.

Temperature (K)	220	260	300	340	460	540	580
Mobility (cm^2/Vs)	3392	2112	1405	983	538	415	107

Table 5. Mobility and the corresponding temperature.

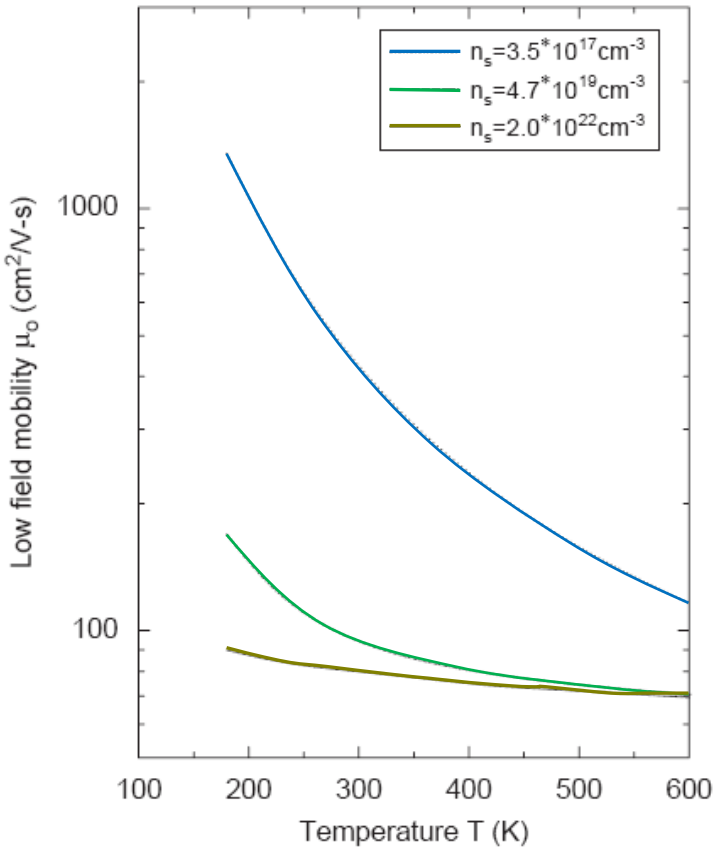

Figure 8. Dependence of low-field mobility μ_o (cm^2/Vs) on temperature T(K) [From 4].

In Figure 8, it can be seen that the mobility decreases with the increasing temperature. In different sheet carrier concentration, the higher the sheet carrier concentration is, the lower the mobility is.

b. Effects of Substrate

The thermal characteristics of various substrate materials have been studied in many researches. Figure 9, from Manju's paper [4], presents the temperature dependence of inverse of thermal conductivity, i.e. $\frac{1}{K}$ of various materials that can be used as substrates in AlGaN/GaN HEMTs. Manju pointed out that if the total epilayer thickness in devices is significantly smaller than the device length, the thermal

conductivity of the substrate plays a significant role in determining the temperature distribution in the epilayer structure and the heat removal from the active region of the device.

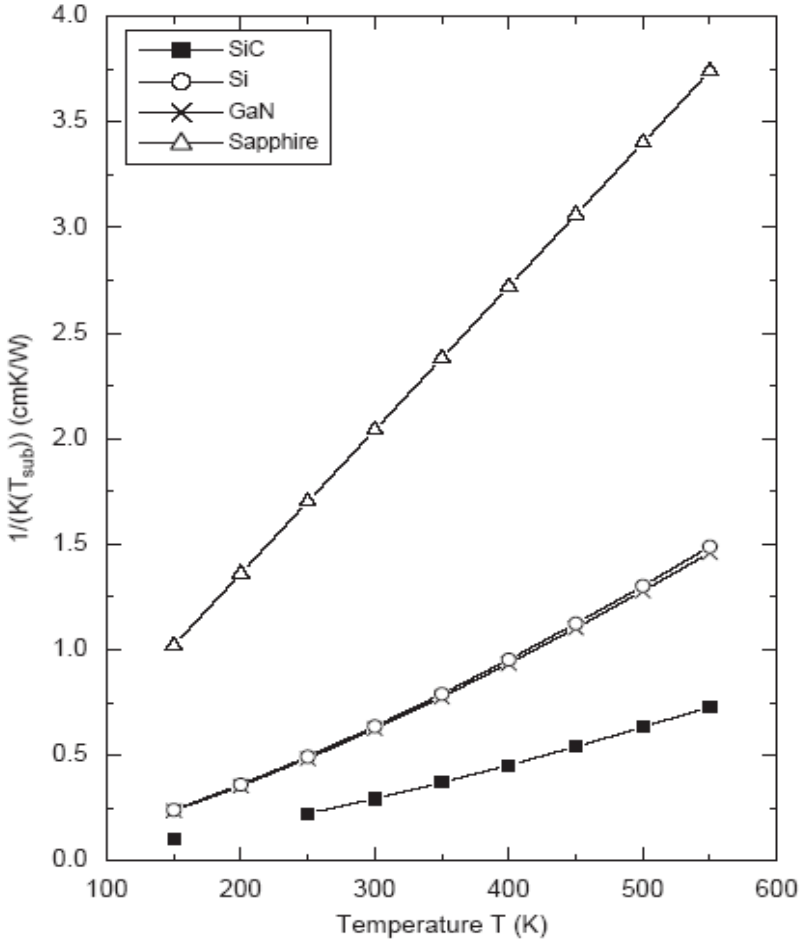

Figure 9. Inverse thermal conductivity $\frac{1}{K(T_{sub})}$ (cm K/W) variation with temperature T(K) for different substrate materials viz. SiC , Si , GaN , Sapphire [From 4].

The values of $\frac{1}{K(T_{sub})}$ for each material are listed in Table 6.

Material	SiC	Si	GaN	Sapphire
$\frac{1}{K(T_{sub})}$ (cm K/W)	0.294	0.625	0.637	2.041

Table 6. Inverse thermal conductivity.

B. SP3 DEVICE

Since the model used in this thesis was modified from the SP3 device, we will briefly discuss the SP3 device which has been demonstrated in [8].

1. Device Construction

The sp3 device fabricated by AFRL, with the epilayer provided by Nitronex and SOD substrate provided by sp3, is a GaN HEMT with a silicon substrate separated by a thin diamond on silicon layer as well as a bonding layer. It has a gate length of .35 microns and a 150 x 2 micron gate width. The source-drain spacing is 4.5 microns with the source contact length of 15 microns and drain contact length of 30 microns. The 30 microns drain contact is modeled as a 15 microns contact since it is situated halfway between a double-fingered gate. The contacts are constructed with Ti/Al/Ni/Au metal deposition. The gate is constructed with 200 Å nickel and 3800 Å gold and has a 1000 Å SiN passivation layer.

Because of the high thermal conductivity of the diamond, the idea is that the heat will spread away from the device region through the diamond. Figure 10 depicts the basic structure of this device. It illustrates the expected heat flow pattern with the high thermal conductivity diamond deposited close to the device layer.

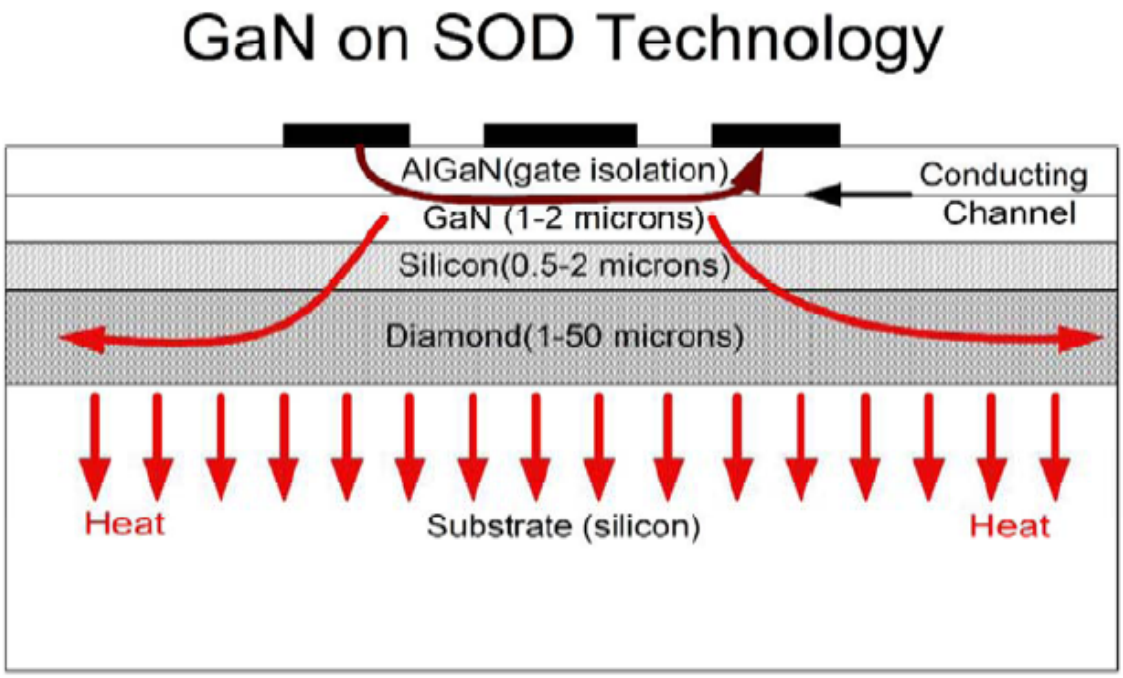

Figure 10. SP3 generic device layers [From 17].

Later we will discuss how this model was modified in the previous thesis in order to explore the DC characteristics of AlGaN/GaN HEMT.

2. Device Testing

Figure 11 shows the drain voltage versus the drain current curves. The two sets of curves represent static DC (the red curve) and pulsed DC (the black curve). The pulsed DC allows DC to be applied to the device, but eliminates most of the heating effects as the device is not constantly heating due to switching on and off. Specifically, the pulsed DC waveform is 200ns with a 1ms period. Notice the peak current with Vgs = +2V is around 0.2A while the knee of the curve begins around Vds = 4V. Figure 12 describes the device of Gm versus V_{ds} .

The transient nature of the pulsed-IV data with investigation of Method 3104 allows us to study transient thermal effects in GaN HEMTs.

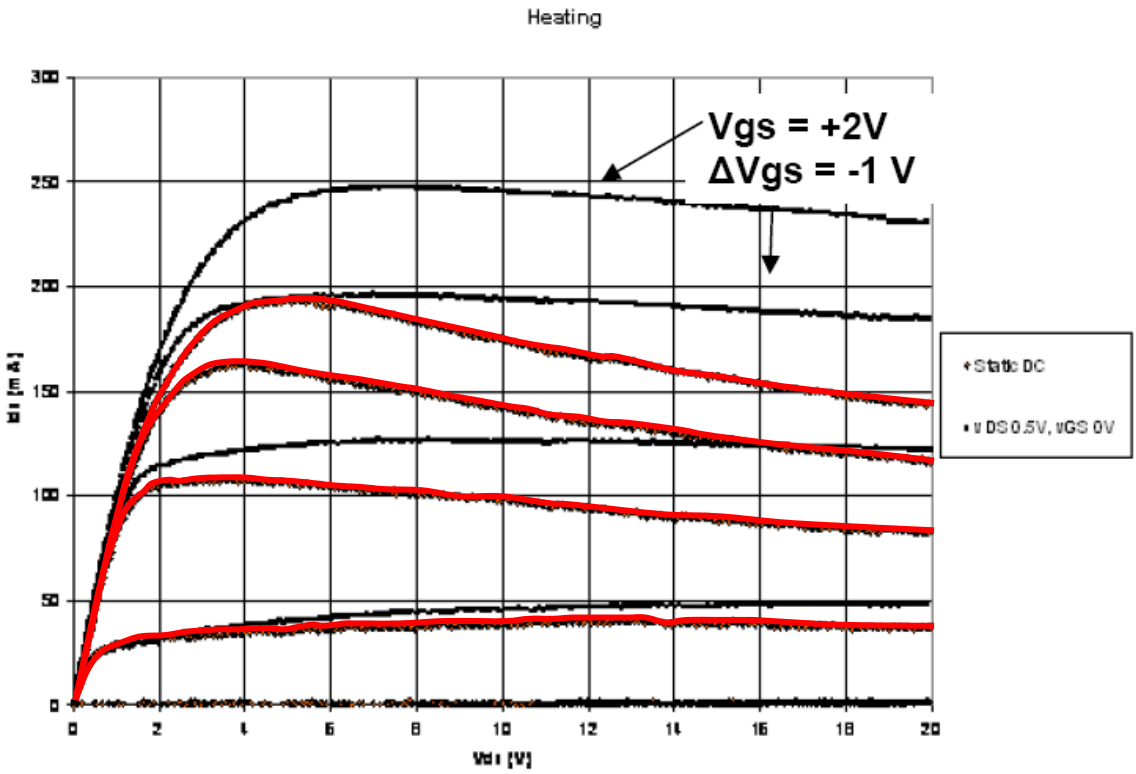

Figure 11. V_{ds} vs. I_d curves for SP3 device [From 8].

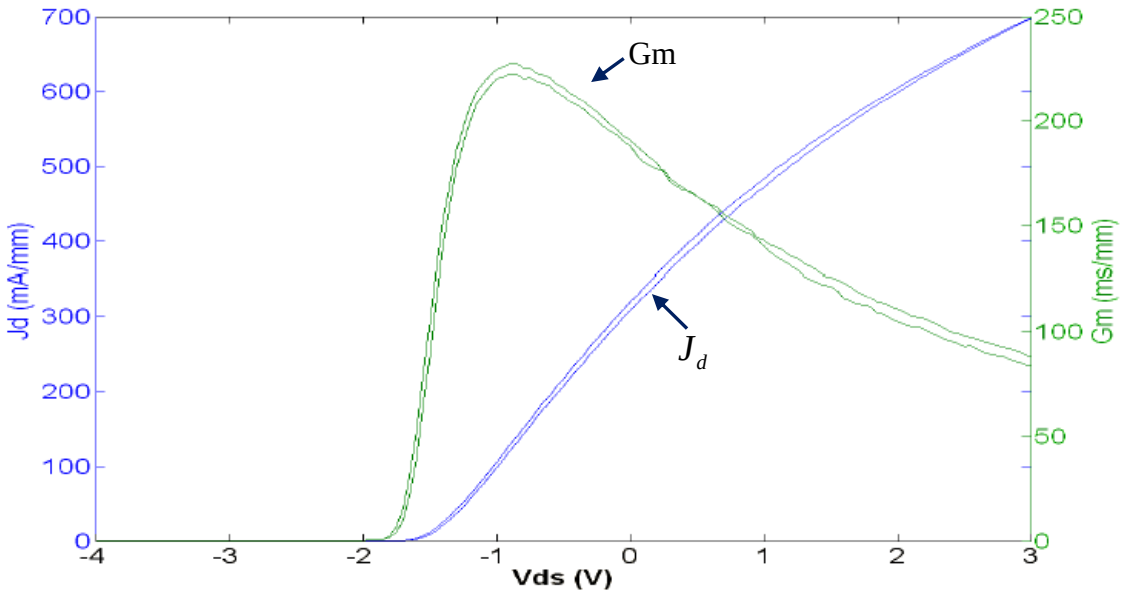

Figure 12. V_{ds} vs. J_d curves for SP3 device [From 8].

THIS PAGE INTENTIONALLY LEFT BLANK

III. METHOD 3104 OF MIL-STD-750D

The military standard, MIL-STD 750D, is designed by Department of Defense. It establishes uniform methods for testing semiconductor devices, including basic environmental tests to determine resistance to deleterious effects of natural elements and conditions surrounding military operations, and physical and electrical tests. The Method 3104 [13], one of the test methods, is originally designed to measure the thermal resistance of GaAs MESFETs. In this thesis, we used the Method 3104 of MIL-STD 750D to measure the thermal resistance of the AlGaN/GaN HEMT and most importantly to determine the location of the HEMT structure that the gate voltage measurement relates to.

We now describe the method 3104 as in the following section.

A. APPARATUS

The test circuit shown on Figure 13 consists of a DUT (Device Under Test), a voltage source (V_H), a current source (I_M), and an electronic switch (S_1). The forward-biased gate–source junction diode voltage (V_{GSf}) is used as a Temperature-Sensitive Parameter (TSP).

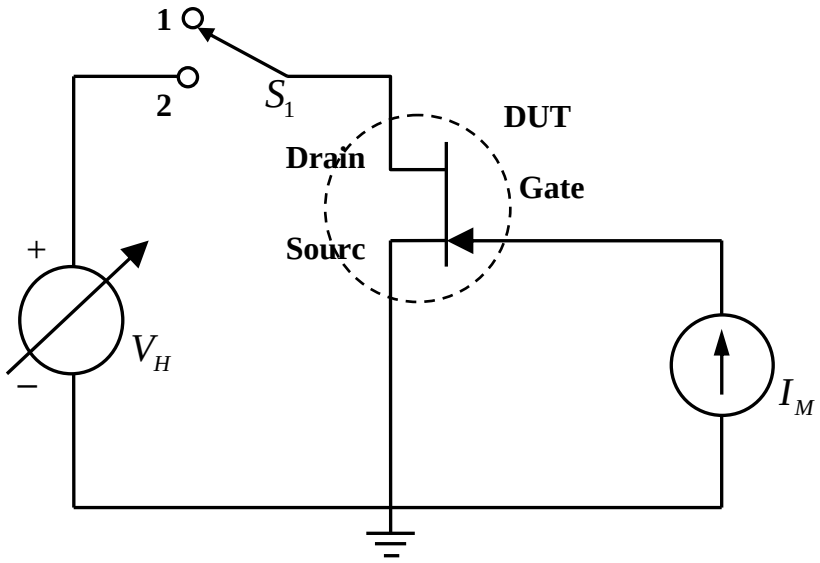

Figure 13. Thermal resistance measurement circuit.

B. CALIBRATION

From MIL-HBK-217, during the calibration phase, the S_1 switch is open (in position 1). A constant forward current, I_M, flows through the gate-source diode. In the experiment the DUT has to be placed in a temperature controlled environment able to keep the device temperature constant within ± 1 K during the calibration procedure, and the case reference temperature has to be measured using a thermocouple with accuracy of ± 0.5 K. Following with the various ambient temperatures, the corresponding V_{GSf} and the junction temperature T_J are recorded with resolution of at least 1mV for V_{GSf}. The plot of the measured V_{GSf} values versus T_J values is the calibration curve. I_M should be chosen so that V_{GSf} is a linearly decreasing function over the expected T_J range. I_M must be large enough to ensure that the gate-source junction is turned on but not large enough to cause significant self-heating or device destruction. An example calibration curve is shown on Figure 14.

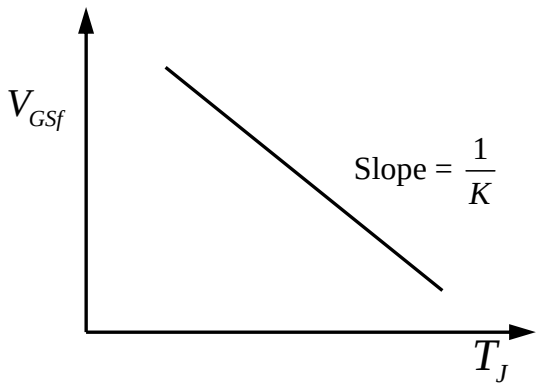

Figure 14. Calibration Curve.

A calibration factor K (which is the reciprocal of the slope of the curve on Figure 14) can be defined as:

$$K = \left| \frac{T_{J1} - T_{J2}}{V_{GSf1} - V_{GSf2}} \right| {}^{o}c / mV \tag{3}$$

It has been found, experimentally, that the K factor should vary less than several % for all devices within a given device type class. The usual procedure is to perform a K factor calibration on a 10 to 12 piece sample from a device lot and determine the average K and standard deviation (σ). If σ is less than or equal to 3 % of the average value of K, then the average value of K can be used for all devices within the lot. If σ is greater than the average value of K, then all the devices in the lot should be calibrated and the individual values of K should be used in thermal resistance calculations.

C. MEASUREMENT

During the measurement phase, the current source I_M and the voltage source V_H are kept constant. A heating pulse with heating time t_H will be generated by switching the switch S_1. And a reference point temperature T_X is established in order to modify the procedure or correct the value of the thermal resistance in the next phase. The reference point is usually chosen to be on the bottom of the transistor case directly below the semiconductor chip. Reference temperature point location must be specified and its

temperature should be monitored using the thermocouple with the accuracy $\pm 0.5^0 C$. If it is ascertained that T_{Xf} increases by more than +5°C during the heating power pulse, then either the heating power pulse magnitude must be decreased, the DUT must be mounted in a temperature controlled heat sink, or the calculated value of thermal resistance must be corrected to take into account the thermal resistance associated with the temperature rise of the reference point.

The measurement phase consists of three segments described as below. And Figure 15 shows the waveforms associated with the three segments of the measurement.

1. Prior to the Heating Pulse

The switch S_1 is open (in position 1). This disconnects the V_H source and allows for the measurement of $V_{GSf(i)}$ and T_{Xi} before the heating pulse.

2. During the Heating Pulse

The switch S_1 is switched to position 2. This generates a heating pulse and allows for the measurement of drain heating current I_H. The time width of the heating pulse is noted as t_H .The T_{Xf} is measured at the end of the heating pulse.

3. Post Heating Pulse

The switch S_1 is switched back to position 1 to disconnect the V_H source and allow for the measurement of $V_{GSf(f)}$ after the heating pulse.

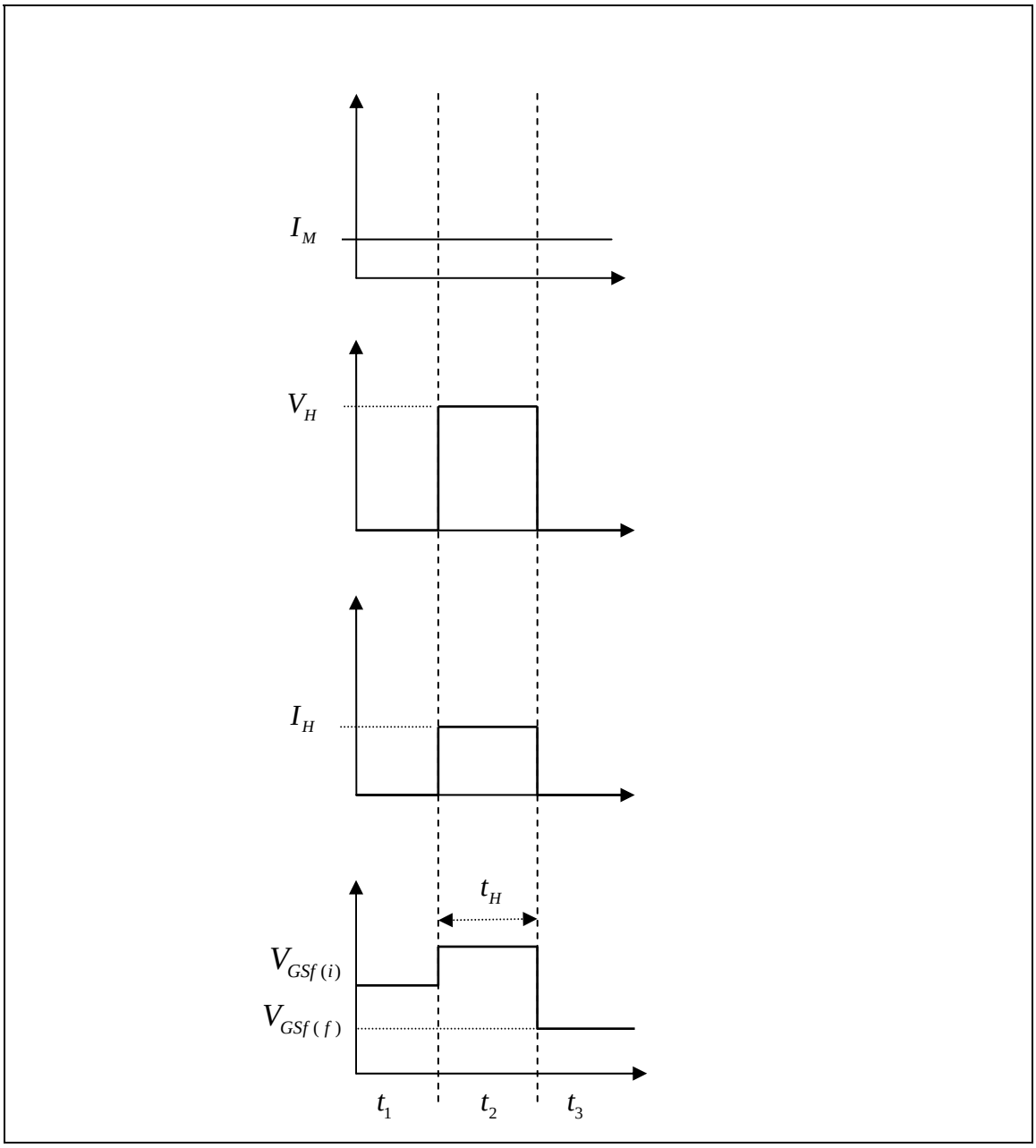

Figure 15. Device waveforms during the three segments of the measurement.

D. CALCULATION OF THERMAL RESISTANCE

The value of thermal resistance, R_{TH}, is calculated from the following formula:

$$R_{TH} = \frac{\Delta T_J}{P_H} = \frac{K\left|V_{GSf(f)} - V_{GSf(i)}\right|}{I_H \times V_H} \tag{4}$$

This value of thermal resistance will have to be corrected if T_{Xf} is greater than T_{Xi}. The correction consists of subtracting out the component of thermal resistance due to the heat flow path from the reference point (typically the device case) to the heat sink and the environment. This thermal resistance component has a value calculated as follows:

$$R_X = \frac{\Delta T_X}{P_H} = \frac{T_{Xf} - T_{Xi}}{I_H \times V_H} \tag{5}$$

Then the corrected thermal resistance will be as follows:

$$R'_{TH} = R_{TH} - R_X \tag{6}$$

Later, we will discuss how to utilize the MIL-STD -Method 3104 to set up the simulation and to calculate the virtual thermal resistance with Silvaco Atlas© simulation tool.

IV. TRANSIENT MODEL OF ALGAN/GAN HEMT

A. MODEL DEVELOPMENT

1. Using Thermal Contact and Albrecht's Model

In the previous Naval Postgraduate School research, McGlone's thesis [8], a model was built to study the DC characteristics of AlGaN/GaN HEMT. The model was modified from Berkeley device in order to incorporate the characteristics of the AFRL device. First, the Y.MIN parameter in the AlGaN region statement and the Y.MAX parameter in the GaN region statement were removed to simulate the abrupt heterojunction between two materials of different bandgaps. Further modifying the structure, the SOD and AlN layers were added to the device meshing to begin simulating the sp3 device. And the 400 micron thick silicon layer was removed and being instead of a thermal contact in order to avoid slowing the simulation due to the meshing in the large Silicon region. The simulated structure is shown in Figure 16 and Figure 17. According to McGlone's simulation result, the replacement of the thermal contact would result in the identical temperature profile and IV curve as shown on Figure 18 and Figure 19.

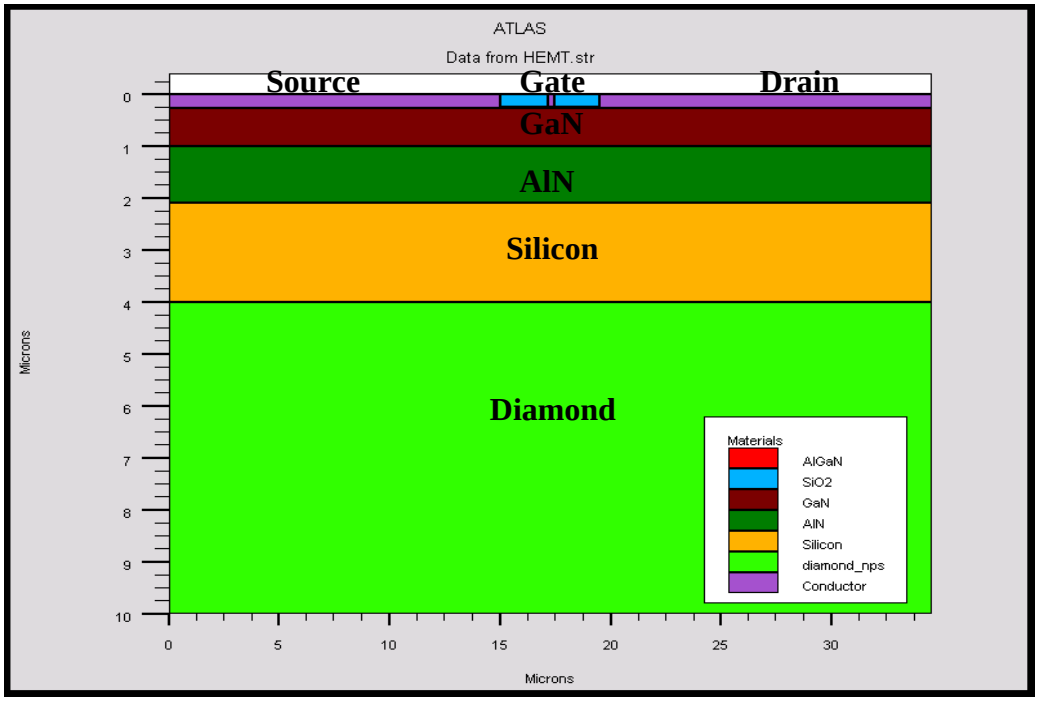

Figure 16. The 2D Structure Plot of AlGaN/GaN HEMT.

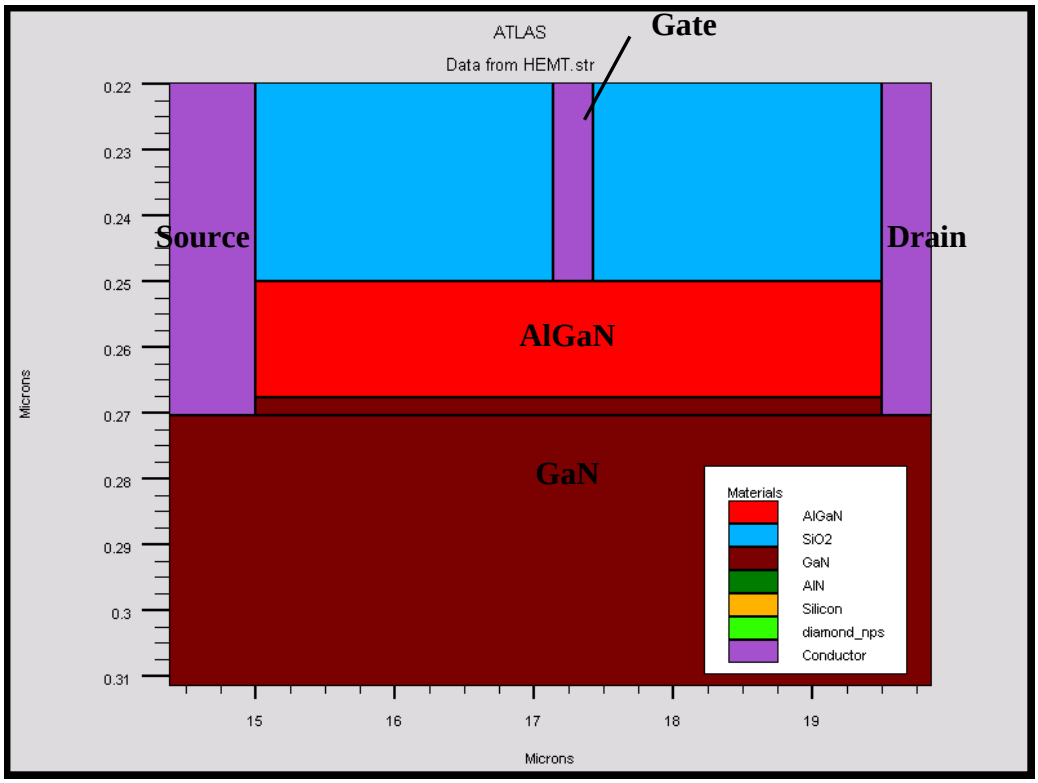

Figure 17. Electrodes and Heterostructure.

In Figure 18, the left one is with silicon layer and the right one is replaced with Thermal resistance.

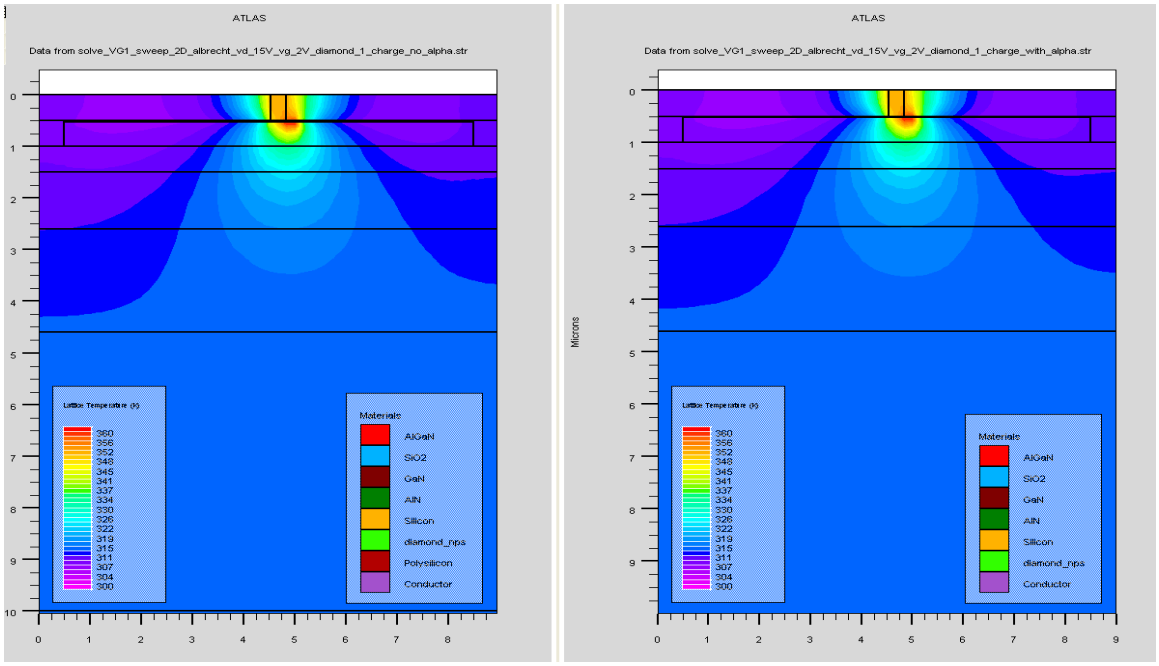

Figure 18. Comparison of with Silicon Layer and with Thermal resistance [From 8].

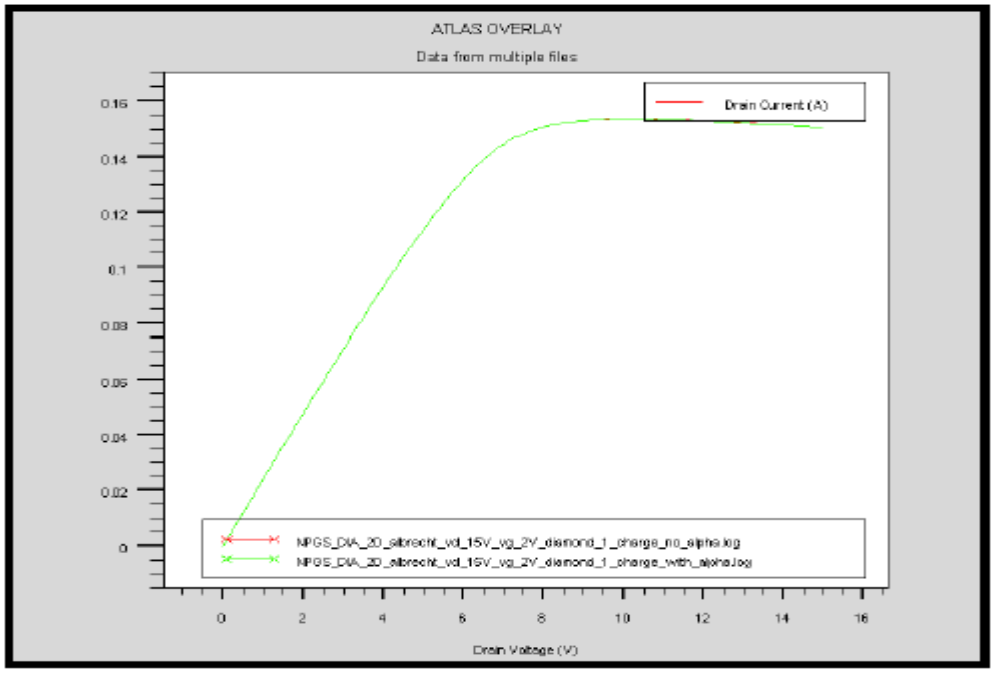

Figure 19. I-V curves. [From 8].

In the previous thesis, the Low Field Mobility Model chosen to simulate the device operation was Albrecht's model. It is a doping and temperature dependent low field mobility model. It determines the low field mobility is mostly affected by temperature, ionized impurity and compensation ratio dependences of the drift mobility in bulk GaN. The effects of applying various parameters of Albrecht's model and the comparison with high field mobility model have been further discussed in Gibson's thesis [13] and McGlone's thesis [8] respectively.

In this thesis, we will continue to use the same structure and the same model in the simulation.

2. Transient Pulse

Based on the previous model structure, we are going to build a transient simulation from the earlier DC simulations. Afterward, the modeling would be used to do the simulations of method 3104 first and to study other transient analysis later.

a. MixedMode Simulator

In Silvaco© software, there are various simulators for different purposes. In order to simulate the pulsed wave, we first chose MixedMode simulator to generate the pulsed input. MixedMode is a circuit simulator that can include elements simulated using device simulation, as well as compact circuit models. The statement of MixedMode can be easily implemented to the input file to replace the "solve" statement. As shown in Appendix A., in the first part of the statement we started with the SPICE-like input file to describe the circuit and specified the device "ahemt" which was indicated as the structure saved at first. Then the second part was used to define physical models, material parameters, and numerical methods for the device. All statements specifying the device properties and models were just supplemented by the "device=ahemt" parameter.

Using MixedMode to describe the circuit and to generate the pulsed wave is much easier than using "solve" statements in Atlas©. And another beneficial is the structure plot files can be automatically saved into the solution file and you just need to specify how many time steps to save a file by using the "write" parameter. However, we

encountered a convergence problem of applying a constant gate current in the simulation. After meeting with Silvaco's engineers, we accept their recommendation to use "solve" statement in Atlas© to generate the pulsed wave in the simulation rather than MixedMode.

b. Atlas

Atlas© is a physically-based two and three dimensional device simulator. It predicts the electrical behavior of specified semiconductor structures and provides insight into the internal physical mechanisms associated with device operation.

To generate a pulsed wave, we ramped the drain voltage by using the "solve" statement in Atlas©. As described in method 3104, a constant gate current supply is needed rather than a gate voltage. Therefore, we used the "contact" parameter to change the gate electrode to current control and to supply a constant gate current. Different from McGlone's model, we set the distributed contact resistance of the source and the drain electrodes as zero and used "Newton" method instead of "Block" in order to avoid the convergence problem we encountered in transient modeling. We also added the material statement for Silicon in order to activate the temperature-dependent thermal conductivity model and the temperature-dependent heat capacity model for Silicon and modified the material statement for AlGaN activate the the temperature-dependent heat capacity model for AlGaN. The difference between with and without specifying these thermal conductivity and heat capacity models for Silicon and AlGaN is shown on Figure 20 and Figure 21.

In both figures, it can be seen that the drain current and the temperature of with specifying are slightly lower than without specifying. The maximum difference of drain current is 9 mA and the maximum difference of temperature is 1.4 ^{o}C

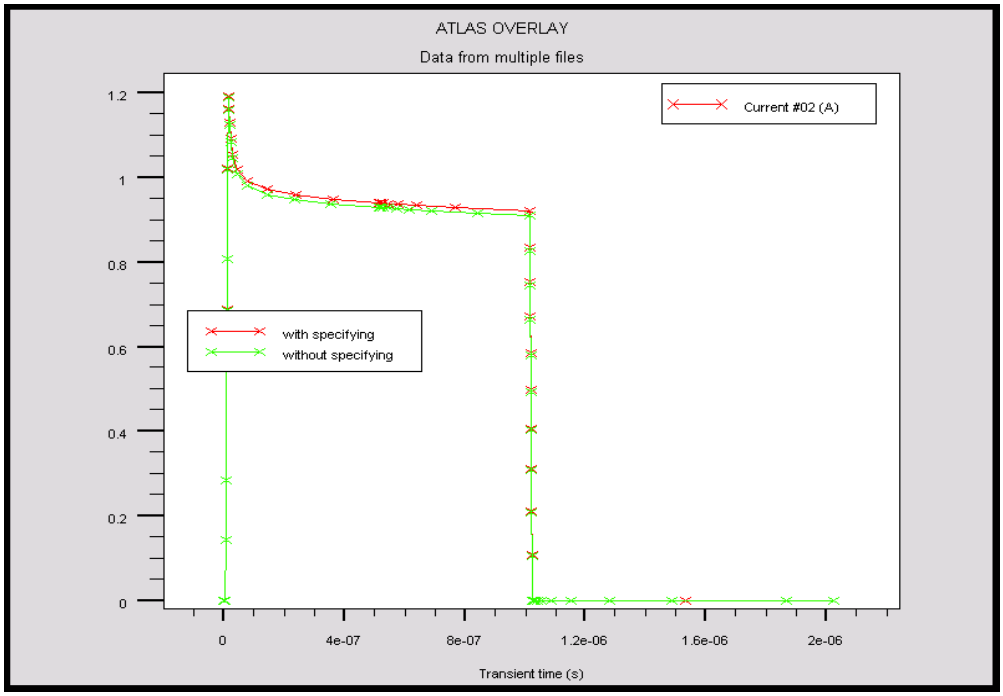

Figure 20. Comparison of drain current.

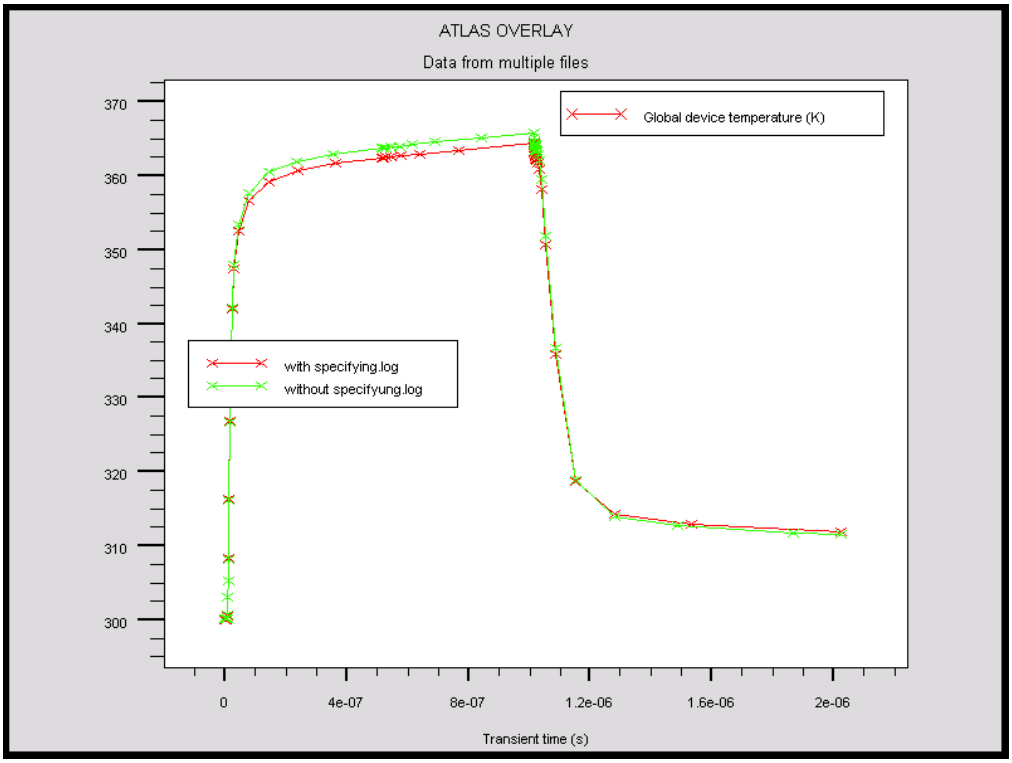

Figure 21. Comparison of temperature.

B. SIMULATION OF MIL-STD 750D METHOD 3104

1. K factor Calibration Setup

In this simulation, we used the AlGaN/GaN HEMT structure as shown in Figure 16 previously. In order to extract the thermal resistance, we first set up the K factor calibration. We set both of the drain current and the drain voltage as zero and only applied a constant gate current I_M = 0.01 mA, flows through the gate-source diode. Then we ramped the ambient temperature from 300 K to 360 K to obtain the corresponding values of V_{GSf} and T_J which can be read from the plot generated by Tonyplot as shown in Figure 22. Finally, we could use Equation (3) to calculate out the average value of K factor is 436.93 (^{o}C/V).

It should be noted that ramping the ambient temperature requires to set the same temperature in the "Model" statement and the "Thermcontact" statement in Atlas©. In this simulation, we also needed to use the "Probe" parameter to extract the junction temperature. However the junction temperature was exactly the same with the Global device temperature in this simulation.

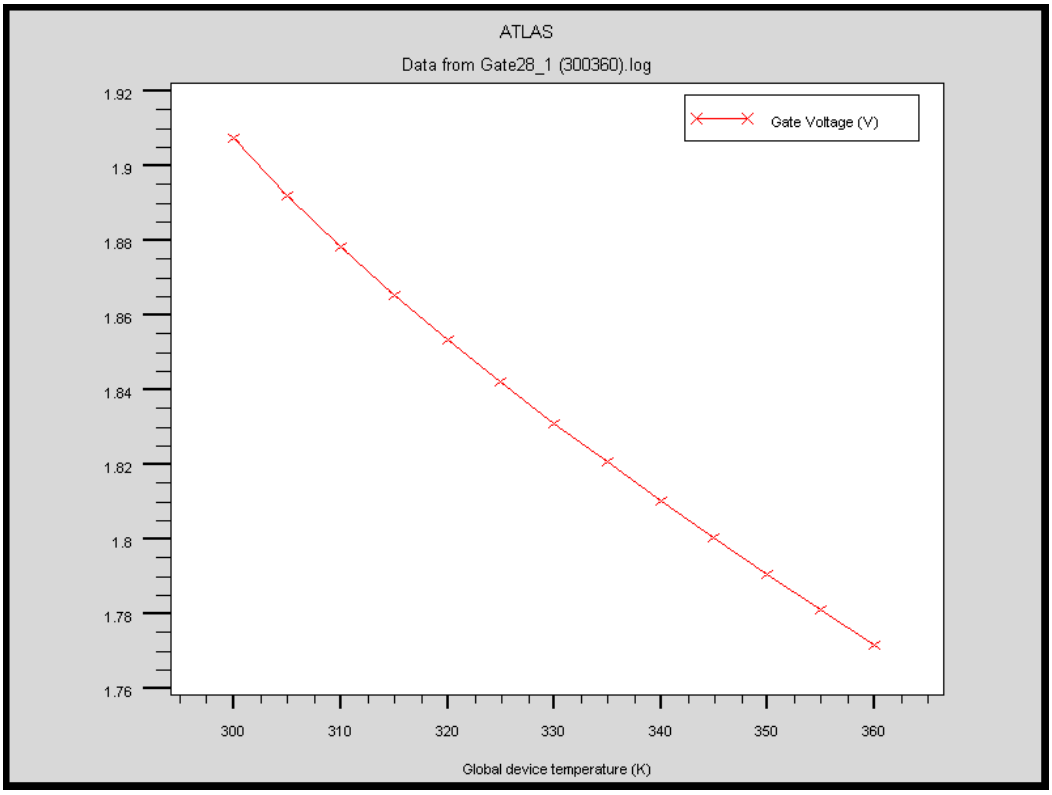

Figure 22. Gate voltage vs. Temperature.

2. Extracting the Thermal Resistance

After obtaining the K factor, we were going to simulate the measurement phase. In this phase, we kept the external temperature at 300 K and applied the same constant gate current I_M =0.01 mA and a drain voltage pulse V_H =10 V with rise time t_r = 10 ns, fall time t_f = 10 ns and pulse time t_H = 0.1ms as shown in Figure 23. Then we read the value of $V_{GSf(i)}$ in the beginning of the pulse and the value of $V_{GSf(f)}$ in the end of the pulse from the tonyplot as shown in Figure 24. Then we could use Equation (4) to calculate out the thermal resistance of the AlGaN/GaN HEMT device:

$$R_{Th} = \frac{K\left|V_{GSf(f)} - V_{GSf(i)}\right|}{I_H \times V_H} = \frac{436.93\left|1.6334 - 1.9075\right|}{0.685 \times 10} = 17.48(K/W)$$

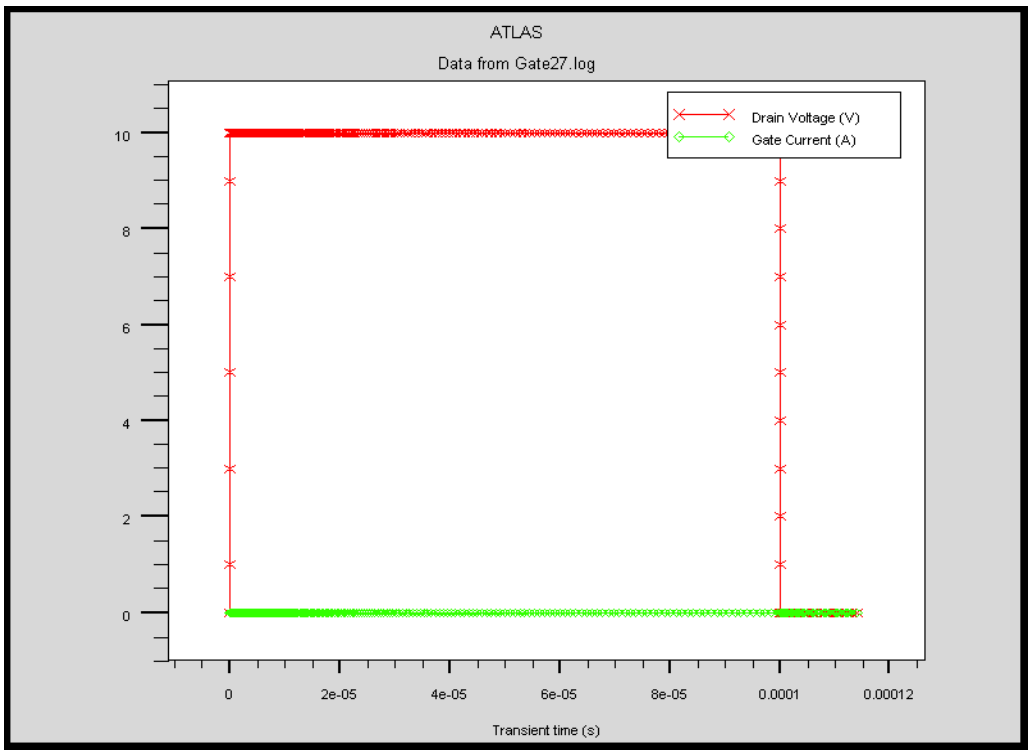

Figure 23. Constant Gate current and Drain Voltage Pulse.

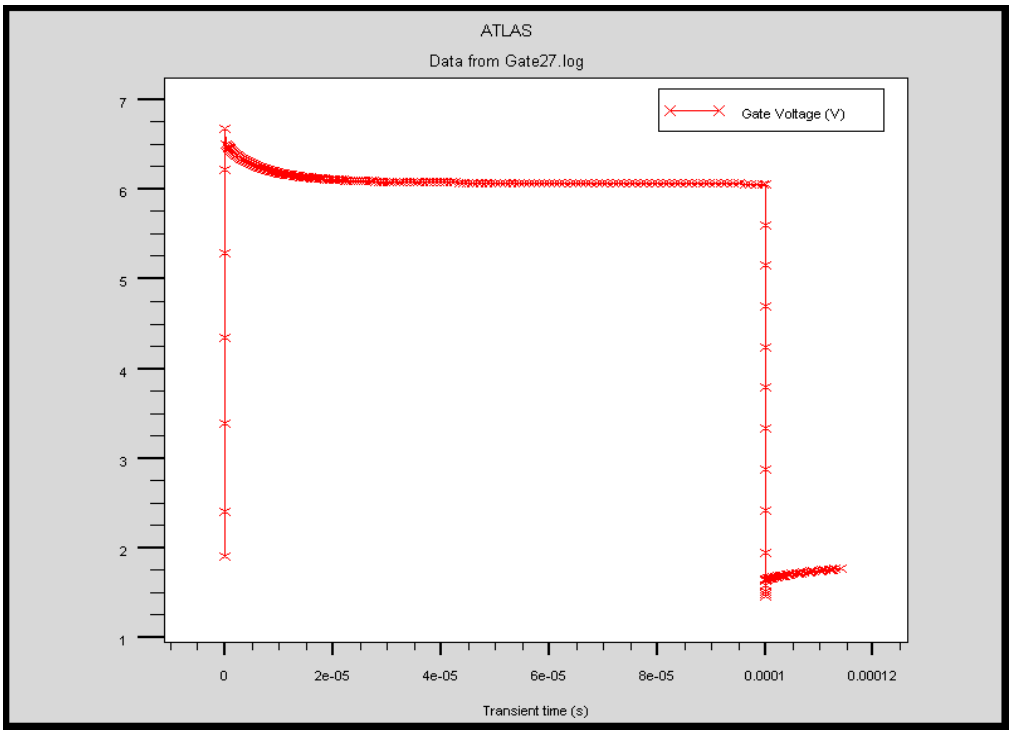

Figure 24. V_G vs. Time (Measurement of $V_{GSf(i)}$ and $V_{GSf(f)}$).

3. Determining the Location of the HEMT Structure that Gate Voltage Measurement Relates to

One of the objectives in this thesis is to verify if Vg changes based on the temperature of a specific area in the HEMT structure. To verify this presumption, first we choose a point at the specified time “a” after the pulse in the previous Figure 24 (Vg vs. Time) and read the corresponding gate voltage value “b”. Then we look into the previous Figure 22 (Vg vs. Temperature) and obtain the corresponding temperature ”c” at Vg=b. Finally, we open the structure plot saved at time “a” and find out the spot where the temperature is “c”. The whole process is illustrated in Figure 25.

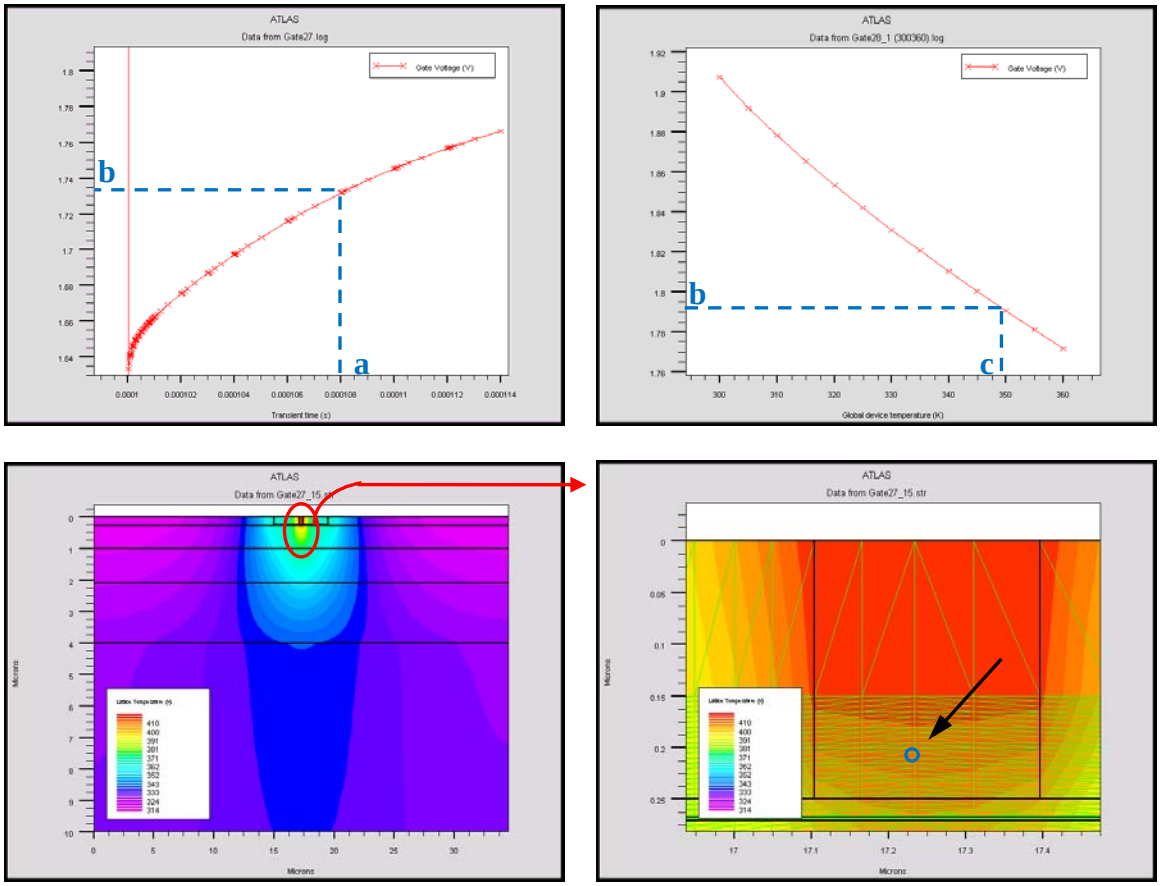

Figure 25. The process of determining the location to which the gate voltage measurement relates.

In Tonyplot, it allows us to use the ”Probe” tool to read the values of the impurity (potential, temperature, electron concentration, electric field and current density…,etc) in a specified location of the structure. The specified location is actually not just one point but a mesh triangle consisted of three points. And the Probe tool will show you the values of the impurity in the three points. Therefore the accuracy of the values depends on how small the mesh triangle is. So it is very important how you define the mesh. Good definition of the mesh will enhance the accuracy. In this simulation we redefined the mesh of the structure to make the mesh triangle in the observed area reduce from $0.00143um^2$ to $0.00019um^2$. (The simulation code is attached as Appendix B.)

We repeated this process for a couple of times at various time points after the pulse to check if all the spots located in a concentrated area inside the structure rather than to spread over the structure widely. Table 7 lists the corresponding temperatures extracted from the structure plot in 1us time length.

a	Time (us)	100.1	100.2	100.3	100.4	100.5	100.6	100.7	100.8	100.9	101
b	Vg (V)	1.641	1.646	1.649	1.652	1.654	1.656	1.657	1.659	1.661	1.662
c	Correspo-nding Temp	**416.7**	**414.4**	**412.9**	**411.9**	**410.9**	**410.1**	**409.3**	**408.6**	**407.9**	**407.2**

Table 7. Gate voltage and the corresponding temperature (short time range).

According to the data of Table 7, we first found that in a short time length, from 100.1us to 101us, and small temperature change, from 416 K to 407 K, the corresponding area could be determined in a small area which is inside the gate electrode as shown in Figure 26. The blue box specifies the corresponding area located in x =17.165 to x=17.31 and y=0.195 to y=0.21 (um).

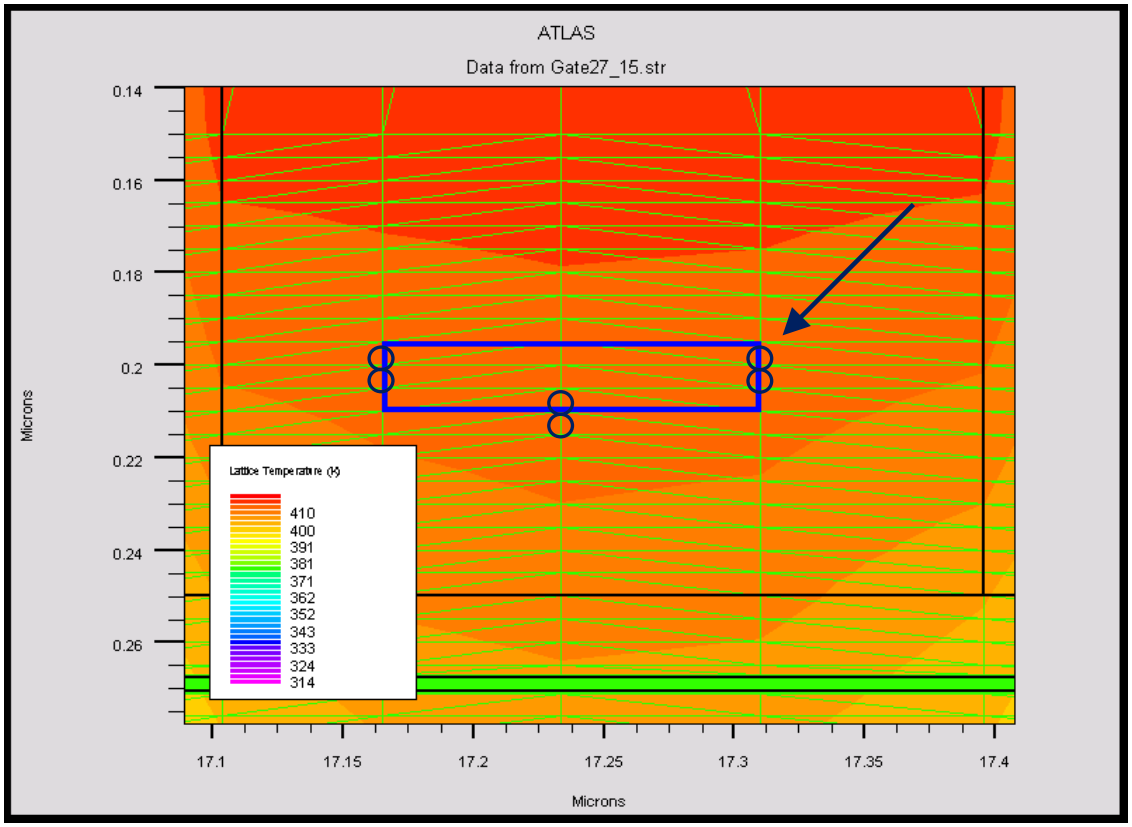

Figure 26. Temperature profile of structure.

However, if we extent the observing time and then extracted the corresponding temperatures as listed in Table 8, we found it would be hard to determine the corresponding area in a specific location. Since the corresponding area was dynamic following the heat retreating away from the gate electrode as show in Figure 27. But we could still conclude that the specific location was inside the gate electrode and above the channel.

a	Time (us)	102	103	104	106	108	110	112	114
b	Vg (V)	1.6752	1.6866	1.6971	1.7158	1.7317	1.7453	1.7567	1.7663
c	Corresponding Temp	**401.5**	**396.5**	**391.9**	**383.8**	**376.8**	**370.9**	**365.9**	**361.7**

Table 8. Gate voltage and the corresponding temperature (long time range).

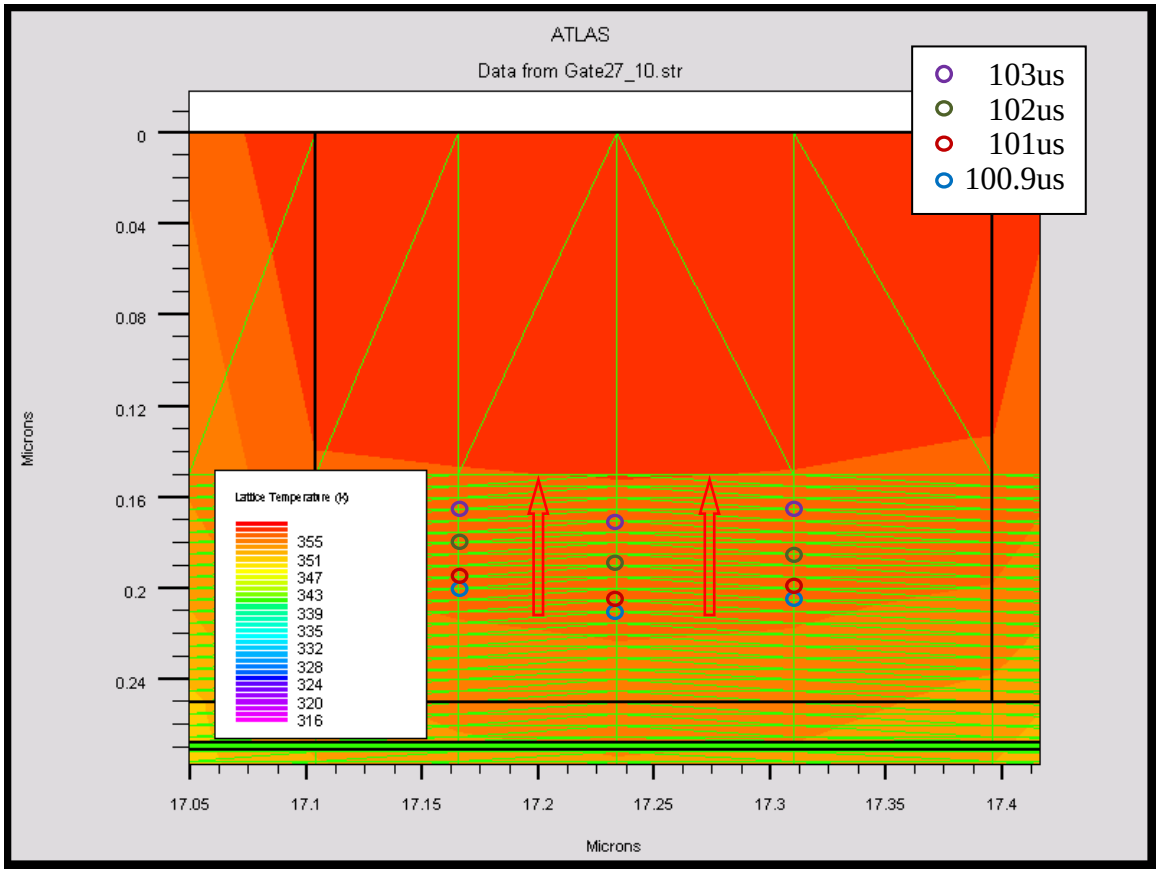

Figure 27. The specific location was dynamic and above the channel.

C. THERMAL RESISTANCE, HEAT CAPACITANCE AND THERMAL TIME CONSTANT FOR EACH LAYER

In order to understand more about the thermal characteristics of the AlGaN/GaN HEMT, we were interested to determine the thermal resistance, heat capacitance and thermal time constant for each material layer.

Since in the Silvaco© software the temperature of each layer does not change with various external temperature as the drain voltage is zero. Therefore, we could not use Method 3104 to set up K factor but simply used the equation "$R_{Th} = \frac{\triangle T}{P}$" to determine the thermal resistance for each layer. We still applied a constant gate current I_M =0.01

mA and a drain voltage pulse V_H =10 V with pulse time 1ms and used the “Probe” and “Extract” parameters to obtain the temperature curves for each material layer as shown in Figure 28.

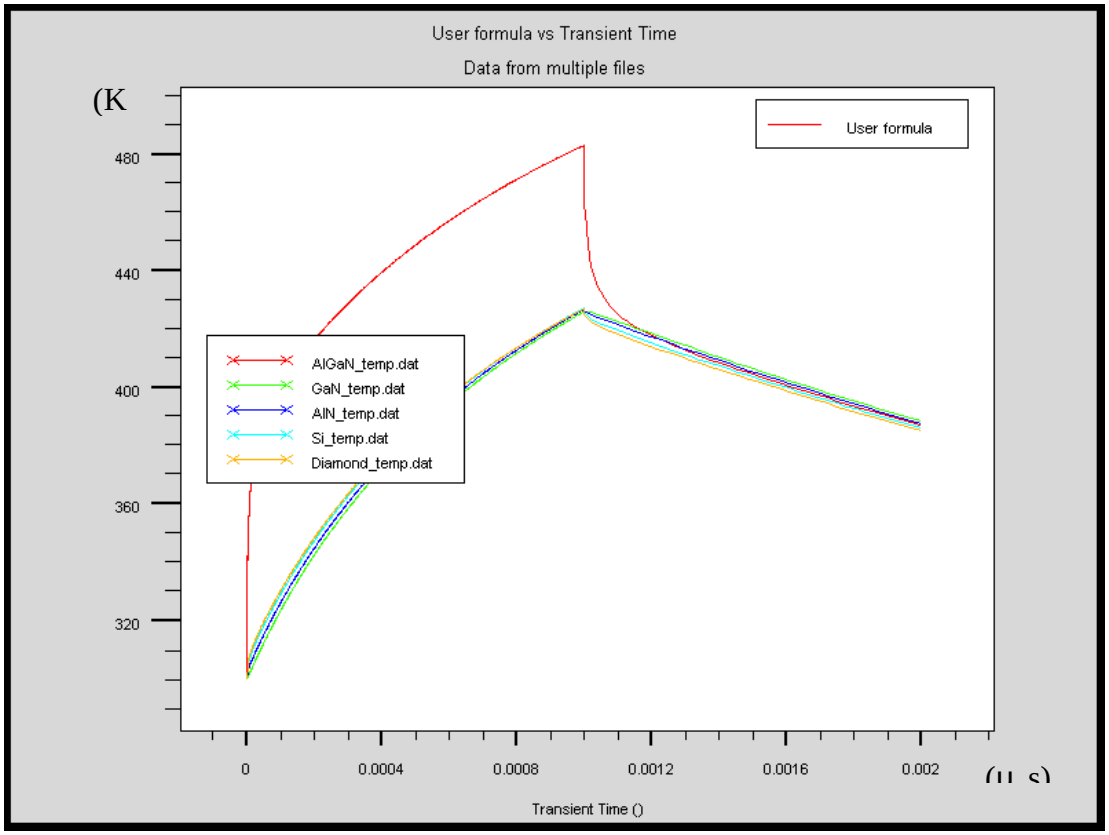

Figure 28. Temperature for each material Layer.

In Figure 28, it can be seen that the temperature curves for GaN , AlN ,Silicon and Diamond are very close but AlGaN seems have a larger heat capacitance and a slow time constant to hold much more heat and to hold it longer.

The thermal resistance, heat capacitance and thermal time constant for each material layer was calculated as Table 9.

	AlGaN	GaN	AlN	Si	Diamond
Rth (K/W)	3.704E+01	2.549E+01	2.565E+01	2.574E+01	2.569E+01
C (J/K)	2.700E-05	3.923E-05	3.899E-05	3.885E-05	3.893E-05
Tau (s)	2.351E-04	4.449E-04	4.355E-04	4.186E-04	4.077E-04

Table 9. Thermal Resistance, Heat Capacitance and time Constant for each material layer.

THIS PAGE INTENTIONALLY LEFT BLANK

V. THERMAL CHARACTERISTICS OF PULSED WAVE

In the previous chapters, we have used a single drain voltage pulse and Method 3104 to discuss the thermal resistance, thermal time constant and heat capacitance of AlGaN/GaN HEMT. In this chapter, we will discuss more about the electrical and thermal performance of AlGaN/GaN HEMT under the multiple pulses and also compare with DC modeling in various conditions.

A. MULTIPLE PULSES

Basically we generated 10 pulses, 50 pulses and 120 pulses with the same applied constant gate voltage at 3V and the same peak value of drain voltage at 10V and then compared the performance between them. All of them have the same pulse duration of $2\,us$ and duty cycle of 50%. The simulation code for 10 pulses is attached as Appendix C.

1. 10 Pulses

The drain voltage and drain current is shown in Figure 29.

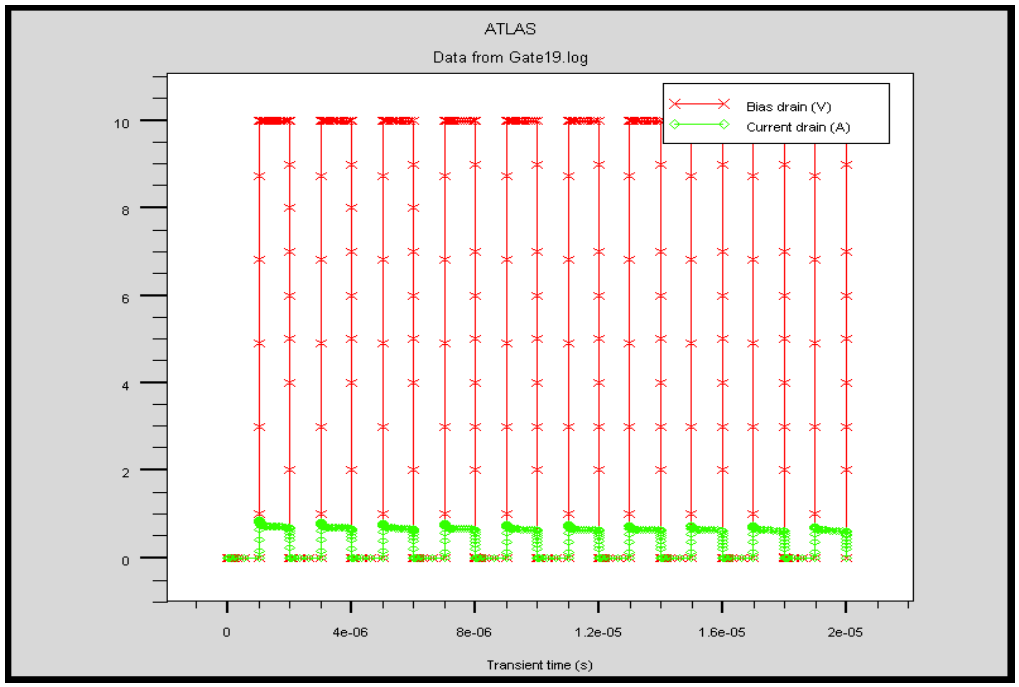

Figure 29. V_d vs I_d.

In Figure 30, the temperature of the pulsed wave rose from 300 K up above 350 K very fast in the beginning, then increased slowly until it achieved the local maximum temperature. After the local maximum, the temperature started to decrease until the beginning of the next pulse. Finally, the temperature achieved the maximum in the end of the pulsed wave. The maximum temperature of the 1st pulse is 354.1 K and the maximum temperature of the 10th pulse is 374.62 K, 105.8% of the 1st pulse. The local maximum temperature increases 5.8% during 20us. If we point out every local maximum and draw a line to connect them together linearly, it can be clearly observed that the temperature increased less and less as the time was getting longer.

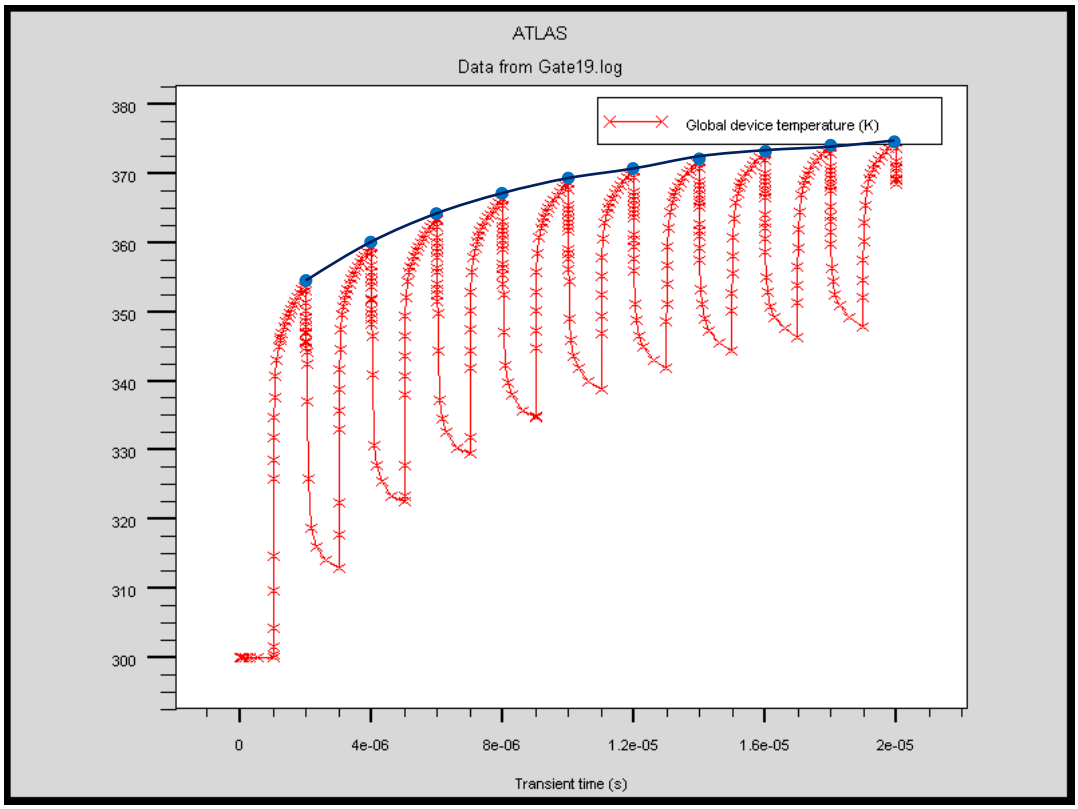

Figure 30. Device temperature of 10 pulses.

Besides the temperature, we are also interested in the performance of the drain current. In Figure 31, it can be seen that the drain current decreased with time due to the increasing temperature in each pulse and has the minimum value in the end of the 10th pulse where the temperature has the maximum value.

The average drain current of the 1st pulse is calculated as 0.714A and the average drain current of the 10th pulse is 0.624A, 87.4% of the 1st pulse. The drain current average drops 12.6% over 20us. This results in the average power dropping from 3.57 W to 3.12 W. The average power of the whole pulsed wave is 3.27 W.

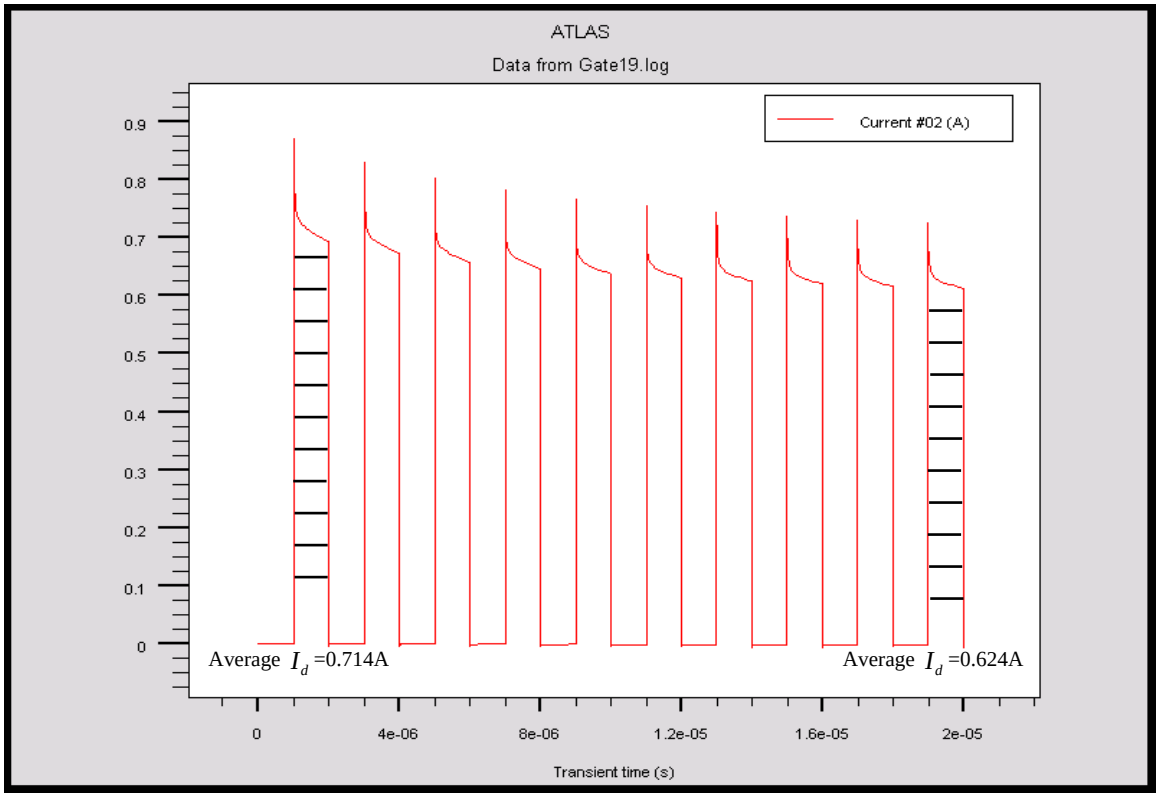

Figure 31. Drain Current of 10 pulses.

2. 50 Pulses

Next, we observed that the performance of a 50 pulses pulsed wave. In Figure32, we observed that the maximum temperature of the 50th pulse is 383.86 K, 108.4% of the 1st pulse. The local maximum temperature increases 8.4% during 0.1ms.

In Figure 33, we obtained the average drain current of the 50th pulse is 0.571A, 80% of the 1st pulse. The drain current averagely drop 20% during 0.1ms.This also result in that the average power drops from 3.57 W to 2.855 W. The average power of the whole pulsed wave is 3 W.

As a result, the local maximum temperature increases 5.8% in the first 10 pulses and only increases 2.6% in the post 40 pulses. The average drain current drops 12.6% in the 10 pulses and only drops 7.4% in the post 40 pulses. The average power decreases 0.45 W in the first 10 pulses and 0.265 W in the post 40 pulses.

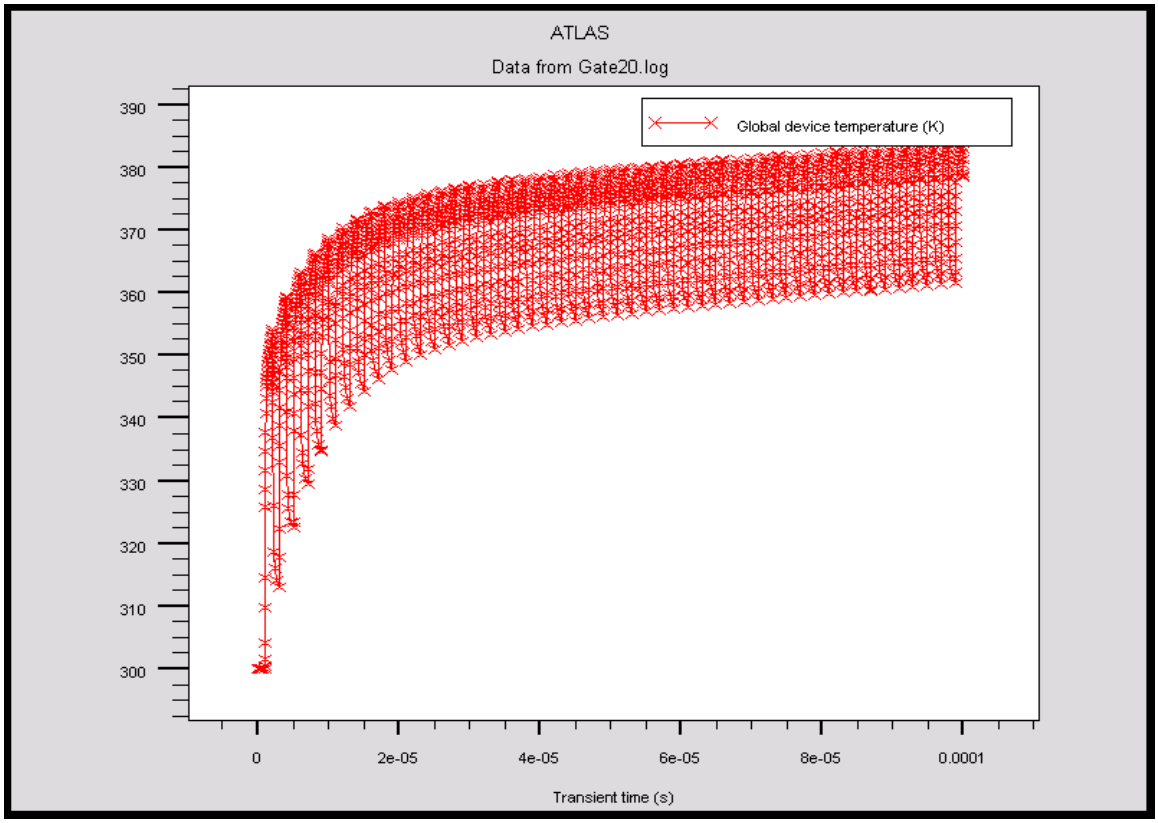

Figure 32. Device temperature of 50 pulses.

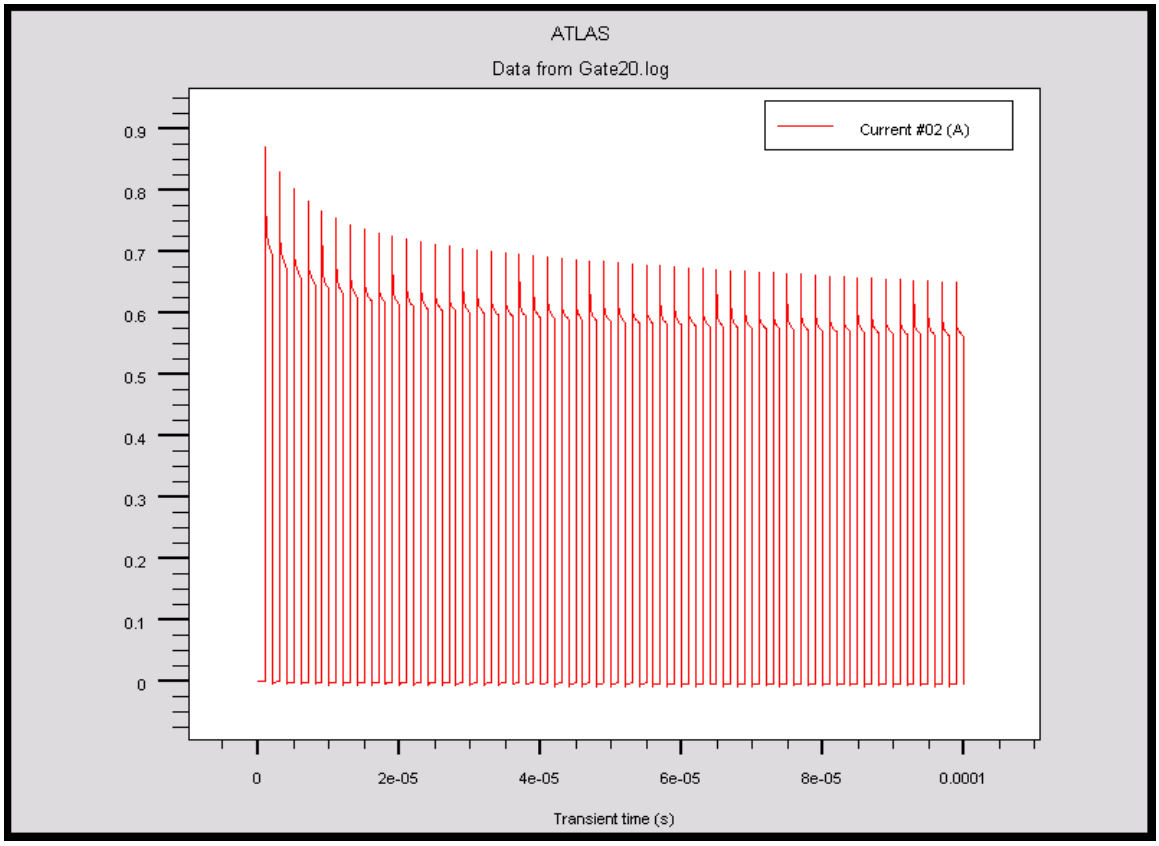

Figure 33. Drain current of 50 pulses.

3. 120 Pulses

When we extend the pulsed wave to 0.1ms with 120 pulses, it can be observed more obviously how the temperature increased less and less with time as well as how the average drain current decreased less and less with the temperature.

The local maximum temperature of 120th pulse is 392.54 K, 110.86% of the 1st pulse. The average drain current of 120th pulse is 0.527A, 73.8% of the 1st pulse.

As a result, the local maximum temperature increases 5.06% in the past 110 pulses and the average drain current drops 13.6%.

The result data of the 10, 50 and 120 pulses is listed in Table 10.

	1st pulse	10 Pulses (20us)	50 Pulses (0.1ms)	120 Pulses (0.24ms)
T_{max} (K) (local maximum temperature of the last pulse)	354.1	374.62	383.86	392.54
I_d (A) (average drain current of the last pulse)	0.714	0.624	0.571	0.527
T_{max} Increment (%) Compared with 1st pulse		5.8	8.4	10.86
I_d Decrement (%) Compared with 1st pulse		12.6	20	26.2
P (Watt) (average power of the last pulse)	3.57	3.12	2.855	2.835

Table 10. Comparison between 10, 50 and 12 pulses.

4. Comparison between External Temperature at 300 K and 400 K

Here, we only increased the external temperature from 300 K to 400 K and observed the changes of the temperature and of the drain current. Then we compared the performance of 10 pulses pulsed wave between the external temperature of 300 K and 400 K.

In Figure 34, we observe that the maximum temperature of 1st pulse is 430.43 K and the temperature of the 10th pulse is 444.7 K, 103.3% of the 1st pulse.

In Figure 35, we observe that the average drain current of 1st pulse is 0.379A and that of the 10th pulse is 0.357A, 94.2% of the 1st pulse. The average power of the whole pulsed wave is 1.73 W.

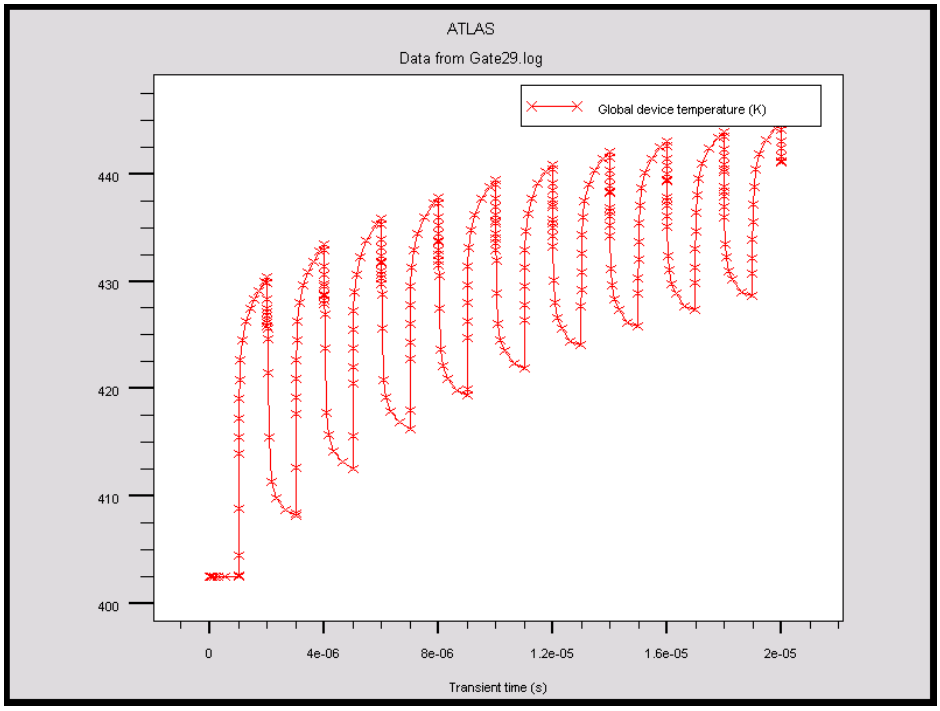

Figure 34. Device temperature of 10 pulses at external temperature of 400 K.

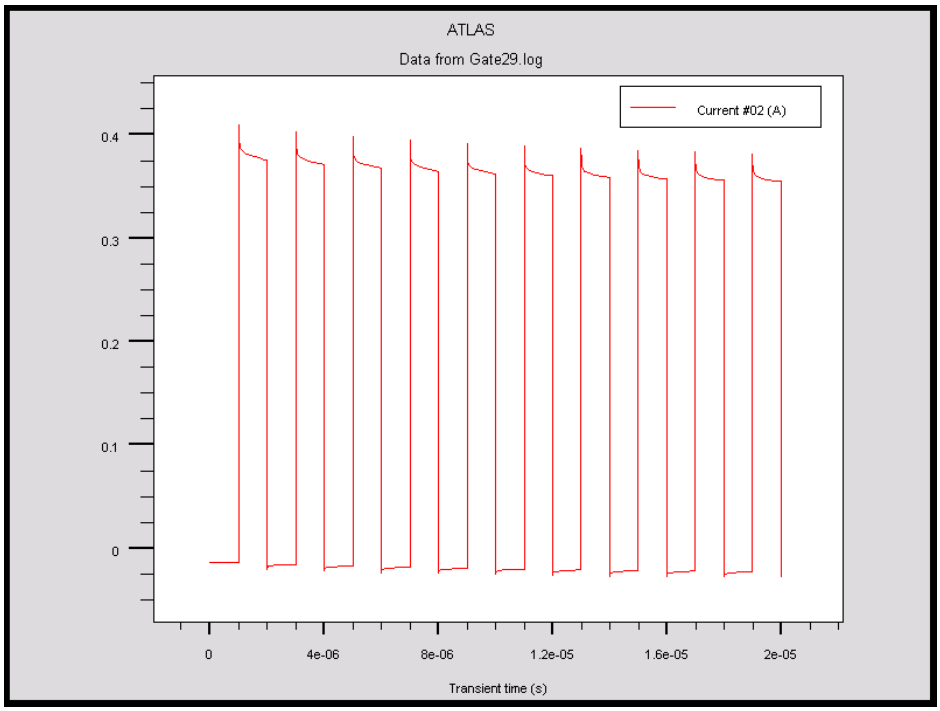

Figure 35. Drain current of 10 pulses at external temperature of 400 K.

External Temperature	300 K		400 K	
	1st pulse	10th pulse	1st pulse	10th pulse
T_{max} (K) (maximum temperature)	354.1	374.62	430.43	444.7
I_d (A) (average drain current)	0.714	0.624	0.379	0.357
T_{max} Increment (%) (compared with the 1st pulse)		**5.8**		**3.3**
I_d Decrement (%) (compared with the 1st pulse)		**12.6**		**5.8**
P (Watt) (average power)	**3.57**	3.12	**1.895**	1.785
Average Power of the whole pulsed wave	**3.27**		**1.73**	

Table 11. Comparison between external temperatures of 300 K and 400 K.

In Table 11, it can be seen that how the external temperature impacted the performance of the transient modeling of the AlGaN/GaN HEMT. The average power of 1st pulse was reduced from 3.57 W to 1.895 W when the external temperature changed from 300 K to 400 K. The average power of the whole pulsed wave was also reduced from 3.27 W to 1.73 W though the T_{max} Increment and I_d Decrement were both lower in external temperature 400 K.

B. SINGLE PULSE AND MULTIPLE PULSES

Here, we compared and discussed the performance between single pulse and multiple pulses. In Figure 36, it can be seen that the operation time of the pulsed wave was 20 us the same with the pulse duration of the single pulse. The maximum temperature of the single pulse was 394.62 K and the maximum temperature of the pulsed wave was 374.62 K.

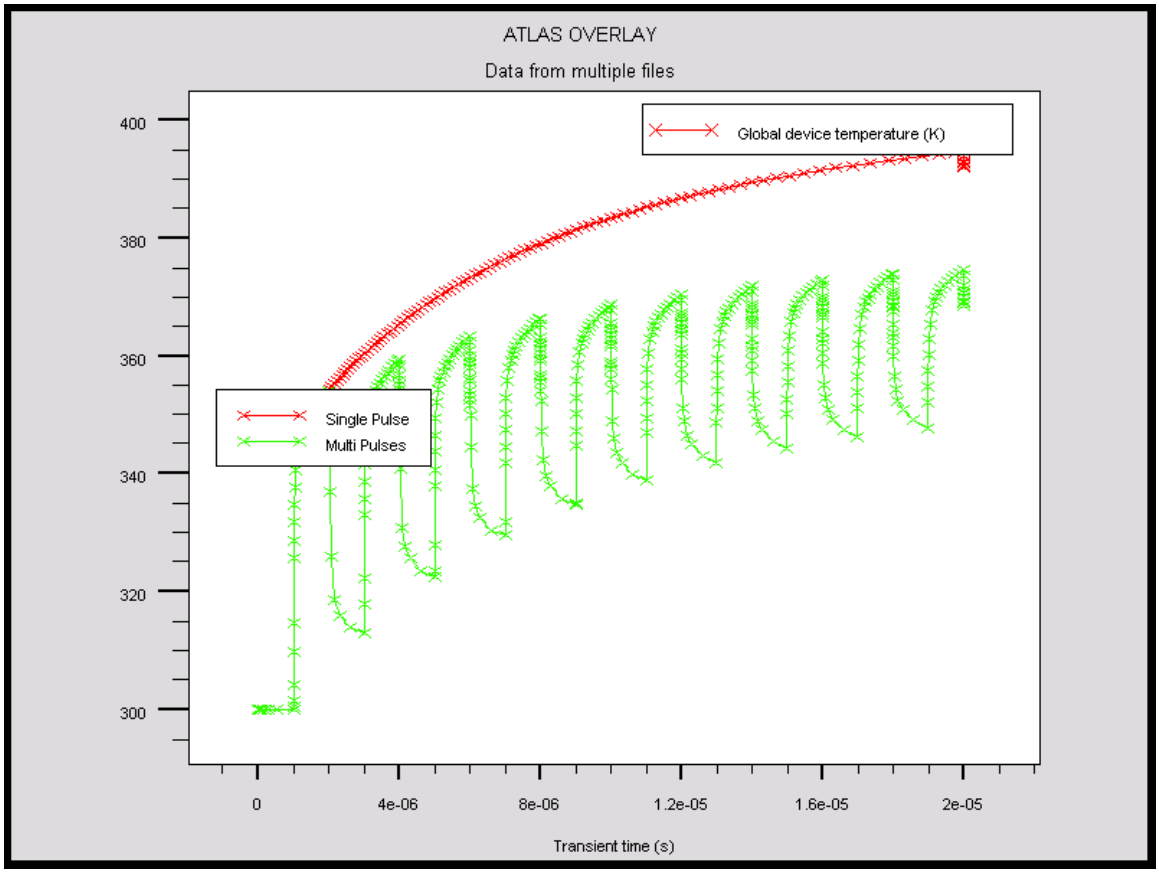

Figure 36. Comparison of temperature between single pulse and multiple pulses.

In Figure 37, it can be readily observed that the peak value of drain current of the single pulse was lower than the pulsed wave and the difference gradually increased with time. The average drain current of the single pulse was calculated as 0.6A and the average peak value of drain current of the pulsed wave was 0.654A. However, the average power of the single pulse was 6 W and the average power of the pulsed wave was only 3.27 W due to its 50% duty cycle.

As a result, the single pulse had the higher maximum temperature of 394.62 K, 105.33% of 374.62 but had a better performance on average power of 6 W, 183.5% of 3.27 W.

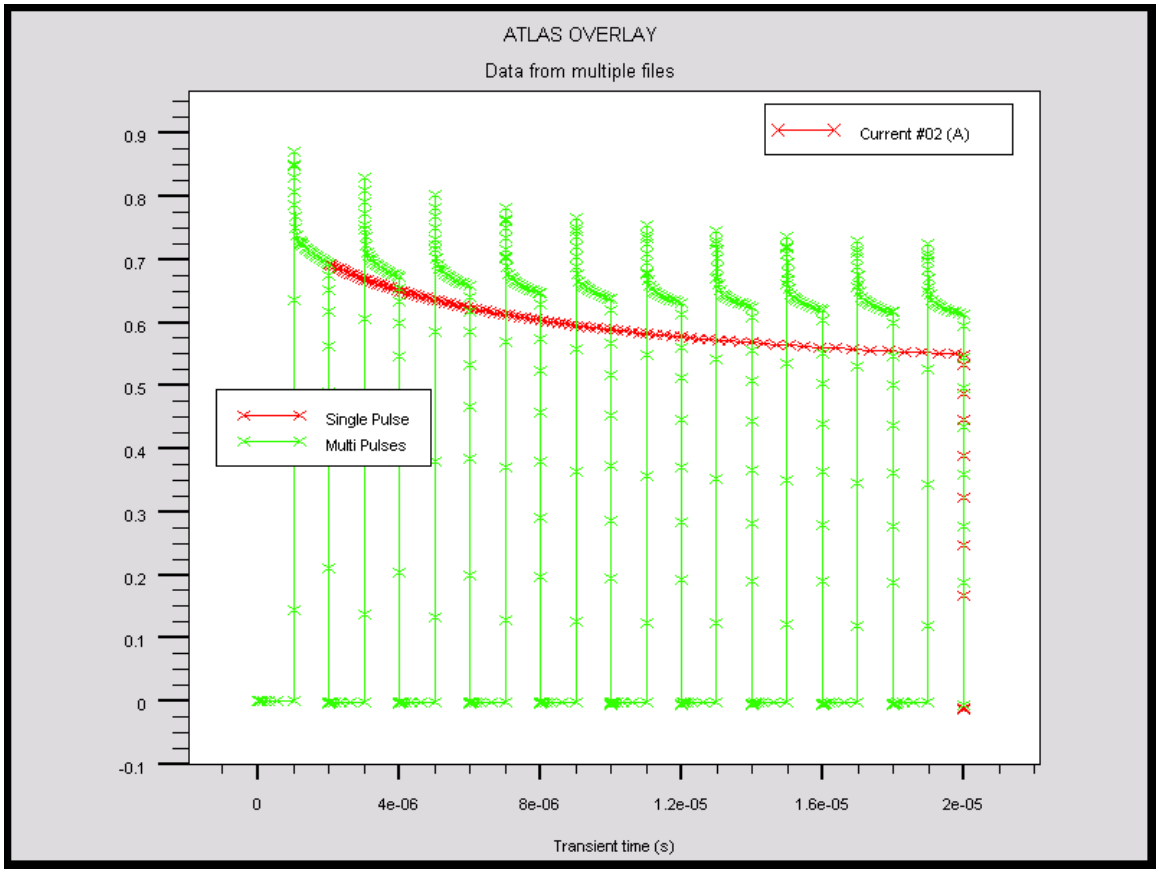

Figure 37. Comparison of drain current between single pulse and multiple pulses.

C. COMPARISON BETWEEN DC MODEL AND TRANSIENT MODEL WITH THE SAME POWER

To compare the performance between DC modeling and the 10 pulses pulsed wave generated previously in Chapter V, A., 1., the DC modeling was modeled with the same power with the 10 pulses pulsed wave. By applying the same constant gate voltage V_g =3V and a proper constant drain voltage 22.6V, the DC modeling had the value of power as 3.267 W which was close to 3.27 W of the 10 pulses average power.

Figure 38 illustrated I_d vs. V_d and T vs. V_d in DC modeling. In Figure 38, it can be seen that the saturation value of drain current was 0.217A and the knee voltage was 5.9V. The temperature increased approximately linearly when the drain voltage was greater than the knee voltage and finally rose up to the maximum value 630.76 K.

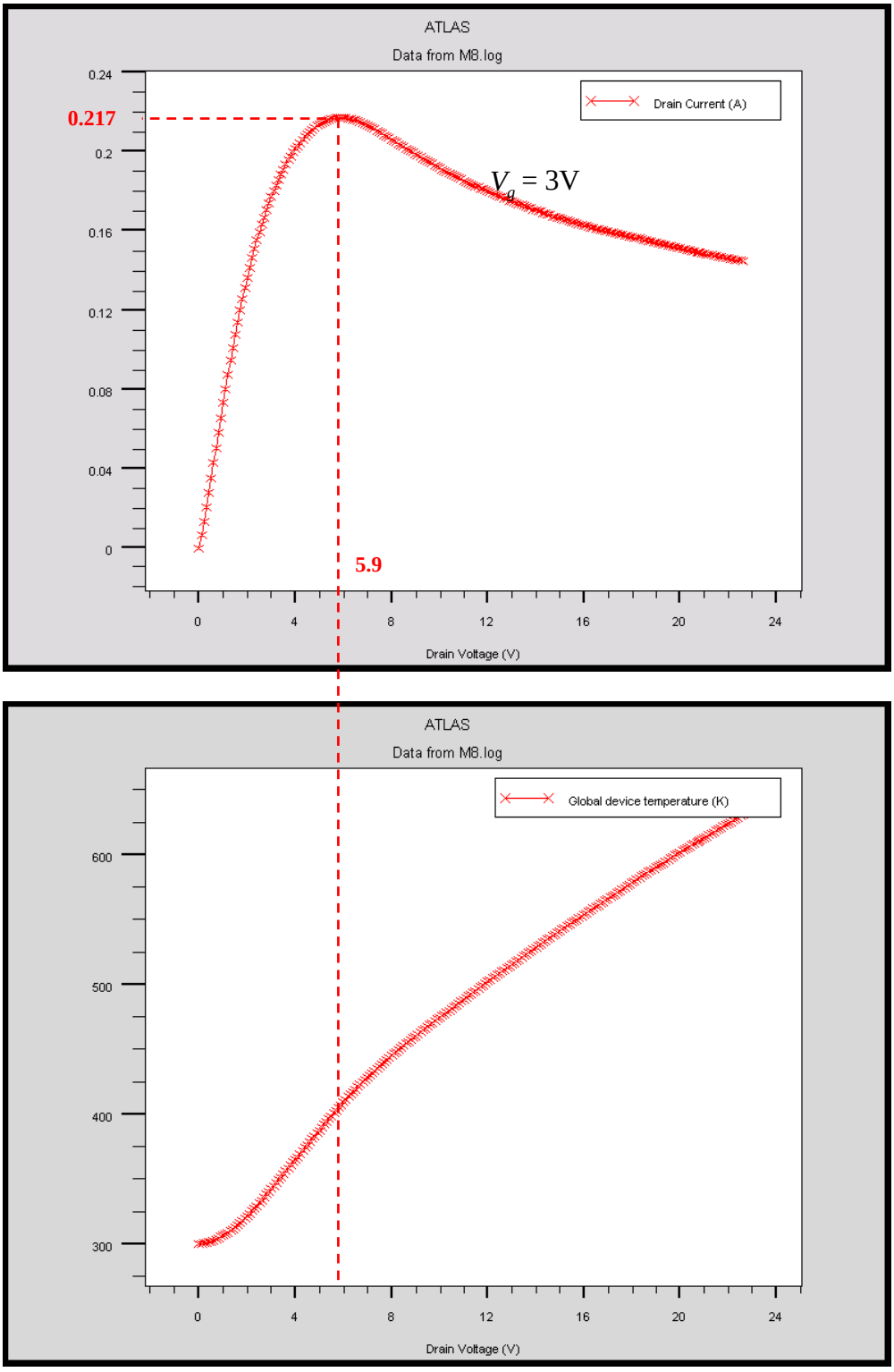

Figure 38. I_d vs. V_d and T vs. V_d in DC modeling.

Although the maximum temperature (630.76 K) of DC modeling was much higher than the maximum temperature (374.62 K) of the 10 pulses pulsed wave, the pulsed wave was only 20us and not achieved the equilibrium condition yet. Therefore, in order to have a correct analysis, we need a pulsed wave which achieves the equilibrium condition to be compared with the DC modeling.

However, it was very lengthy in computational time to make a pulsed wave to achieve the equilibrium in simulation. Even we reduced the pulse duration from 50% to 5%, but the device temperature continued to increase slightly.

Finally, we used the time constant technique to predict the temperature and the power in equilibrium for multiple pulses. As shown in Figure 39 and Figure 40, we extracted the values of the peak temperature and average drain current of each pulse in the 50 pulses pulsed wave generated previously in Chapter V, A., 2. and made the two curves.

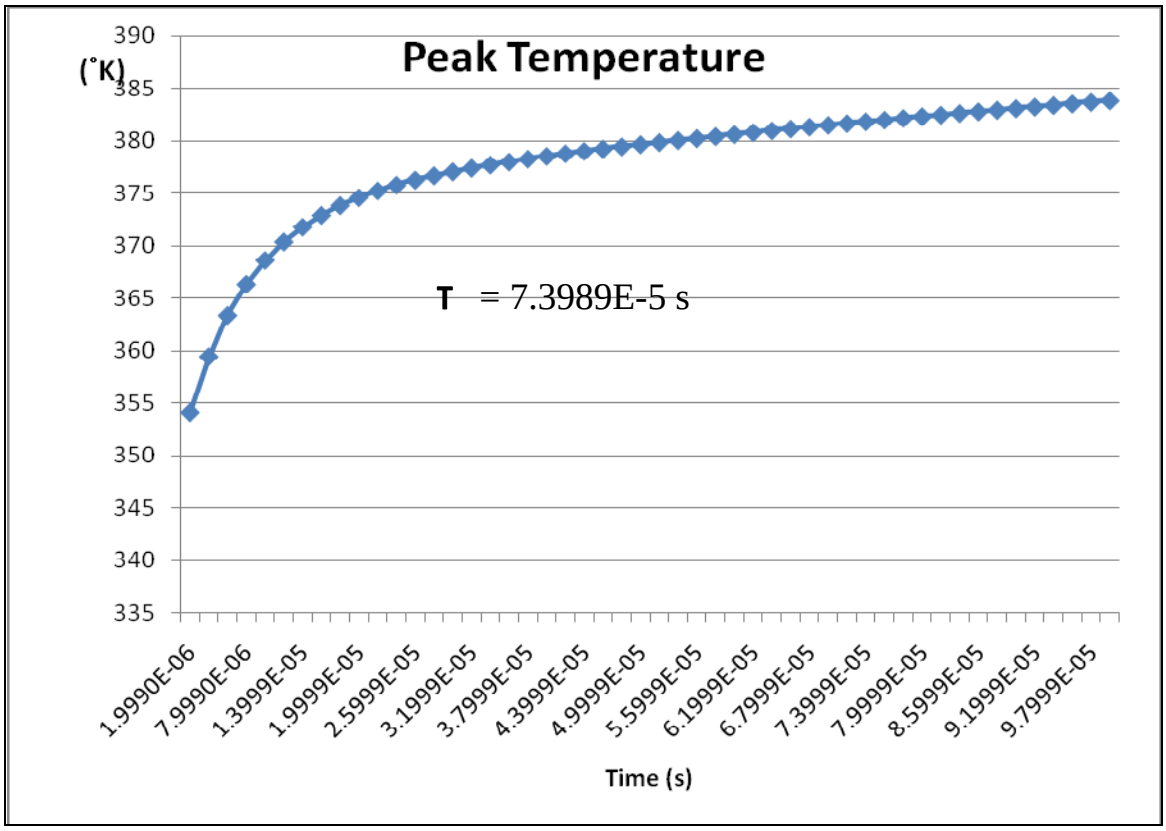

Figure 39. Peak temperature of each pulse.

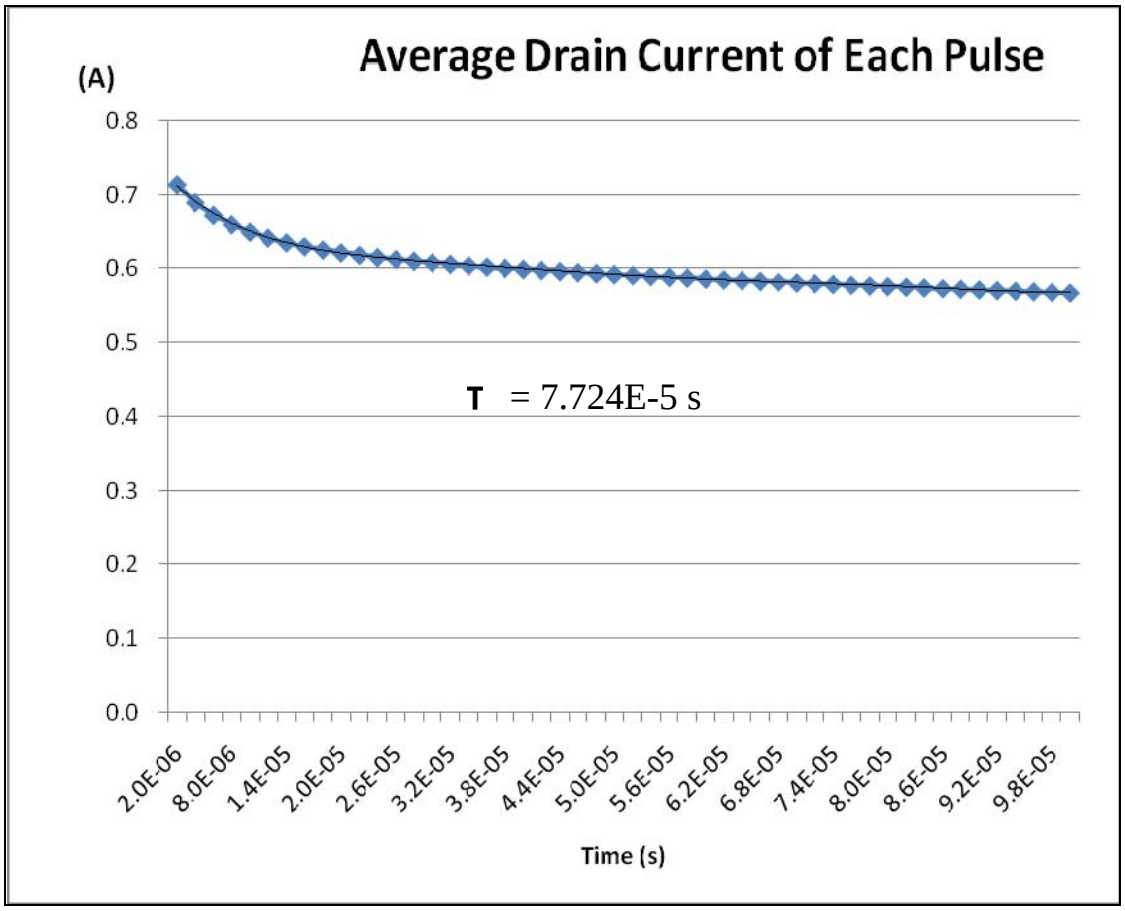

Figure 40. Average drain current of each pulse.

We further calculated the average time constants for the peak temperature and the average drain current curves respectively as 7.3989E-5 s and 7.724E-5 s. With the time constants we were able to obtain the peak temperature and the average drain current in equilibrium respectively as 402.61 K and 0.4737A. Then the power in equilibrium was calculated as 2.37W. Back to Figure 38, we found the same power at I_d =0.17051A and at V_d =13.9V in DC modeling. The corresponding temperature was 527.01 K.

As a result, with the same power, the temperature in multiple pulses was 402.61 K which was much lower than in DC modeling with 124.4^{o}C difference. The simulation result suggests that running multiple pulses in GaN HEMT instead of DC modeling will reduce the self-heating effect.

D. CHANGED SUBSTRATE

As mentioned previously, SOD technology can reduce the self-heating effect due to the high thermal conductivity of diamond. In this chapter we compared the performance of AlGaN/GaN HEMTs by changing the thickness of silicon layer and diamond layer.

1. Comparison for Single Pulse

We first compared the performance of three different cases in single pulse simulation. As shown in Figure 41, the three structures had the same thickness of substrates but each substrate was consisted of different thickness of silicon layer and diamond layer. The thickness of the whole substrate is 7.9 *um* (from Y=2.1 *um* to Y=10 *um*). In the left structure, the substrate is 7.9 *um* of a silicon layer. In the middle structure, the substrate is 1.9 *um* silicon and 6 *um* diamond. In the right structure, the substrate is 0.4 *um* silicon and 7.5 *um* diamond. It can be seen clearly that the right structure had a better heat dissipation. The three structure plots were made in the end of the single pulse. The single pulse was generated by applying 10 volts drain voltage and 3 volts gate voltage and the pulse duration is 20 *us*.

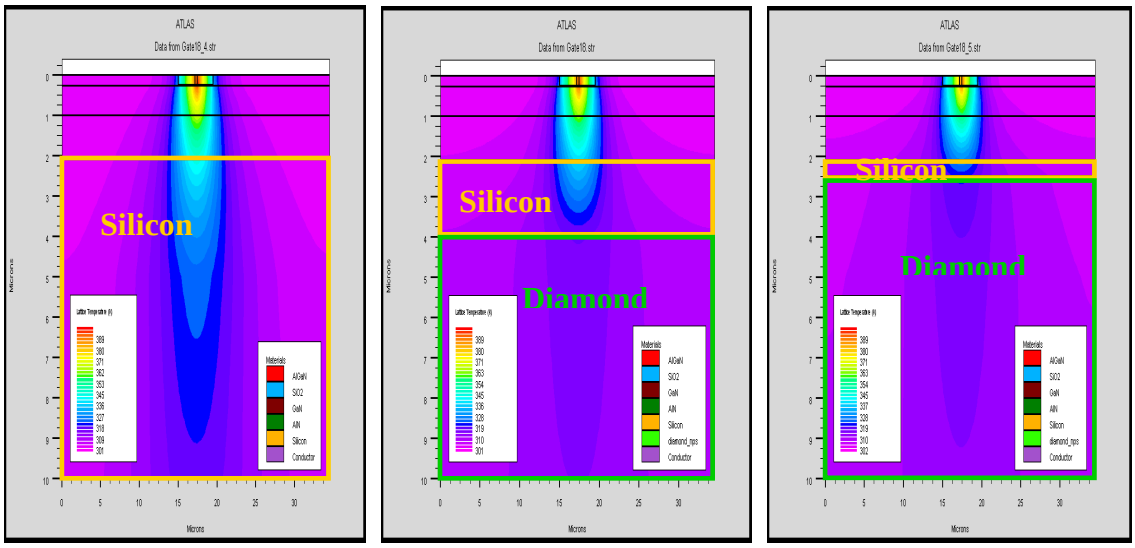

Figure 41. Structures of different composition ratio of diamond.

In Figure 42, it can be seen that the left case had the highest temperature at 397.41 K and the right case with the larger diamond had the lowest temperature at 390.02 K.

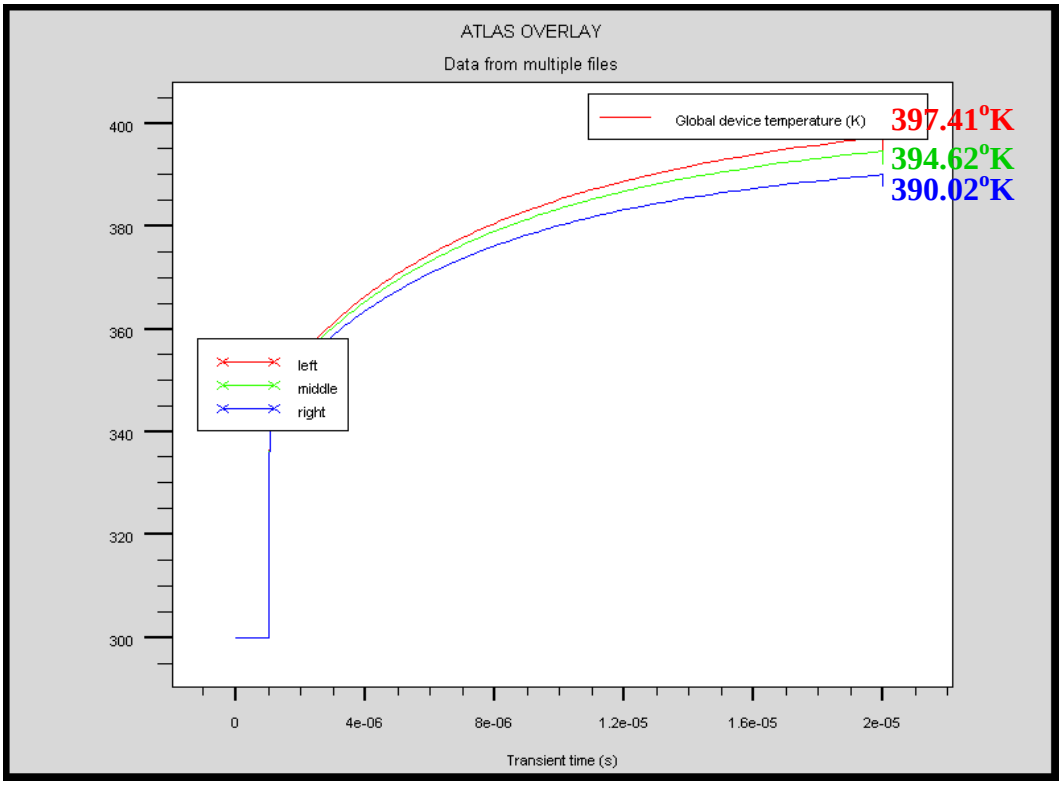

Figure 42. Temperatures for Various Substrates.

In Figure 43, it can be seen that the left case (all silicon) had the smallest drain current and the right case with the larger diamond had the biggest drain current. The average drain current and the average power for the three cases from the left to the right were separately calculated as 0.552 A, 0.57 A, 0.584 A and 11.04 W, 11.4 W, 11.68 W respectively.

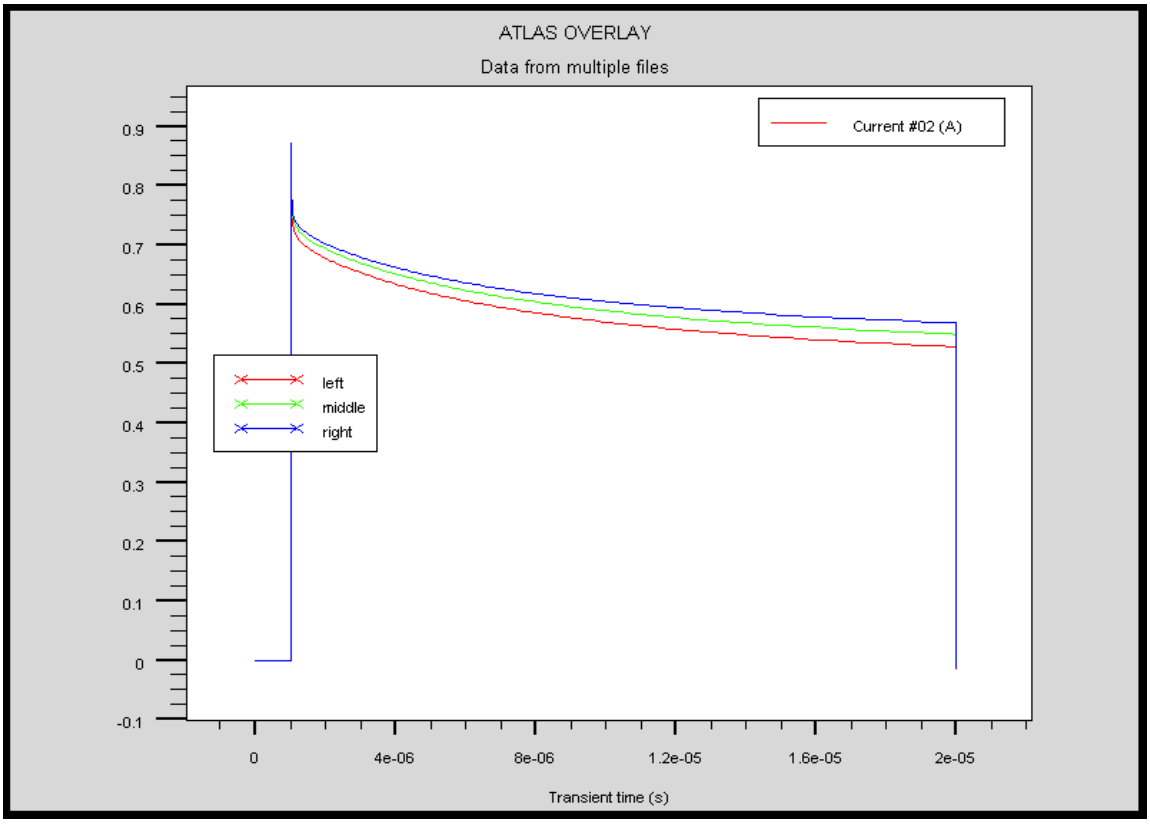

Figure 43. Drain current for various substrates.

2. Comparison for Multiple Pulses

After the single pulse, we compared the performance of the previous three structures in simulation of multiple pulses. The multiple pulse simulation had 10 pulses. The pulse duration was 2 *us* and the duty cycle was 50%.The applied drain voltage was 10 volts and the applied gate voltage was 3 volts.

In Figure 44, it can be seen that the left case (all silicon) had the highest temperature at 376.59 K and the right case with the larger diamond had the lowest temperature at 371.52 K in the end of the pulsed wave.

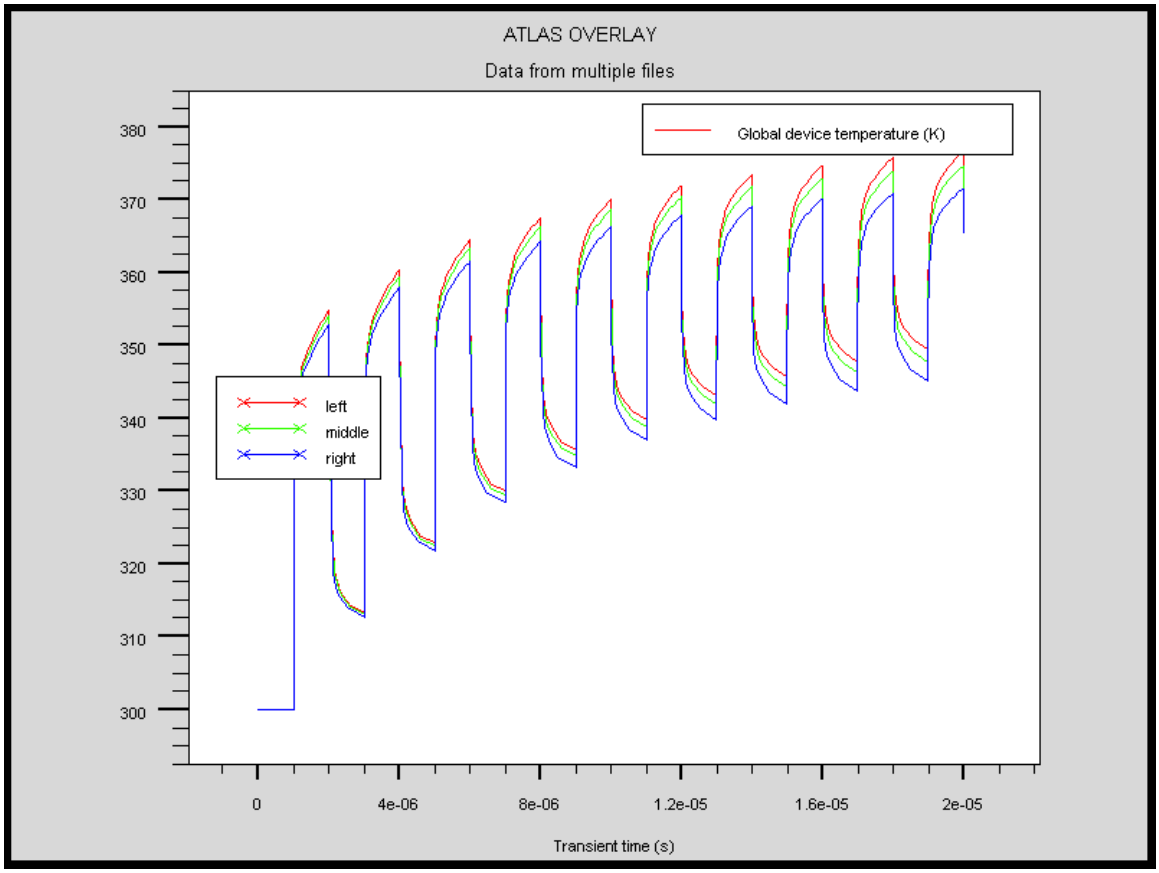

Figure 44. Temperatures for Various Substrates in multiple pulses.

In Figure 45, it can be seen that the left case had the smallest drain current and the right case with the larger diamond had the biggest drain current. The average drain current and the average power for the three cases from the left to the right were separately calculated as 0.636 A, 0.654 A, 0.665 A and 6.36 W, 6.54 W, 6.65 W, respectively.

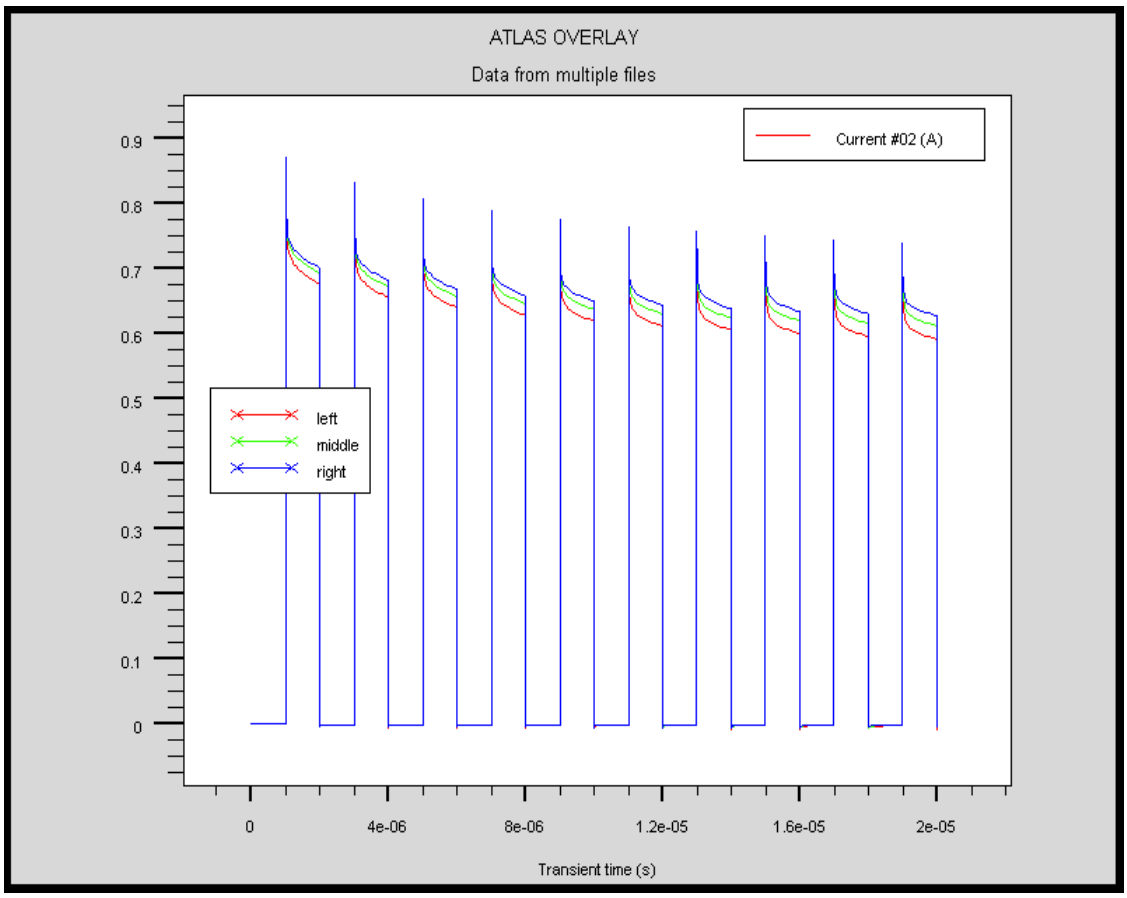

Figure 45. Drain current for Various Substrates in multiple pulses.

Finally, the results of the two simulations in single pulse and multiple pulses suggest that increasing the thickness of diamond in SOD substrate can reduce the self-heating effect and increase the power as shown in Table 12.

	Single Pulse			Multiple Pulses		
	Left	Middle	Right	Left	Middle	Right
Ratio of Silicon in Substrate	100 %	24 %	5 %	100 %	24 %	5 %
Ratio of Diamond in substrate	0	76 %	95 %	0	76 %	95 %
Temperature Decrement(^{o}C) (compared with the left case)		**2.79**	**7.39**		**1.97**	**5.07**
Average Power Increment (compared with the left case)		**3.26 %**	**5.8 %**		**2.83 %**	**4.56 %**

Table 12. Comparison between single pulse and multiple pulses.

E. THE RELATIONSHIP BETWEEN THE ELECTRON VELOCITY, DRAIN CURRENT AND THE TEMPERATURE OF TRANSIENT MODEL

It has been studied in many researches [4]–[5] that the increase in temperature due to the self-heating will degrade the performance of the transistor, for instance the decrease in the channel electron mobility and the drain current. Here, we would discuss how the electron mobility changes with temperature in transient modeling of the AlGaN/GaN HEMT.

As shown in Figure 46, we would extract the data of the electron velocity from the two specified spots (x,y) at various time points which the local maximum temperature occurs at. The two spots are chosen inside the 2DEG channel. Spot1 is at (16.341 , 0.268) and Spot2 is at (18.308 , 0.268).

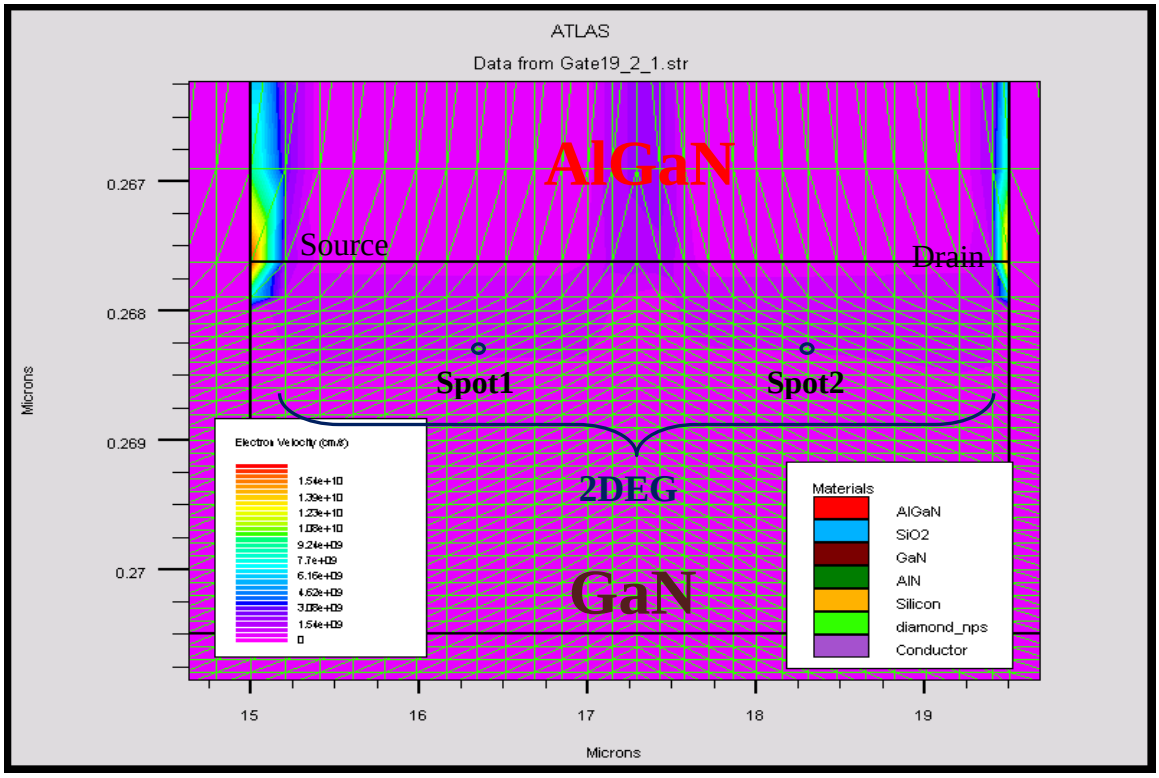

Figure 46. Electron velocity profile of structure.

In Table 13, it lists the drain current and temperature and the extracting data of the electron velocity at various time points.

Time (us)	Electron Velocity (m/s)		Drain Current (A)	Device Temperature (K)
	Spot1	Spot2		
1.999	**7.09267E+08**	**6.86623E+08**	**0.69625**	**354.1**
3.999	**6.96048E+08**	**6.75646E+08**	**0.67233**	**359.44**
5.999	**6.86265E+08**	**6.67410E+08**	**0.65757**	**363.37**
7.999	**6.78717E+08**	**6.60963E+08**	**0.64637**	**366.34**
9.999	**6.72745E+08**	**6.55793E+08**	**0.63764**	**368.62**
11.999	**6.67915E+08**	**6.51559E+08**	**0.63067**	**370.39**
13.999	**6.63932E+08**	**6.48026E+08**	**0.62499**	**371.8**
15.999	**6.60586E+08**	**6.45025E+08**	**0.62027**	**372.93**
17.999	**6.57726E+08**	**6.42436E+08**	**0.61627**	**373.86**
19.999	**6.55242E+08**	**6.40166E+08**	**0.61284**	**374.62**

Table 13. Electron velocity, drain current and temperature.

Based on the data in Table 13,we obtained the curves of electron velocity and drain current versus temperature as shown in Figure 47. It can be seen that the three curves are linearly proportional to the temperature and the curves of Spot1 and Spot2 are almost ideally pareallel. By using the technique of polynominal curve fitting, we could find out how the drain current and the electron velocity depend on the temperature and further described the relationship as the following formulas :

$$I_d = 2T^4 \times 10^{-5} + 0.006T^2 - 0.038T + 0.728 \quad \text{(Drain Current)}$$

$$v_{e-} = 3T^4 \times 10^{-6} + 0.001T^2 - 0.011T + 8.861 \quad \text{(Electron Velocity,at Spot1)}$$

$$v_{e-} = 3T^4 \times 10^{-6} - 9T^3 \times 10^{-5} + 0.001T^2 - 0.01T + 8.845 \quad \text{(Electron Velocity, at Spot2)}$$

It should be noted that the the temperature range for these formulas is between 300 K and 374.62 K. And the formulas are based on the 10 pulses pulsed wave with pulse duration 2us and duty cycle 50%.

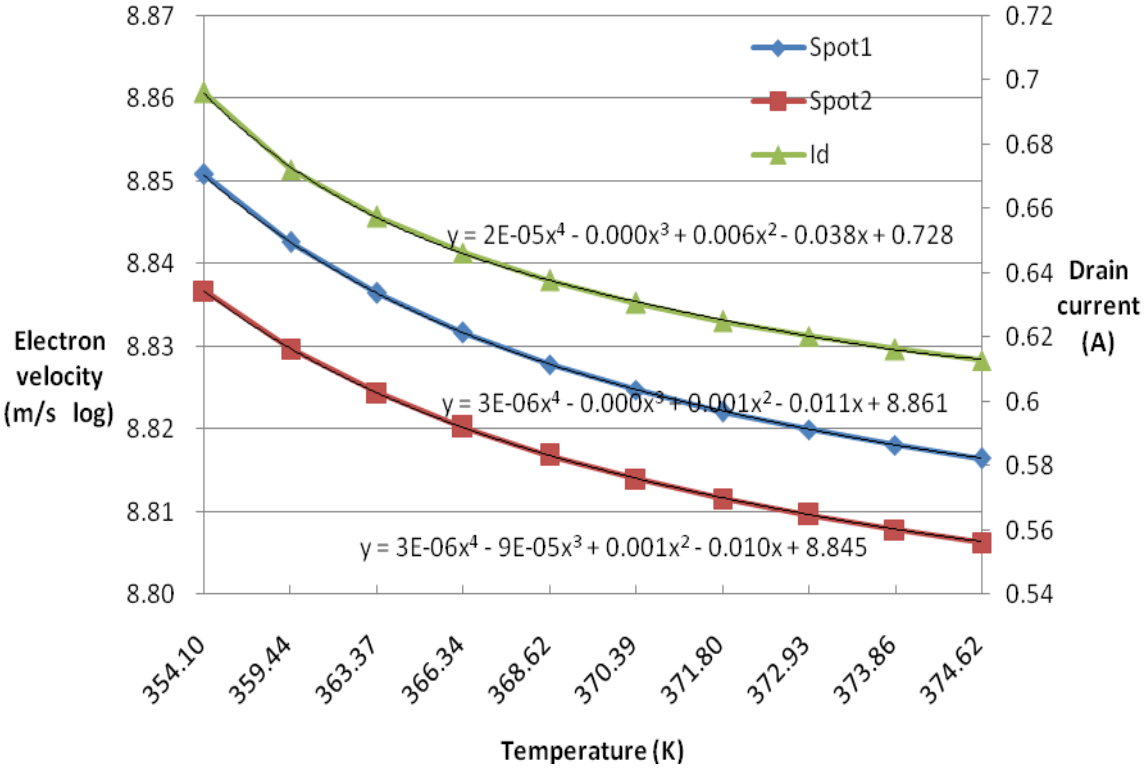

Figure 47. Curves of Electron velocity at spot1 and spot2 and the corresponding I_d.

F. ONE HOT SPOT AND TWO HOT SPOTS

In the simulation of a long single pulse, a phenomenon was observed in the structure that two hot spots occurred in the beginning of the pulse and then the two hot spots gradually diffused into one hot spot with increasing time.

The long pulse was 1ms and had peak drain voltage of 10 volts and constant gate voltage of 3 volts (The simulation code is attached as Appendix D.). In Figure 48 and Figure 49, the temperature profiles of the structure illustrated the phenomenon of one hot spot and two hot spots and also pointed out the temperature difference between the middle and both ends.Figure 48 was saved at 515ns and Figure 49 was saved at 1ms.

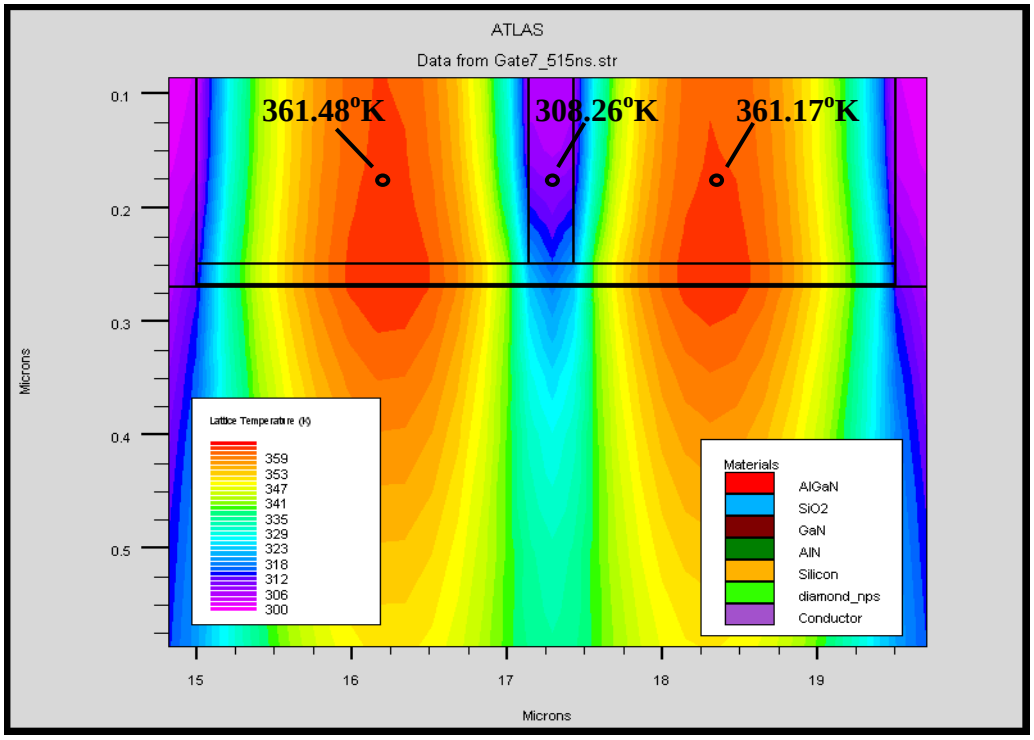

Figure 48. Temperature profile of two hot spots (at 515 ns).

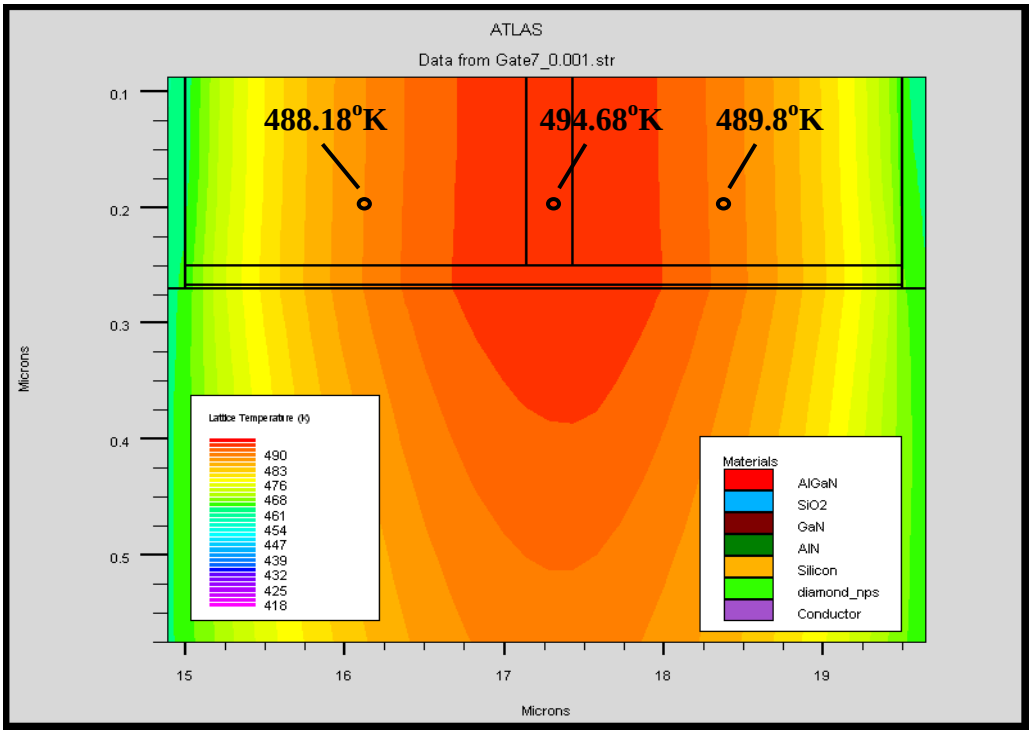

Figure 49. Temperature profile of one hot spot (at 1ms).

To explain this phenomenon, we observed the electric field, current density and Joule heat power profiles of the structure, as shown in Figure 50, Figure 51, and Figure 52 respectively. It can be seen that the electric field and current density were similar in the channel at both time points. The Joule heat power was slightly larger in both ends at 515ns and larger in the middle at 1ms. The instant Joule heat power was gradually accumulated in both ends from the beginning of the pulse due to the self-heating. As the device was filled with heat energy, the gate electrode acted as a heat source and heat dissipated through the gate electrode. Therefore, the gate electrode was cool at first but gradually getting hotter with increasing time as shown in Figure 49.

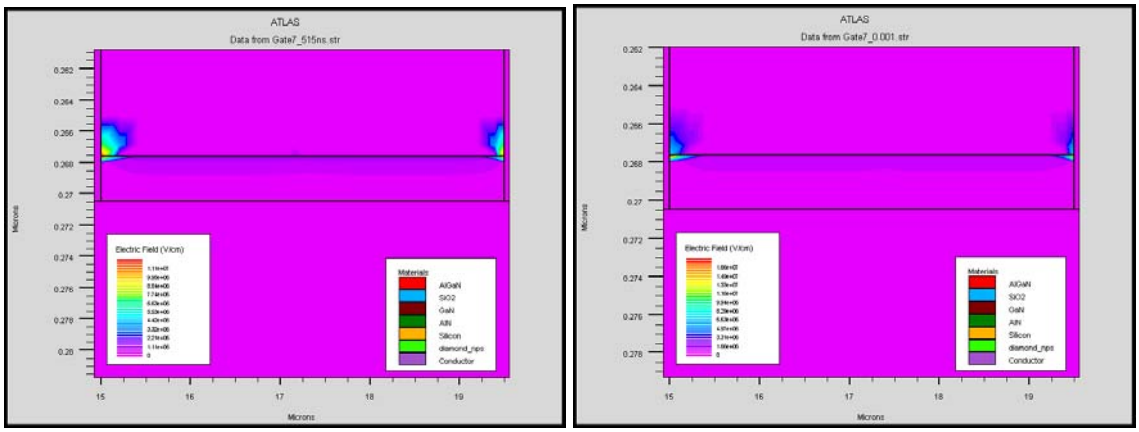

Figure 50. Electric field profile (left at 515ns and right at 1ms).

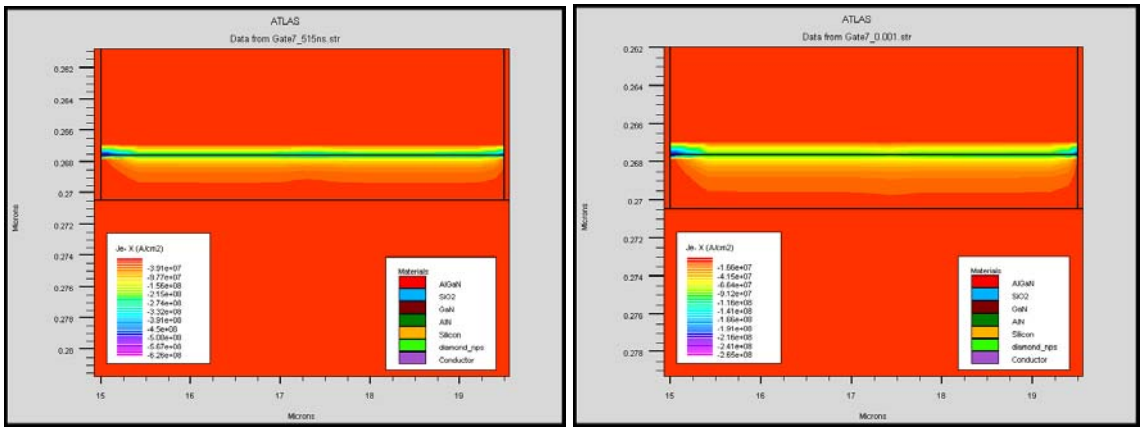

Figure 51. Current density at X direction (left at 515ns and right at 1ms).

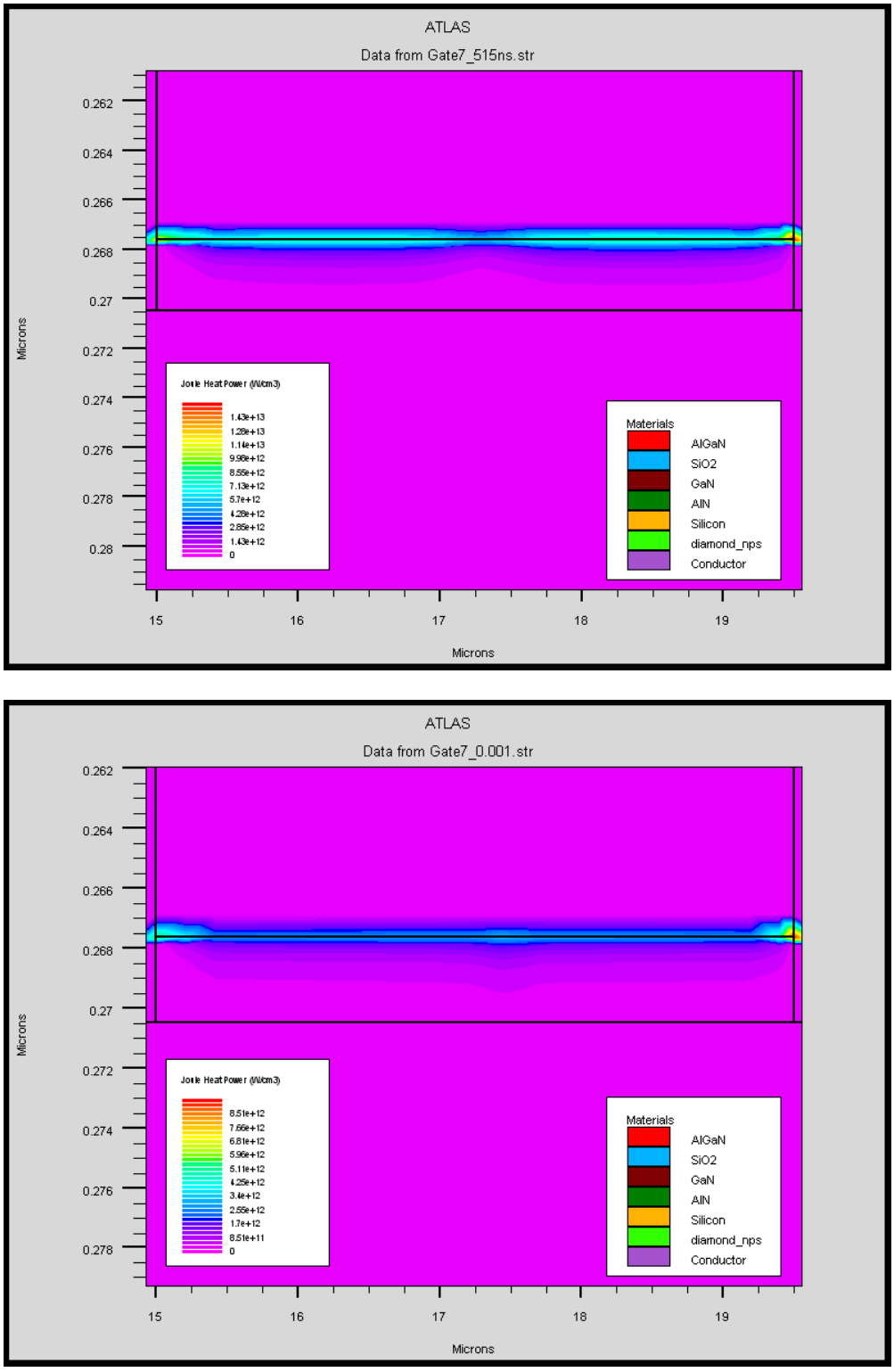

Figure 52. Joule heat power (above at 515ns and below at 1ms).

THIS PAGE INTENTIONALLY LEFT BLANK

VI. CONCLUSIONS AND RECOMMENDATIONS

A. CONCLUSIONS

In this thesis paper, we have presented numerous simulation works which help us to understand more about the electrical and thermal characteristics of GaN HEMTs. First, we have developed a GaN HEMTs transient model. Based on this model we are able to explore transient properties of GaN HEMTs which cannot be done in the practical experimental, i.e. virtually measuring the device temperature at microsecond time or shorter time, at various locations.

We also successfully used Method 3104 technique to determine the location where gate voltage measurement relates to. As a result, the location was inside the gate electrode and above the channel.

In the study of single pulse and multiple pulses, the single pulse appeared to have a higher maximum temperature which would reduce the device life time. But it had a better performance on average output power than multiple pulses. From the simulation result, we can presume that increasing pulse duration results in higher temperature due to the longer heating time but have a larger average output power.

After the study of multiple pulses, we further compared the performance between DC and RF. We presented how to use simulation to uncover thermal time constants and to find out the large difference of device temperature between DC and RF at same output power. The particular simulation result appears that the temperature in RF is 125^{o}C lower than in DC. It also suggests that GaN HEMTs working in RF should have a longer life time.

In this work, the temperature effects of the SOD substrate were studied. We compared the self-heating effects in three cases with different composition ratio of diamond. The simulation result appeared that increasing the composition ratio of diamond in SOD substrate could reduce the heating effects and lead to lower device temperature.

Finally, we discussed the unique transistor heating that dual hot spots in the beginning of single pulse (at sub microsecond time) gradually diffused into one hot spot in the end of the single pulse (at 1ms). We first found that Joule power continued to increase in both sides and this explains the observation of dual hot spots in the beginning. It was presumed that the Joule heat accumulated in the device then dissipated through gate electrode after the gate electrode was filled with heat. That means gate electrode acts as a heat sink.

As in the previous NPS research, a lot of efforts have been contributed to advance the simulation of GaN HEMTs. All the simulation results in this thesis paper can lead us to further studies of GaN HEMTs and also help us to design a better GaN transistor.

B. RECOMMENDATIONS

A lot of simulation work has been done in this thesis paper and experiments to validate the simulation accuracy are needed i.e. the simulation of Method 3104 and the comparison between DC and RF.

Pertaining to the observation of dual hot spots, it was concluded that gate electrode acts as a heat sink which the accumulating heat dissipates through. A study is needed to further understand the heating effects. Placing another thermal contact on the top of the structure and below the electrodes should be investigated.

For these simulations, we have discussed a lot about self-heating effects but we did not include the trapping effects. It has been reported that the electrical performances are strongly affected by surface and substrate traps. The trapping effects can also limit the output power performance of microwave field-effect transistors (FETs) [18–19].

In Chapter 3, 3., 3. “Traps and Defects” of the ATLAS user’s manual© [20], various models are introduced to include the trapping effects. For instance, “Trap-Assisted Tunneling” which can be enabled by specifying TRAP.TUNNEL in the Models statement models the trap-to-band phonon-assisted tunneling effects for Dirac wells. Therefore, a possible next step to improve the transient modeling would be including the trapping effects model.

LIST OF REFERENCES

[1] DoD,"Department of Defense Fiscal Year (FY) 2009 Budget Estimates February 2008," DoD. pp. 378, February 2008.

[2] Jianfeng XU, Wen-Yan YIN, Junfa MAO, *and* Le-Wei LI," Thermal Effect Simulation of GaN HFETs under CW and Pulsed Operation," The Institute of Electronics, Information and Communication Engineers, vol. E90, pp.204 -207, January 2007.

[3] Chenggang Xie and Anthony Pavio, "Development of GaN HEMT based high power high efficiency distributed power amplifier for military applications," Military Communications Conference, MILCOM 2007. IEEE, Oct 2007.

[4] Manju K. Chattopadhyay and Sanjiv Tokekar, " Thermal model for dc characteristics of AlGaN/GaN HEMTs including self-heating effect and non-linear polarization," Microelectronics Journal, vol. 39, pp. 1181–1188, 2008.

[5] E.R. Heller and A. Crespo, "Electro-thermal modeling of multifinger AlGaN/GaN HEMT device operation including thermal substrate effects," Microelectronics Reliability, vol.48, pp.45-50, January 2008.

[6] John C. Zolper, "Status, Challenges, and Future Opportunities for Compound Semiconductor Electronics," Gallium Arsenide Integrated Circuit (GaAs IC) Symposium, IEEE,pp. 3 – 6, 2003.

[7] Sangmin Lee, Ramakrishna Vetury, Jeffrey D. Brown, Shawn R. Gibb, Will Z. Cai, Jinming Sun, Daniel S. Green and Jeff Shealy, "Reliability Assessment of AlGaN/GaN HEMT Technology on SiC for 48V applications," IEEE CFP08RPS-CDR 46th Annual International Reliability Physics Symposium, pp. 446-449,2008.

[8] David Allen McGlone, "Modeling of Gallium Nitride High Electron Mobility Transistors on Silicon/Diamond," M.S. thesis, Naval Postgraduate School, Monterey, California, 2008,[Electronic].

[9] Mark Rosker, "The Wide and the Narrow: DARPA/MTO Programs for RF Applications in Wide Bandgap and Antimonide-Based Semiconductors," Compound Semiconductor Integrated Circuit Symposium, CSIC IEEE, vol. 30, pp. 13-16, November 2005.

[10] Mark J. Rosker, "Recent Advances in GaN-on-SiC HEMT Reliability and Microwave Performance within the DARPA WBGS-RF Program," Compound Semiconductor Integrated Circuit Symposium, CSIC IEEE, 2007.

[11] Katerina Raleva, Dragica Vasileska, and Stephen M. Goodnick, “Is SOD Technology the Solution to Heating Problems in SOI Devices?,” IEEE ELECTRON DEVICE LETTERS, vol. 29, NO. 6, pp. 621-624, June 2008.

[12] SP3 Incorporated, http://www.sp3diamondtech.com/pdf/20090414_SODAvailability_PR-FINAL.pdf, June 8, 2009.

[13] William Alexander Gibson, “Comparison of Gallium Nitride high electron mobility transistors modeling in two and three dimensions,” M.S. thesis, Naval Postgraduate School, Monterey, California, 2007, [Electronic].

[14] MIL-STD 750D Method 3104, “Thermal resistance measurements of GaAs MOSFETs.”

[15] Sanghyun Seo, “AlGaN/GaN High Electron Mobility Transistors (HEMTs),” http://www.eecs.umich.edu/dp-group/classes/2003_EECS521/AlGaN_GaN_HEMT_SanghyunSeo_EECS521_ProjectII_Winter_2003.pdf, June 8, 2009.

[16] Lester F. Eastman and Umesh K. Mishra, “The toughest,” IEEE Spectrum, pp. 28-33, May 2002.

[17] J. Zimmer and G. Chandler, “Advances in Large Diameter GaN on Diamond Substrates,” CS Mantech 2008.

[18] Steven C. Binari, P. B. Klein and Thomas E. Kazior,” Trapping effects in GaN and SiC microwave FETs,” Proceedings of the IEEE, vol.90, pp.1048-1058, June 2002.

[19] S. Augaudy, R. Quere, J.P. Teyssier, M.A. Di Forte-Poisson, S. Cassette, B. Dessertenne and S.L Delage,” Pulse characterization of trapping and thermal effects of microwave GaN power FETs,” Microwave Symposium Digest, vol.1,pp. 427-430, May 2001.

[20] Silvaco International, “Silvaco International, ATLAS User’s Manual,” September 2007.

APPENDIX A. MIXEDMODE CODE

```
################### Mixmode Transient State ######################
go atlas

.begin
Vg 2 0 0 pulse 0 3 0ns   200ns 100ns 3000ns 4300ns
Vd 1 0 0 pulse 0 1 100ns 100ns 100ns 3000ns 4200ns
ahemt 0=source 1=drain 2=gate infile=AFRL.str
.Numeric toldc=1e-6
.Options fulln print relpot write=10
.print DC Vg(ahemt) Vd(ahemt) Vs(ahemt) ig(ahemt) id(ahemt)
.log outfile=AFRL_2.2.1
.save master=AFRL_2.2.1
.tran 1ns 200ns
.end

#################################################################

# material device=ahemt mat=diamond_nps user.group=insulator \
# user.default=oxide TCON.POLYN TC.A=.125 TC.B=0 TC.C=0 permittivity=5.7

# AlGaN
material device=ahemt region=1 taun0=1.e-9 taup0=1.e-9 TCON.POLYN TC.A=1.47 \
         TC.B=0 TC.C=0 HC.A=1.54 HC.B=0.0 HC.C=0.0 HC.D=0.0 align=0.75

# GaN
material device=ahemt region=3 taun0=1.e-9 taup0=1.e-9 TCON.POLYN TC.A=0.666 \
         TC.B=0 TC.C=0 HC.A=1.97 HC.B=0.00036 HC.C=0.0 HC.D=0.0
material device=ahemt region=4 taun0=1.e-9 taup0=1.e-9 TCON.POLYN TC.A=0.666 \
         TC.B=0 TC.C=0 HC.A=1.97 HC.B=0.00036 HC.C=0.0 HC.D=0.0

# AlN
material device=ahemt region=5 taun0=1.e-9 taup0=1.e-9 TCON.POLYN TC.A=0.03 \
         TC.B=0.00156 TC.C=1.65e-6 HC.A=1.97 HC.B=0.00036 HC.C=0.0 HC.D=0.0

contact device=ahemt name=gate work=4.3
contact device=ahemt name=source con.resist=.1e-6
contact device=ahemt name=drain con.resist=.1e-6

interface device=ahemt charge=0.85e13 y.min=.265 y.max=.2685 s.s

mobility device=ahemt albrct.n an.albrct=2.1e-4 bn.albrct=2.3e-4 \
         cn.albrct=1.36e-2

models device=ahemt print srh albrct lat.temp

thermcontact device=ahemt num=1 y.min=10 y.max=10 ext.temp=300 boundary \
             alpha=125

output con.band val.band charge e.velocity h.velocity

quit
```

THIS PAGE INTENTIONALLY LEFT BLANK

APPENDIX B. CODE FOR GATE VOLTAGE MEASUREMENT

```
go atlas simflags="-P 2"

mesh auto width=300

# x plane meshing
x.m l=0.0 s=0.25
x.m l=15 s=0.2
x.m l=17 s=0.05
x.m l=18 s=0.15
x.m l=19.4 s=0.2
x.m l=19.5 s=0.25
x.m l=34.5 s=.25

# y plane meshing
y.m l=0 s=0.25
y.m l=0.15 s=0.2
y.m l=0.23 s=0.005
y.m l=0.24 s=0.005
y.m l=0.25 s=0.005
y.m l=0.26 s=0.005
y.m l=0.268 s=0.0001
y.m l=0.2685 s=0.0001
y.m l=0.2705 s=0.0001

y.m l=0.271 s=0.005

y.m l=0.3 s=0.05
y.m l=0.4 s=0.1
y.m l=1.0 s=0.2
y.m l=1.5 s=0.15
y.m l=2.1 s=0.1
y.m l=2.6 s=0.15
y.m l=3.9 s=0.15
y.m l=4.6 s=0.15
y.m l=10 s=5
#y.m l=20 s=10
#y.m l=400 s=10

######################### Region Definitions ################
region num=1 x.min=15 x.max=19.5 y.max=0.2675  mat=AlGaN    x.comp=0.27
region num=2 x.min=0.0 x.max=34.5 y.min=0.0     y.max=0.25      mat=oxide
region num=3 x.min=15 x.max=19.5 y.min=0.2675  mat=GaN      donors=1e15
region num=4 x.min=0 x.max=34.5 y.min=0.2705  y.max=1.0 mat=GaN donors=1e15
region num=5 x.min=0.0 x.max=34.5 y.min=1.0    y.max=2.1 mat=AlN
region num=6 x.min=0.0 x.max=34.5 y.min=2.1    y.max=4.0 mat=silicon donors=1e16
region num=7 x.min=0.0 x.max=34.5 y.min=4.0     y.max=10.0
user.material=diamond_nps
#region num=8 x.min=0.0 x.max=34.5 y.min=10.0     y.max=400.0
user.material=silicon_nps

elec num=1 name=source x.min=0   x.max=15 y.min=0 y.max=.2705
elec num=2 name=drain  x.min=19.5 x.max=34.5   y.min=0 y.max=.2705
elec num=3 name=gate   x.min=17.1   x.max=17.45   y.min=0 y.max=0.25
elec num=4 substrate

material mat=diamond_nps user.group=insulator user.default=oxide TCON.POLYN
TC.A=.125 TC.B=0 TC.C=0 permittivity=5.7
```

```
#material mat=silicon_nps user.group=insulator user.default=oxide TCON.POLYN
TC.A=.666 TC.B=0 TC.C=0 permittivity=11.8

#AlGaN
#material region=1 taun0=1.e-9 taup0=1.e-9 TCON.POLYN TC.A=1.47 TC.B=0 TC.C=0
HC.A=1.54 HC.B=0.0 HC.C=0.0 HC.D=0.0 align=0.75
material material=AlGaN taun0=1.e-9 taup0=1.e-9 TCON.POLYN tc.a=0.666 tc.b=0
tc.c=0 hc.std hc.a=1.97 hc.b=0.00036 hc.c=0 hc.d=-3.7e4 align=0.75

#GaN
material region=3 taun0=1.e-9 taup0=1.e-9 TCON.POLYN TC.A=0.666 TC.B=0 TC.C=0
HC.A=1.97 HC.B=0.00036 HC.C=0.0 HC.D=0.0
material region=4 taun0=1.e-9 taup0=1.e-9 TCON.POLYN TC.A=0.666 TC.B=0 TC.C=0
HC.A=1.97 HC.B=0.00036 HC.C=0.0 HC.D=0.0

#AlN
material region=5 taun0=1.e-9 taup0=1.e-9 TCON.POLYN TC.A=0.03 TC.B=0.00156
TC.C=1.65e-6 HC.A=1.97 HC.B=0.00036 HC.C=0.0 HC.D=0.0

#Silicon
material region=6 taun0=1.e-9 taup0=1.e-9 TCON.POLYN TC.A=0.03 TC.B=0.00156
TC.C=1.65e-6 hc.std HC.A=1.97 HC.B=0.00036 HC.C=0.0 HC.D=-3.7e4

contact name=gate work=4.3
#contact name=source con.resist=.1e-6
#contact name=drain con.resist=.1e-6

interface charge=0.85e13 y.min=.265 y.max=.2685 s.s

mobility albrct.n an.albrct=2.1e-4 bn.albrct=2.3e-4 cn.albrct=1.36e-2

models print srh albrct lat.temp heat.full

thermcontact num=1 y.min=10 y.max=10 ext.temp=300 boundary alpha=125

output con.band val.band charge e.velocity h.velocity

method newton

solve init
save outf=Gate27.str

solve name=gate Vgate=0 vfinal=2 vstep=0.1
contact name=gate current
solve previous
solve Igate=1e-5

log outf=Gate27.log

solve Vdrain=0 tstep=1e-9 tstop=5e-9
solve Vdrain=10 ramptime=10e-9 tstep=1e-9 tstop=15e-9
solve Vdrain=10 tstep=1e-7 tstop=0.000100015
solve Vdrain=0 ramptime=10e-9 tstep=1e-9 tstop=0.000100025
save outf=Gate27_1.str

solve Vdrain=0 tstep=1e-9 tstop=0.0001001
save outf=Gate27_11.str

solve Vdrain=0 tstep=1e-9 tstop=0.0001002
save outf=Gate27_12.str

solve Vdrain=0 tstep=1e-9 tstop=0.0001003
```

```
save outf=Gate27_13.str

solve Vdrain=0 tstep=1e-9 tstop=0.0001004
save outf=Gate27_14.str

solve Vdrain=0 tstep=1e-9 tstop=0.0001005
save outf=Gate27_15.str

solve Vdrain=0 tstep=1e-9 tstop=0.0001006
save outf=Gate27_16.str

solve Vdrain=0 tstep=1e-9 tstop=0.0001007
save outf=Gate27_17.str

solve Vdrain=0 tstep=1e-9 tstop=0.0001008
save outf=Gate27_18.str

solve Vdrain=0 tstep=1e-9 tstop=0.0001009
save outf=Gate27_19.str

solve Vdrain=0 tstep=1e-9 tstop=0.000101
save outf=Gate27_2.str

solve Vdrain=0 tstep=1e-9 tstop=0.000102
save outf=Gate27_3.str

solve Vdrain=0 tstep=1e-9 tstop=0.000103
save outf=Gate27_4.str

solve Vdrain=0 tstep=1e-9 tstop=0.000104
save outf=Gate27_5.str

solve Vdrain=0 tstep=1e-9 tstop=0.000106
save outf=Gate27_6.str

solve Vdrain=0 tstep=1e-9 tstop=0.000108
save outf=Gate27_7.str

solve Vdrain=0 tstep=1e-9 tstop=0.00011
save outf=Gate27_8.str

solve Vdrain=0 tstep=1e-9 tstop=0.000112
save outf=Gate27_9.str

solve Vdrain=0 tstep=1e-9 tstop=0.000114
save outf=Gate27_10.str

log off

quit
```

THIS PAGE INTENTIONALLY LEFT BLANK

APPENDIX C. CODE FOR 10 PULSES

```
go atlas simflags="-P 2"

mesh auto width=300

# x plane meshing
x.m l=0.0 s=0.25
x.m l=15 s=0.2
x.m l=17 s=0.15
x.m l=18 s=0.15
x.m l=19.4 s=0.2
x.m l=19.5 s=0.25
x.m l=34.5 s=.25

# y plane meshing
y.m l=0 s=0.25
y.m l=0.15 s=0.2
y.m l=0.23 s=0.02
y.m l=0.24 s=0.005
y.m l=0.25 s=0.005
y.m l=0.26 s=0.005
y.m l=0.268 s=0.0001
y.m l=0.2685 s=0.0001
y.m l=0.2705 s=0.0001

y.m l=0.271 s=0.005

y.m l=0.3 s=0.05
y.m l=0.4 s=0.1
y.m l=1.0 s=0.2
y.m l=1.5 s=0.15
y.m l=2.1 s=0.1
y.m l=2.6 s=0.15
y.m l=3.9 s=0.15
y.m l=4.6 s=0.15
y.m l=10 s=5
#y.m l=20 s=10
#y.m l=400 s=10

######################### Region Definitions ################
region num=1 x.min=15 x.max=19.5 y.max=0.2675  mat=AlGaN    x.comp=0.27
region num=2 x.min=0.0 x.max=34.5 y.min=0.0     y.max=0.25      mat=oxide
region num=3 x.min=15 x.max=19.5 y.min=0.2675  mat=GaN      donors=1e15
region num=4 x.min=0 x.max=34.5 y.min=0.2705  y.max=1.0 mat=GaN donors=1e15
region num=5 x.min=0.0 x.max=34.5 y.min=1.0    y.max=2.1 mat=AlN
region num=6 x.min=0.0 x.max=34.5 y.min=2.1    y.max=4.0 mat=silicon donors=1e16
region num=7 x.min=0.0 x.max=34.5 y.min=4.0     y.max=10.0
user.material=diamond_nps
#region num=8 x.min=0.0 x.max=34.5 y.min=10.0     y.max=400.0
user.material=silicon_nps

elec num=1 name=source x.min=0   x.max=15 y.min=0 y.max=.2705
elec num=2 name=drain  x.min=19.5 x.max=34.5   y.min=0 y.max=.2705
elec num=3 name=gate   x.min=17.1   x.max=17.45   y.min=0 y.max=0.25
elec num=4 substrate

material mat=diamond_nps user.group=insulator user.default=oxide TCON.POLYN
TC.A=.125 TC.B=0 TC.C=0 permittivity=5.7
```

```
#material mat=silicon_nps user.group=insulator user.default=oxide TCON.POLYN
TC.A=.666 TC.B=0 TC.C=0 permittivity=11.8

#AlGaN
#material region=1 taun0=1.e-9 taup0=1.e-9 TCON.POLYN TC.A=1.47 TC.B=0 TC.C=0
HC.A=1.54 HC.B=0.0 HC.C=0.0 HC.D=0.0 align=0.75
material material=AlGaN taun0=1.e-9 taup0=1.e-9 TCON.POLYN tc.a=0.666 tc.b=0
tc.c=0 hc.std hc.a=1.97 hc.b=0.00036 hc.c=0 hc.d=-3.7e4 align=0.75

#GaN
material region=3 taun0=1.e-9 taup0=1.e-9 TCON.POLYN TC.A=0.666 TC.B=0 TC.C=0
HC.A=1.97 HC.B=0.00036 HC.C=0.0 HC.D=0.0
material region=4 taun0=1.e-9 taup0=1.e-9 TCON.POLYN TC.A=0.666 TC.B=0 TC.C=0
HC.A=1.97 HC.B=0.00036 HC.C=0.0 HC.D=0.0

#AlN
material region=5 taun0=1.e-9 taup0=1.e-9 TCON.POLYN TC.A=0.03 TC.B=0.00156
TC.C=1.65e-6 HC.A=1.97 HC.B=0.00036 HC.C=0.0 HC.D=0.0

#Silicon
material region=6 taun0=1.e-9 taup0=1.e-9 TCON.POLYN TC.A=0.03 TC.B=0.00156
TC.C=1.65e-6 hc.std HC.A=1.97 HC.B=0.00036 HC.C=0.0 HC.D=-3.7e4

contact name=gate work=4.3
#contact name=source con.resist=.1e-6
#contact name=drain con.resist=.1e-6

interface charge=0.85e13 y.min=.265 y.max=.2685 s.s

mobility albrct.n an.albrct=2.1e-4 bn.albrct=2.3e-4 cn.albrct=1.36e-2

models print srh albrct lat.temp heat.full

thermcontact num=1 y.min=10 y.max=10 ext.temp=300 boundary alpha=125

output con.band val.band charge e.velocity h.velocity

method newton

solve init

solve name=gate Vgate=0 vfinal=3 vstep=0.1

log outf=Gate19.log

solve Vdrain=0 tstep=1e-9 tstop=1e-6
solve Vdrain=10 ramptime=1e-9 tstep=1e-10 tstop=1.001e-6
solve Vdrain=10 tstep=1e-9 tstop=1.999e-6
solve Vdrain=0 ramptime=1e-9 tstep=1e-10 tstop=2e-6
save outf=Gate19_1.str

solve Vdrain=0 tstep=1e-9 tstop=3e-6
solve Vdrain=10 ramptime=1e-9 tstep=1e-10 tstop=3.001e-6
solve Vdrain=10 tstep=1e-9 tstop=3.999e-6
solve Vdrain=0 ramptime=1e-9 tstep=1e-10 tstop=4e-6
save outf=Gate19_2.str

solve Vdrain=0 tstep=1e-9 tstop=5e-6
solve Vdrain=10 ramptime=1e-9 tstep=1e-10 tstop=5.001e-6
solve Vdrain=10 tstep=1e-9 tstop=5.999e-6
solve Vdrain=0 ramptime=1e-9 tstep=1e-10 tstop=6e-6
save outf=Gate19_3.str
```

```
solve Vdrain=0 tstep=1e-9 tstop=7e-6
solve Vdrain=10 ramptime=1e-9 tstep=1e-10 tstop=7.001e-6
solve Vdrain=10 tstep=1e-9 tstop=7.999e-6
solve Vdrain=0 ramptime=1e-9 tstep=1e-10 tstop=8e-6
save outf=Gate19_4.str

solve Vdrain=0 tstep=1e-9 tstop=9e-6
solve Vdrain=10 ramptime=1e-9 tstep=1e-10 tstop=9.001e-6
solve Vdrain=10 tstep=1e-9 tstop=9.999e-6
solve Vdrain=0 ramptime=1e-9 tstep=1e-10 tstop=10e-6
save outf=Gate19_5.str

solve Vdrain=0 tstep=1e-9 tstop=11e-6
solve Vdrain=10 ramptime=1e-9 tstep=1e-10 tstop=11.001e-6
solve Vdrain=10 tstep=1e-9 tstop=11.999e-6
solve Vdrain=0 ramptime=1e-9 tstep=1e-10 tstop=12e-6
save outf=Gate19_6.str

solve Vdrain=0 tstep=1e-9 tstop=13e-6
solve Vdrain=10 ramptime=1e-9 tstep=1e-10 tstop=13.001e-6
solve Vdrain=10 tstep=1e-9 tstop=13.999e-6
solve Vdrain=0 ramptime=1e-9 tstep=1e-10 tstop=14e-6
save outf=Gate19_7.str

solve Vdrain=0 tstep=1e-9 tstop=15e-6
solve Vdrain=10 ramptime=1e-9 tstep=1e-10 tstop=15.001e-6
solve Vdrain=10 tstep=1e-9 tstop=15.999e-6
solve Vdrain=0 ramptime=1e-9 tstep=1e-10 tstop=16e-6
save outf=Gate19_8.str

solve Vdrain=0 tstep=1e-9 tstop=17e-6
solve Vdrain=10 ramptime=1e-9 tstep=1e-10 tstop=17.001e-6
solve Vdrain=10 tstep=1e-9 tstop=17.999e-6
solve Vdrain=0 ramptime=1e-9 tstep=1e-10 tstop=18e-6
save outf=Gate19_9.str

solve Vdrain=0 tstep=1e-9 tstop=19e-6
solve Vdrain=10 ramptime=1e-9 tstep=1e-10 tstop=19.001e-6
solve Vdrain=10 tstep=1e-9 tstop=19.999e-6
solve Vdrain=0 ramptime=1e-9 tstep=1e-10 tstop=20e-6
save outf=Gate19_10.str

log off

quit
```

THIS PAGE INTENTIONALLY LEFT BLANK

APPENDIX D. CODE FOR LONG PULSE

```
go atlas simflags="-P 2"

mesh auto width=300

# x plane meshing
x.m l=0.0 s=0.25
x.m l=15 s=0.2
x.m l=17 s=0.15
x.m l=18 s=0.15
x.m l=19.4 s=0.2
x.m l=19.5 s=0.25
x.m l=34.5 s=.25

# y plane meshing
y.m l=0 s=0.25
y.m l=0.15 s=0.2
y.m l=0.23 s=0.02
y.m l=0.24 s=0.005
y.m l=0.25 s=0.005
y.m l=0.26 s=0.005
y.m l=0.268 s=0.0001
y.m l=0.2685 s=0.0001
y.m l=0.2705 s=0.0001

y.m l=0.271 s=0.005

y.m l=0.3 s=0.05
y.m l=0.4 s=0.1
y.m l=1.0 s=0.2
y.m l=1.5 s=0.15
y.m l=2.1 s=0.1
y.m l=2.6 s=0.15
y.m l=3.9 s=0.15
y.m l=4.6 s=0.15
y.m l=10 s=5
#y.m l=20 s=10
#y.m l=400 s=10

######################### Region Definitions ################
region num=1 x.min=15 x.max=19.5 y.max=0.2675  mat=AlGaN    x.comp=0.27
region num=2 x.min=0.0 x.max=34.5 y.min=0.0     y.max=0.25      mat=oxide
region num=3 x.min=15 x.max=19.5 y.min=0.2675  mat=GaN      donors=1e15
region num=4 x.min=0 x.max=34.5 y.min=0.2705  y.max=1.0 mat=GaN donors=1e15
region num=5 x.min=0.0 x.max=34.5 y.min=1.0    y.max=2.1 mat=AlN
region num=6 x.min=0.0 x.max=34.5 y.min=2.1    y.max=4.0 mat=silicon donors=1e16
region num=7 x.min=0.0 x.max=34.5 y.min=4.0     y.max=10.0
user.material=diamond_nps
#region num=8 x.min=0.0 x.max=34.5 y.min=10.0     y.max=400.0
user.material=silicon_nps

elec num=1 name=source x.min=0   x.max=15 y.min=0 y.max=.2705
elec num=2 name=drain  x.min=19.5 x.max=34.5   y.min=0 y.max=.2705
elec num=3 name=gate   x.min=17.1   x.max=17.45   y.min=0 y.max=0.25
elec num=4 substrate

material mat=diamond_nps user.group=insulator user.default=oxide TCON.POLYN
TC.A=.125 TC.B=0 TC.C=0 permittivity=5.7
```

```
#material mat=silicon_nps user.group=insulator user.default=oxide TCON.POLYN
TC.A=.666 TC.B=0 TC.C=0 permittivity=11.8

#AlGaN
#material region=1 taun0=1.e-9 taup0=1.e-9 TCON.POLYN TC.A=1.47 TC.B=0 TC.C=0
HC.A=1.54 HC.B=0.0 HC.C=0.0 HC.D=0.0 align=0.75
material material=AlGaN taun0=1.e-9 taup0=1.e-9 TCON.POLYN tc.a=0.666 tc.b=0
tc.c=0 hc.std hc.a=1.97 hc.b=0.00036 hc.c=0 hc.d=-3.7e4 align=0.75

#GaN
material region=3 taun0=1.e-9 taup0=1.e-9 TCON.POLYN TC.A=0.666 TC.B=0 TC.C=0
HC.A=1.97 HC.B=0.00036 HC.C=0.0 HC.D=0.0
material region=4 taun0=1.e-9 taup0=1.e-9 TCON.POLYN TC.A=0.666 TC.B=0 TC.C=0
HC.A=1.97 HC.B=0.00036 HC.C=0.0 HC.D=0.0

#AlN
material region=5 taun0=1.e-9 taup0=1.e-9 TCON.POLYN TC.A=0.03 TC.B=0.00156
TC.C=1.65e-6 HC.A=1.97 HC.B=0.00036 HC.C=0.0 HC.D=0.0

#Silicon
material region=6 taun0=1.e-9 taup0=1.e-9 TCON.POLYN TC.A=0.03 TC.B=0.00156
TC.C=1.65e-6 hc.std HC.A=1.97 HC.B=0.00036 HC.C=0.0 HC.D=-3.7e4

contact name=gate work=4.3
#contact name=source con.resist=.1e-6
#contact name=drain con.resist=.1e-6

interface charge=0.85e13 y.min=.265 y.max=.2685 s.s

mobility albrct.n an.albrct=2.1e-4 bn.albrct=2.3e-4 cn.albrct=1.36e-2

models print srh albrct lat.temp heat.full

thermcontact num=1 y.min=10 y.max=10 ext.temp=300 boundary alpha=125

output con.band val.band charge e.velocity h.velocity

method newton

solve init

solve name=gate Vgate=0 vfinal=3 vstep=0.1

contact name=gate current
solve previous

log outf=Gate7.log

solve Vdrain=0 tstep=1e-9 tstop=5e-9
save outf=Gate7_5ns.str

solve Vdrain=1 ramptime=1e-9 tstep=1e-9 tstop=6e-9
save outf=Gate7_6ns.str

solve Vdrain=5 ramptime=4e-9 tstep=1e-9 tstop=10e-9
save outf=Gate7_10ns.str

solve Vdrain=10 ramptime=5e-9 tstep=1e-9 tstop=15e-9
save outf=Gate7_15ns.str

solve Vdrain=10 tstep=1e-9 tstop=515e-9
save outf=Gate7_515ns.str
```

```
solve Vdrain=10 tstep=1e-9 tstop=1015e-9
save outf=Gate7_1015ns.str

solve Vdrain=10 tstep=1e-9 tstop=0.001
save outf=Gate7_0.001.str

solve Vdrain=5 ramptime=5e-9 tstep=1e-9 tstop=0.001000005
save outf=Gate7_0.001000005.str

solve Vdrain=0 ramptime=5e-9 tstep=1e-9 tstop=0.001000010
save outf=Gate7_0.001000010.str

solve Vdrain=0 tstep=1e-9 tstop=0.001002010
save outf=Gate7_0.001002010.str

log off

quit
```

THIS PAGE INTENTIONALLY LEFT BLANK

INITIAL DISTRIBUTION LIST

1. Defense Technical Information Center
   Ft. Belvoir, Virginia

2. Dudley Knox Library
   Naval Postgraduate School
   Monterey, California

3. Professor Todd R. Weatherford, Code EC(590)/Wt
   Department of Electrical and Computer Engineering
   Naval Postgraduate School
   Monterey, California

4. Professor Gamani Karunasiri, Code PH/Kg
   Department of Physics
   Naval Postgraduate School
   Monterey, California